THE Marquardt CORPORATION

16 OCTOBER 1964

REPORT 6077

COPY NO. 7

(Title -- Unclassified)

OPTIMIZATION STUDY OF MASS EXPULSION ATTITUDE CONTROL SYSTEMS BY MEANS OF ADVANCED LIMIT CYCLE TECHNIQUES

UNCLASSIFIED

(Title -- Unclassified)
OPTIMIZATION STUDY OF
MASS EXPULSION ATTITUDE CONTROL SYSTEM
BY MEANS OF
ADVANCED LIMIT CYCLE TECHNIQUES

Contract NAS 8-11232

Project 350

PREPARED BY

R. W. Adlhoch

W. C. Englehart

CHECKED BY

W. C. Englehart
Project Engineer

APPROVED BY

A. Rose
Manager, Space Equipment

W. P. Boardman
Manager, Advanced
Product Development

UNCLASSIFIED

THE Marquardt CORPORATION
VAN NUYS, CALIFORNIA

FOREWORD

This analytical, three-axis thrust vector, cross-coupled, error study demonstrates the feasibility of using advanced attitude control techniques. The study is directed toward the ultimate goal of optimizing mass expulsion attitude control systems for space vehicles. This contract was performed within the Advanced Product Development Department of the Power Systems Division of The Marquardt Corporation. The authors gratefully acknowledge the assistance and contributions of the following personnel within The Marquardt Corporation:

S. A. Lunn
D. P. Muhonen
D. F. Reeves
D. R. Slagle
M. E. Winter

CONTENTS

TMC A673

ILLUSTRATIONS

ILLUSTRATIONS
(continued)

LIST OF TABLES

I. SUMMARY

The purpose of this study was to introduce and evaluate attitude control techniques which may be more efficient in terms of propellant consumption and rocket engine duty cycle than other methods used to date. The method of evaluating the "Advanced Limit Cycle Control Techniques" is based on a three-axis thrusting cross-coupled, error digital computer program.

Much effort was spent on formulating usable and meaningful criteria for performance evaluation of three-axis control systems in terms of component errors. To this end, a method which uses the system errors as inputs and has as outputs the propellant consumption and number of engine firings was selected. The method of treatment (either analytical or by computer program) for any of the control techniques under consideration is relatively straightforward. The program becomes considerably more difficult when the three-axis thrust vector error cross-coupling effects are taken into consideration and a valid comparison between control techniques is desired.

The feasibility of the advanced control techniques was demonstrated by investigating the effects of errors for the specific conditions of interest. The error sources considered in this study include:

1. Impulse magnitude errors (Normally distributed)
2. Impulse magnitude error variations with pulse width
3. Thrust vector angular error (Normally distributed)
4. Hardware installation angular errors
5. Specific impulse variation with pulse width
6. Sensor errors
7. Timing errors

Since the thrust errors are not limited to the plane in which the thrust is commanded, control interaction results. The general behavior of an attitude control system is not only dependent on error values but also upon the nature of error distributions. A statistical survey of available test data was therefore conducted to establish the error values and distributions. Various thrust levels and pulse widths were analyzed. Specific errors were applied to the vehicle and engine configurations of interest. These errors, along with their causes and effects, are a principal factor in the investigation.

TMC A673

Three engine and vehicle configurations were analyzed with three different angular acceleration values for each. Five control techniques were investigated for each of these angular acceleration values. Two simple limit cycle techniques (open loop) and three advanced limit cycle techniques (damped) were investigated. The two simple limit cycle methods were the box and the diamond error matrix with rate switching option. The three advanced limit cycle techniques are best defined by the extent and quality of the sensing information which was assumed. The nonlinearities of these control systems are also incorporated in the analysis. Equations for each axis of each configuration of interest were developed to provide convenient evaluation of error rates in terms of the individual system errors. These equations present the three-axis thrust vector error cross-coupling effects in terms of resulting angular error rates.

The damped control techniques presented herein can directly damp out any disturbance rate in the minimum time and with the minimum propellant without exceeding the vehicle accuracy band. This eliminates the need for any separate acquisition phase.

This study shows that the degree to which the mass expulsion system compares with alternate techniques depends not only on the performance of the torque producing element but to an even greater extent on the integration of this torque producing element in an overall control system. Parametric trends were established for the important parameters of the program. This study program provides the necessary analytical evaluation of the advanced control techniques. The results have furnished a valid evaluation of the "Advanced Limit Cycle Control Techniques". The necessity for developing these control methods was established as a result of the sizable propellant savings and reduction of the engine firings with the Advanced Limit Cycle Techniques.

II. INTRODUCTION

The problem of space vehicle attitude control has received much attention over the past few years. The evolution of attitude control systems, to date, has followed a course which has led to the nonoptimal design of mass expulsion control systems. The current systems leave much to be desired in terms of system weight, control circuitry, energy utilization, and actuator duty cycle. This has not caused much concern in present systems, but as the mission durations are increased and the mission requirements become more demanding, the problem of obtaining efficient, versatile, and economical attitude control systems becomes one of paramount importance.

The requirements imposed on three-axis attitude control systems are in general twofold. An extended quiescent period must be obtained in order to conserve the total energy consumed, since any mass or energy expended must be treated

as a direct burden on the payload or mission duration. However, the general satellite or spacecraft attitude control problem requires a system with more flexibility than one which simply has the ability to follow the attitude reference changes. In particular, the torque producing elements of the control system must also be capable of providing the high torque requirements needed to control stage separation transients, internal movements, maneuvering sequences, and the thrust vector errors of prime propulsion units. These varied and conflicting requirements usually lead to the design of control systems with two or more modes of operation; for example, high and low thrust reaction jets or a combination of methods such as reaction jets with reaction wheel devices. Systems which couple the mass expulsion system with other modes of control often become unduly complex and redundant. This is true, in many cases, since the mass expulsion system with the proper control circuitry is capable of handling the high torque functions while also providing a maximum quiescent period. For the sake of simplicity in logic circuitry, system weight, and reliability of the control system, it seems desirable to use only one active control mode for an entire mission, if possible.

Although mass expulsion systems with controllable impulse outputs are available, none of these units possess a proportional or linear transfer characteristic between impulse output and impulse command. The significant nonlinearity occurs near zero signal and unless compensated for (present system), makes precise attitude control impossible and/or causes excessive propellant consumption during limit cycle operation. However, the mass expulsion systems are desirable since they are capable of producing much higher, rapid response torque levels than other systems. The mass expulsion systems have, therefore, been used to provide the coarse control and momentum dumping function of attitude control. However, if damping could be provided through control techniques, this same hardware might be used to provide maximum quiescent periods. This problem is resolved by designing the control system to make use of the modulation possible with the mass expulsion systems to achieve nonlinear damping.

Much effort has been expended in obtaining methods of converging to the minimum impulse limit cycle. The "advanced limit cycle techniques" discussed herein illustrate the fact that the minimum impulse limit cycle is not the limiting design point for mass expulsion systems. By incorporating the mass expulsion system errors and nonlinearities into the control system synthesis, the minimum impulse limit cycle can be damped with the same hardware used for the acquisition phase.

The primary intention of this study was to investigate the feasibility of several proposed concepts. A great deal of thought has been devoted to the general realm of the control philosophies mentioned above. Practically all of these have been of a qualitative nature, leaving the area of quantitative analysis relatively undisturbed. One of the objectives of this study was to establish a firm foundation for an analysis of this type.

Except in a very broad sense, little has been established in the nature of design criteria and development goals for the individual components of a system such as is under consideration here. It is one of the purposes of this study to provide some usable information relative to this area. Before the design of control logic or the adoption of one control technique can be achieved, an important effect had to be considered. Thrust vector errors in one axis can give rise to accelerations in other axes. These errors could produce error rates which are of the same magnitude as the straight limit cycle driving rate. Should this be the case, there would be no justification for pursuing the advanced control techniques.

The "advanced limit cycle control techniques" which reduce the vehicle angular velocity and position to zero (or other referenced position), thereby minimizing the fuel consumption, are logical in nature, include all system errors and nonlinearities, and are inherently simple to mechanize. Other advantages resulting from tailoring the controller to the reaction jet characteristics are

1. Control circuit simplicity (Extensive acquisition phase eliminated)

2. Reduction of system weight and engine duty cycle

3. Direct velocity information not required

4. Increase in reliability

5. Minimum impulse limit cycle not the limiting design point for mass expulsion systems.

The advanced control techniques are examined herein and first order answers as to their values have been obtained. The results of this study will give direction to more sophisticated methods of analysis in the future.

III. SCOPE OF STUDY

The vehicle and control systems under consideration will be limited to those having the following characteristics:

1. The configurations of interest are illustrated in Figure 1.
2. All engines of a given configuration are of the same thrust level. The mass expulsion system which was investigated comprises a fixed thrust, pulse modulated engine in which the pulse modulation takes the form of pulse width modulation alone.
3. The vehicle polar moments of inertia of the pitch and yaw axes are equal.
4. The vehicle polar moments of inertia are constant.
5. Angular accelerations about the pitch and yaw axes which are caused by the nominal thrust level are defined as unity in any convenient dimension. Angular acceleration about the roll axis due to the same nominal thrust level is greater than unity by a factor of between one and one hundred.
6. The vehicle angular velocity is sufficiently small so that Eulerian rigid body mechanics may be neglected.
7. Disturbance torques are neglected.
8. For the parametric study, angular errors are taken to be no greater than 2 degrees, thrust variations no greater than 5% of nominal, and a steady state impulse error of not more than 10% of the command impulse.

A program was evolved which encompassed all five of the following control techniques:

1. Simple box limit cycle (Fixed impulse delivered when position band on each axis is reached.)
2. Advanced limit cycle with velocity information (Accurate position sensing)
3. Advanced limit cycle with velocity calculations (Moderate position sensing)
4. Advanced limit cycle with rate cutoff (Extremely accurate rate and position sensing)

5. Simple diamond error limit cycle with rate switching option (Fixed impulse delivered when coupled axis error signal dictates)

The simple limit cycle techniques are open loop control systems whereas the advanced limit cycle techniques are closed loop in nature and do possess damping.

In order to compare the control techniques, a selected engine and vehicle configuration will be used. This configuration and a selected control technique will be examined in terms of propellant expended and number of engine firings over an extended period of simulated space operation neglecting disturbance torques. Another control technique and/or vehicle configuration will then be substituted and the procedure will be repeated. In order to effectively analyze the control philosophies, the same initial conditions, vehicle design parameters, design thrust levels, accuracy band, etc. will be used in each corresponding control technique comparison.

IV. DESCRIPTIONS OF CONTROL TECHNIQUES

The control systems under consideration possess the general block diagram characteristics shown in the following sketch:

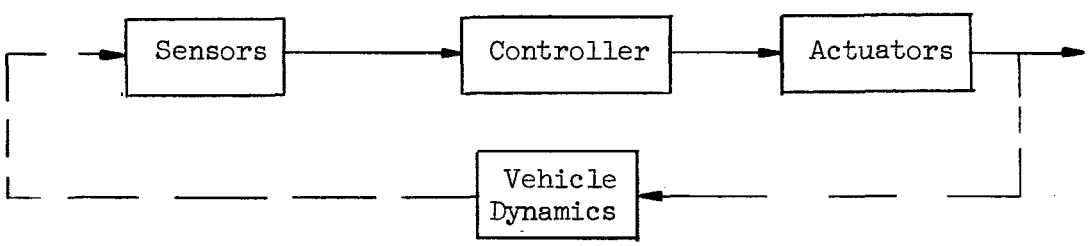

Sketch 1

The controller characteristics for each of the control techniques under consideration are presented in the following discussion.

A. Simple Box Limit Cycle

The most straightforward control mode utilizing this control system is to apply full control torque once the desired accuracy band has been reached. An on-off, single pulse control mode is used. Since natural damping forces do not accompany space missions, a typical no-error, no disturbance torque, vehicle

operation sequence is shown by the position and phase plane plots of Figures 2 and 3. No attempt is made to arrest the angular velocity but merely to limit it to a value which does not exceed that which can be reversed by the application of a minimum impulse bit. Therefore, even under ideal conditions, the vehicle angular position is expected to continually oscillate across the deadband.

In order to determine the theoretical, no-error, mean propellant requirements for this control technique, some insight must be obtained regarding the average pulsing frequency. This is required since the initial rate and disturbance torques are arbitrary in character. Constant vehicle moments of inertia will be assumed and the system dead times, time delays, and pulse widths will be considered negligible compared to the period of oscillation.

If the on-time of the reaction jet is small in comparison with the period, the average off-time of the system per period is

$$T_s = \frac{2\,\theta_s}{\left|\dot{\theta}_{s_1}\right|} + \frac{2\,\theta_s}{\left|\dot{\theta}_{s_2}\right|} \qquad (1)$$

Where the symbols are defined in Figure 3.

The frequency (f_s) is by definition

$$f_s = \frac{1}{T_s} = \frac{\left|\dot{\theta}_{s_1}\right| \left|\dot{\theta}_{s_2}\right|}{2\,\theta_s \left(\left|\dot{\theta}_{s_1}\right| + \left|\dot{\theta}_{s_2}\right|\right)} = \frac{\dot{\theta}_{s_1}\,\Delta\dot{\theta}_o - \dot{\theta}_{s_1}^{\,2}}{2\,\theta_s\,\Delta\dot{\theta}_o} \qquad (2)$$

Where

$$\left|\Delta\dot{\theta}_o\right| = \left|\dot{\theta}_{s_1}\right| + \left|\dot{\theta}_{s_2}\right|$$

Since θ_s is one-half of the total deadband angle and $\Delta\dot{\theta}_o$ is determined by the minimum impulse, the frequency is a function of the random variable (θ_{s_1}) as shown in Figure 4. The statistical mean of the frequency can thus be determined as follows:

MAC A673

Assuming the probability density function of $\dot{\theta}_{s_1}$ to be uniformly distributed between 0 and $\Delta\dot{\theta}_o$,

$$P(\dot{\theta}_{s_1}) = \frac{1}{\Delta\dot{\theta}_o} \qquad 0 \leq \dot{\theta}_{s_1} \leq \Delta\dot{\theta}_o \tag{3}$$

The probability density function of the frequency is defined as

$$P(f_s) \underline{\Delta} P(\dot{\theta}_{s_1}) \frac{d\dot{\theta}_{s_1}}{d f_s} \tag{4}$$

$$\frac{d f_s}{d\dot{\theta}_{s_1}} = \frac{\Delta\dot{\theta}_o - 2\dot{\theta}_{s_1}}{\left[2\theta_s\right]\left[\Delta\dot{\theta}_o\right]} \tag{5}$$

Therefore

$$P(f_s) = \frac{1}{\Delta\dot{\theta}_o}\left[\frac{2\dot{\theta}_s\,\Delta\dot{\theta}_o}{\Delta\dot{\theta}_o - 2\dot{\theta}_{s_1}}\right] = \frac{2\theta_s}{\Delta\dot{\theta}_o - 2\dot{\theta}_{s_1}} \tag{6}$$

The statistical mean of f_s is

$$\overline{f}_s = \int_o^{\Delta\dot{\theta}} f_s\, P(f_s)\, d f_s = \int_o^{\Delta\dot{\theta}} \frac{1}{\Delta\dot{\theta}_o} \frac{\dot{\theta}_{s_1}\Delta\dot{\theta}_o - \dot{\theta}_{s_1}^2}{2\theta_s\,\Delta\dot{\theta}_o} d\dot{\theta}_{s_1} \tag{7}$$

Since Equation (7) describes the frequency of oscillation of the vehicle, the pulsing frequency is twice this value, or

$$f_s' = 2 f_s = \frac{\Delta\dot{\theta}_o}{6\theta_s} \tag{8}$$

MAC A673

The mean propellant consumption is the propellant-used-per-pulse multiplied by the average pulsing frequency. Thus,

$$\bar{\dot{\omega}}_p = \frac{\omega_p}{2} f_s, \tag{9}$$

Making the proper substitutions,

$$\dot{\omega}_p = \frac{\Delta\dot{\theta}_o I}{I_{sp} L} \frac{\Delta\dot{\theta}_o}{6\,\theta_s} = \frac{\Delta\dot{\theta}_o^2 I}{6\, I_{sp} L\, \theta_s} \tag{10}$$

Substituting for $\Delta\dot{\theta}_o$, the mean propellant consumption per axis is

$$\bar{\dot{\omega}}_p = \frac{I_T^2 L}{3\,\theta_s I I_{sp}} \tag{11}$$

for four engines (coupled configuration)

or

$$\bar{\dot{\omega}}_p = \frac{I_T^2 L}{12\,\theta_s I I_{sp}} \tag{11a}$$

for two engines (uncoupled configuration)

B. Advanced Limit Cycle with Velocity Information

It has been shown that the simple limit cycle method does not include damping. Adding damping to the system is one method by which system improvement can be achieved. The problem of improving the straight limit cycle performance involves defining the means of adding damping to the system. The method of system improvement is to reduce the total system mass and to improve the rocket engine duty cycle. The total system mass includes fixed and expendable components. The fixed mass includes the hardware items and the expendable mass is the propellant.

MAC A673

Mass expenditure is the critical component for long term missions and the criterion for reducing the total system mass will be the minimization of the propellant consumption. The criterion used to improve the rocket engine duty cycle requires the minimization of the number of rocket engine firings and duration of each firing.

The optimization criteria for controller design will therefore be the minimization of the number of pulses and the reduction of propellant consumption. The approach employed in this technique involves the application of two pulses in the correction of any angular deviation. Two pulses are a minimum, since one pulse can effectively null only the rate whereas two pulses are required to also null the position. In order to minimize propellant consumption, the second pulse will be a fixed pulse equal to the minimum impulse bit which the engine can accurately and repeatably produce. The first pulse will then vary depending on the initial entering rate and will establish a fixed rate after the pulse firing. The minimum impulse bit will define this fixed leaving rate of the first pulse. Also, the first impulse bit is not determined since it must be of a magnitude sufficient to null the entering rate and produce a minimum leaving rate which the second pulse can null. This will now be shown.

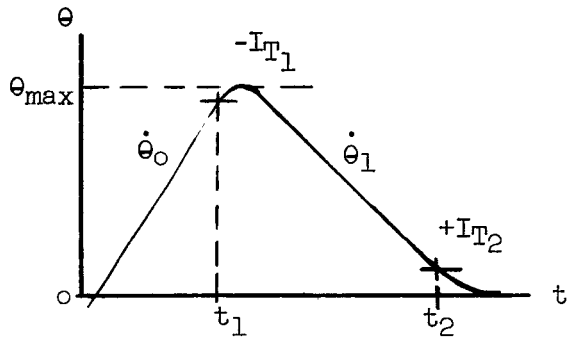

Sketch 2

Where

t_1 = Firing of first pulse

t_2 = Firing of second pulse

$$\ddot{\theta} = \frac{\sum T_y}{I_y} \tag{12}$$

$$\frac{d\dot{\theta}}{dt} = \frac{\sum T_y}{I_y} \tag{13}$$

$$\Delta\dot{\theta} = \int_{t_1}^{t} \frac{\sum T_y}{I_y} \, dt \tag{14}$$

MAC A673

The analyses are further simplified because the effects of disturbance torques are neglected. The rocket engine thrust cannot be taken as a constant with time even though a constant level is commanded from the controller since the rocket system nonlinearities result in an oscillatory thrust output. This will affect the resulting rate and position versus time which is shown in Equation (14) and expressed as

$$\Delta\dot{\theta} = \frac{L}{I_y} \int_{t_1}^{t} F \, dt \tag{15}$$

$$\int_{t_1}^{t_1'} F \, dt \triangleq I_{T_1} \tag{16}$$

Where $t_1' - t_1$ = Pulse width

The defining equation for the first pulse case is

$$\dot{\theta}_1 = -\frac{L \, I_{T_1}}{I_{y_1}} + \dot{\theta}_o \tag{17}$$

Where the sign convention is defined in Figure 2.

The defining equation for the second pulse case is

$$\dot{\theta}_2 = \frac{L \, I_{T_2}}{I_{y_2}} + \dot{\theta}_1 \tag{18}$$

which reduces to

$$\dot{\theta}_1 = -\frac{L \, I_{T_2}}{I_{T_2}} \tag{19}$$

TMC A673

since by definition it is desired to null the rate after the second pulse firing ($\dot{\theta}_2 = 0$). Equation (19) fixes the rate after the first pulse firing and Equation (17) now becomes

$$\frac{L\, I_{T_1}}{I_{y_1}} = \dot{\theta}_o + \frac{L\, I_{T_2}}{I_{y_2}} \tag{20}$$

Since the criterium for minimum propellant consumption dictates that the second pulse should be the minimum impulse bit which the engine can accurately and repeatedly product, Equation (20) becomes

$$\frac{L\, I_{T_1}}{I_{y_1}} = \dot{\theta}_o + \frac{L\, I_{T_{min}}}{I_{y_2}} \tag{21}$$

A constant moment of inertia between the pulse firings of one control cycle is assumed which dictates that the internal mass and equipment remain relatively fixed during this time period. Therefore, $I_{y_1} = I_{y_2}$ and Equation (21) becomes

$$I_{T_1} = K_1 \dot{\theta}_o + I_{T_{min}} \tag{22}$$

$$K_1 = \frac{I_y}{L}$$

The total stored energy to be expended at each pulse is therefore defined.

The diagram and time derivation presented below illustrate the timing or engine firing criteria.

TMC A 673

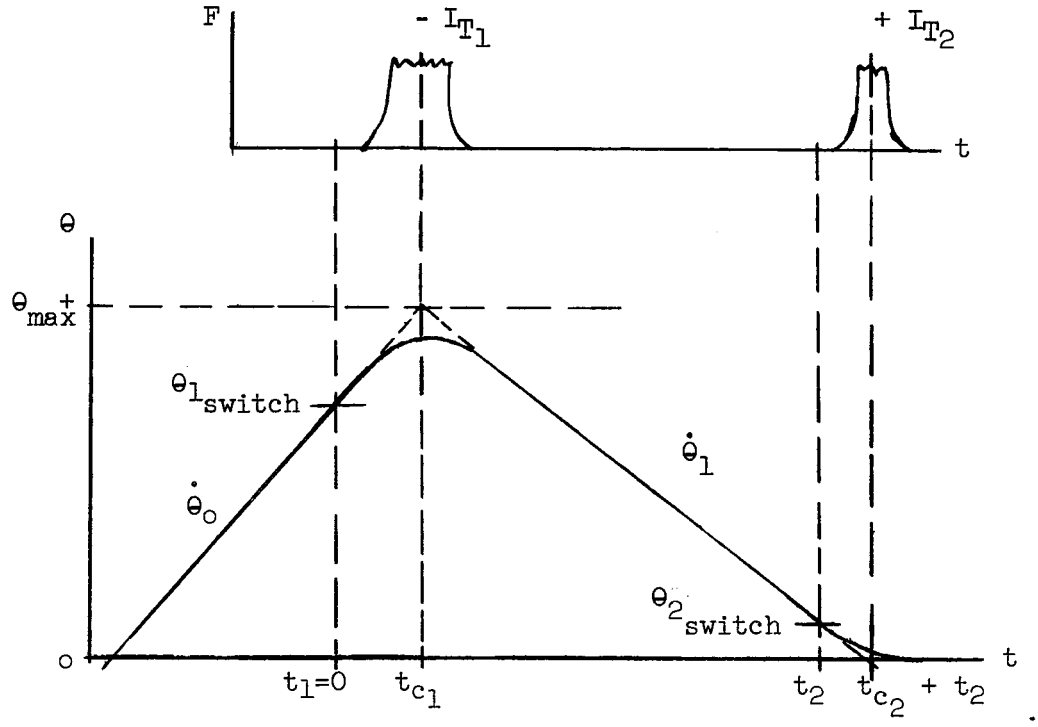

Sketch 3

Where

t_{c_1} and t_{c_2} = The centroid of the individual pulses from electrical signal on time

t_1 and t_2 = Electrical signal on time

The θ_1 switch line can be determined as a function of the mission accuracy requirements and initial rate. Once the θ_1 switch line has been selected, the θ_2 switch line can be determined. However, the use of the θ_2 switch line does not lead to a practical system since errors are introduced due to the position sensor threshold. Therefore, the second pulse will be fired as a function of time rather than position. From the Sketch 3 above,

TMC A673

$$\theta_{max}^{+} = \dot{\theta}_1 (t_{c_2} + t_2 - t_{c_1}) \tag{23}$$

Also

$$\theta_{max}^{+} = \theta_{1_{switch}} + \dot{\theta}_o \, t_{c_1} \tag{24}$$

When $\pm \theta_{max}^{+}$ is assumed to represent the mission position accuracy requirements, Equation (24) is used to determine the θ_1 switch line as a function of initial rate and the pulse centroid. Although θ_{max}^{+} does not represent the actual maximum position reached in the vehicle travel, it does allow a minor degree of conservatism.

The timing of the second pulse firing can now be obtained by combining Equations (23) and (24) as shown below.

$$t_2 = \frac{\theta_{1_{switch}} + \dot{\theta}_o \, t_{c_1}}{\theta_1} + t_{c_1} - t_{c_2} \tag{25}$$

Substituting Equation (19) yields

$$t_2 = \frac{K_1}{I T_{min}} (\theta_{1_{switch}} + \dot{\theta}_o \, t_{c_1}) + t_{c_1} - t_{c_2} \tag{26}$$

C. Advanced Limit Cycle with Velocity Calculations

This method presents an alternate technique which utilizes the control technique to obtain the rate within the accuracy band. A vehicle angular position sensing device with appropriate circuitry is combined into a system which produces a cycle of three pulses firing in alternating directions, the last of which is intended to reduce the angular velocity to zero without the use of angular rate sensors. The average drift velocity during the time between the first and second pulses of the series is obtained by a measure of the elapsed time between these pulses and from a knowledge of the magnitude of the nominal angular position deadband. This information is processed by the system intelligence to

establish the magnitude of the second pulse. The magnitude of the second pulse is such that the difference between it and the third pulse corresponds to an angular velocity increment equal to the average vehicle drift velocity mentioned above. The effect of the second and third pulses combined is to cancel the vehicle angular velocity which exists prior to the second pulse. The third pulse is timed so as to arrest the vehicle velocity at the zero angular position in order to maximize the average time required for the vehicle to drift out of the deadband. The functioning of the advanced limit cycle may be understood more clearly when a typical sequence of operation is followed. Such a typical sequence is shown as follows:

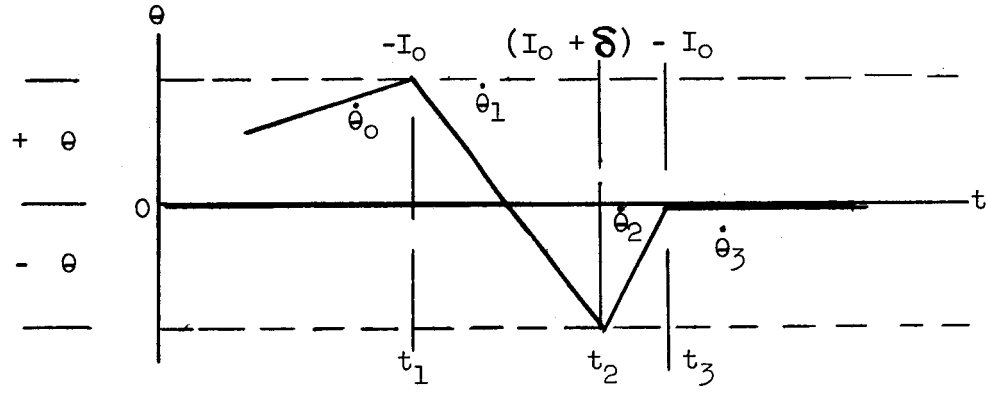

Sketch 4

Prior to the time t_1, the vehicle angular position is drifting with velocity $\dot{\theta}_o$. When the angle $\Delta\theta$ (deadband limit) is reached, the system intelligence calls for a minimum impulse pulse to return the vehicle to its deadband. At time t_2, the vehicle has crossed to the other side of the deadband. The system intelligence measures the elapsed time since the previous pulse and computes the average drift velocity to be $2\Delta\theta/(t_2 - t_1)$. Now if the pulse delivered to the system at the time t_2 were equal in magnitude to that delivered at time t_1, the resulting angular velocity ($\dot{\theta}_2$) would be equal to $\dot{\theta}_o$. In this case, the system would follow the simple limit cycle procedure and would repeat angular velocities after every pair of pulses. However, the system intelligence calls for a pulse which is greater than the minimum repeatable pulse by an amount corresponding to the initial angular velocity ($\dot{\theta}_o$). Therefore, the net result of the first two pulses is to leave a residual velocity ($\dot{\theta}_2$) which corresponds to that of the minimum repeatable pulse. This residual velocity is removed at time t_3 by the application of a minimum pulse. Since the theoretical value of $\dot{\theta}_2$ does not vary from one cycle to another, the time interval ($t_3 - t_2$) is fixed so that the vehicle is at its zero angular position when its angular velocity is arrested.

TMC A673

D. Advanced Limit Cycle with Rate Cutoff

This technique is quite similar to the technique discussed in Section IV-B. The difference arises in the fact that the present method assumes an accurate continuous rate sensor. This sensor is used to provide rate information near zero rate to cut off the final pulse phase of the sequence. The impulse delivered after the electrical signal off is such that it will drive the vehicle to zero rate. This method fires the last pulse not as a function of time but rather when the position sensor switches sign (zero angular position). Therefore this system does not have the integrated effects of system errors which plague the other methods. The only gross errors with this method are the error associated with the impulse bit after electrical off signal and the sensor error.

E. Simple Diamond Error Limit Cycle (Rate Switching Option)

The "Diamond Error Matrix" configurations are as follows:

1. 6-unit configuration with the yaw and roll axes coupled

2. 8-unit configuration with the yaw and roll axes coupled and an independent pitch axis (identical to configuration 1 except a pure couple for the pitch axis is activated rather than a single engine)

3. 8-unit configuration with both the yaw-roll and pitch-roll planes simulated as diamond error matrices. Although this is a possibility, it was not investigated in the computer program.

Since two (or more) axes are coupled in the "Diamond Error Matrix", it is designed to have single engine firings to correct for errors in both axes. For example, if a combined error command in (+) yaw and (+) roll has exceeded the diamond error band, the appropriate engine (Engine 53 in Figure 5) will be fired. In the special cases in which two or three error bands are crossed simultaneously, the computer printout will indicate all engines fired.

The "Diamond Error Matrix" for the yaw-roll axes in the 6-unit configuration is shown in Figure 5. Also shown in Figure 5 are the designated engines to be fired for the indicated error signals. The single axis errors are defined as

$$\text{Yaw} \quad -- \quad \epsilon_Y = a_1 \theta_Y + b_1 \dot{\theta}_Y \tag{27}$$

$$\text{Roll} \quad -- \quad \epsilon_R = a_2 \theta_R + b_2 \dot{\theta}_R \tag{28}$$

$$\text{Pitch} \quad -- \quad \epsilon_P = a_3 \theta_P + b_3 \dot{\theta}_P \tag{29}$$

TMC A 673

The equations describing the linear combination of yaw and roll error command band, along with the engine to be fired when this error band is exceeded, are as follows

Equation	Fire Engine (N)
$\frac{\epsilon_Y}{\epsilon_{Y_{max}}} + \frac{\epsilon_R}{\epsilon_{R_{max}}} - 1 = 0$	53
$\frac{\epsilon_Y}{\epsilon_{Y_{max}}} - \frac{\epsilon_R}{\epsilon_{R_{max}}} - 1 = 0$	63
$\frac{\epsilon_Y}{\epsilon_{Y_{max}}} + \frac{\epsilon_R}{\epsilon_{R_{max}}} + 1 = 0$	54
$\frac{\epsilon_Y}{\epsilon_{Y_{max}}} - \frac{\epsilon_R}{\epsilon_{R_{max}}} - 1 = 0$	64

Associated with these error bands are special or unique cases in which two of the error limit equations intersect. Since these points occur when either the yaw or roll error is zero, a pure "couple"is necessary to drive the system back into its allowable error band.

The pitch error deadband in the 6-unit case is a straight deadband and is identical to the previously described simple box system with the exception of the addition of a rate dependent error contribution.

The 8-unit error command band configurations are shown in Figure 6. It can be seen in Figure 6 that the Type 1, 8-unit, configuration is identical to that shown in the 6-unit configuration with the exception that in the pitch axis error band, a pure couple is fired rather than a single engine. The Type 2, 8-unit, configuration mixes the error signals of both the yaw-roll and pitch-roll axes in obtaining the intelligence necessary to fire the appropriate engine(s).

The equations describing the linear combination of pitch and roll error command band along with the engine to be fired when this error band is exceeded are as follows:

Equation	Fire Engine (N)
$\frac{\epsilon_P}{\epsilon_{P_{max}}} + \frac{\epsilon_R}{\epsilon_{R_{max}}} - 1 = 0$	36
$\frac{\epsilon_P}{\epsilon_{P_{max}}} - \frac{\epsilon_R}{\epsilon_{R_{max}}} - 1 = 0$	46
$\frac{\epsilon_P}{\epsilon_{P_{max}}} + \frac{\epsilon_R}{\epsilon_{R_{max}}} + 1 = 0$	35
$\frac{\epsilon_P}{\epsilon_{P_{max}}} - \frac{\epsilon_R}{\epsilon_{R_{max}}} - 1 = 0$	45

This is the most complex (controller or computer circuitry) of the control techniques investigated to this time. However, the computer logic is basically an extension of the uncoupled pitch-roll configurations except for additional special cases. In all instances in which two or three error limits are reached simultaneously, the control or computer logic will be such to command the minimum number of engines necessary for corrective action. Computer runs were made to determine the effect of biasing the switching logic as a function of the rate as well as position. With the addition of rate switching, it becomes more realistic to include a firing delay time, since a rate change by itself may be enough to exceed another error band.

V. THRUST VECTOR AND IMPULSE ERRORS

It is evident that in the absence of outside torques, the vehicle angular velocity would be reduced to zero after the first cycling of an ideal damped, advanced limit cycle system. However, in the case of real systems which inherently contain errors, the mean time between cycling is finite. In the discussion which follows, the errors are determined which were used in the computer program to establish quantitative relationships between the system errors and the pulsing frequency or mean propellant consumption.

Errors are known to exist in thrust magnitude, pointing direction, and pulse widths. Some of these errors may be associated with a particular system or unit such as mounting or installation errors. These errors are fixed throughout the history of the unit in question, but they may vary from one system to another. Other system errors may be assumed to be time dependent. In the general case, the total error is due to errors of both kinds. Since the important factor to be considered in thrusting errors is the error of total impulse delivered about each control axis, the pulse width errors are included at the same time as the thrust magnitude and orientation errors. The errors are a function of thrust level and pulse width. The parameters of interest include

1. Total impulse per pulse errors
2. Steady state thrust level variations
3. Time from electrical on signal to
   a. Start of valve travel
   b. 90 percent full thrust
   c. Centroid of pulse
   d. Electrical signal off
   e. 90 percent full thrust on tail off
   f. End of pulse
4. Total impulse contributions due to
   a. Rise transient
   b. Steady state
   c. Decay transient
   d. Shutdown transient-after electrical signal off
5. Specific impulse variations with pulse width

The recorded pulse errors include instrumentation errors which are difficult to compensate. The instrumentation errors could be a major constituent of the recorded error especially for small pulse widths, and therefore any rigorous treatment of pulse errors should treat the instrumentation errors. The purpose of this task was to provide data which would allow more valid assumptions concerning the associated pulse errors. A more refined treatment of the pulse errors was not dictated under this contract since state of the art errors continue to change, and the treatment of the control techniques and errors were in a general form so that any range of errors and error distribution could be used in this program.

The pulse characteristics of most importance to the present study are the following:

1. Total impulse per pulse errors

2. Impulse error associated with the shutdown transient (after electrical signal off)

3. Specific impulse variations

A survey of existing data was made. The pulse errors arising from typical hypergolic bipropellant pulse rocket engines were investigated in order to better establish the statistical range and distributions of the pulse errors. The mean value of an individual parameter was not of particular concern in this task but the associated error and the nature of the error distribution have a large influence on the performance of the more sophisticated attitude control systems.

Due to the limited nature of this task only a minimum of test data could be reduced. The problem found was that although sufficient data exist to statistically determine the parameters of interest, the programs under which this data were obtained did not require error data because of the control techniques which were employed. Therefore, there is scarcity of pertinent information.

A total of 48 data points of a 66.84 Newton bipropellant thruster were considered. These points are divided between two groups of pulse width commands of 10 and 12 milliseconds. Each group was analyzed separately.

The group associated with the 10 millisecond command contained 20 data points. The mean value of these points is given as

$$\bar{X} = \frac{1}{N} \sum_{i=1}^{N} X_i \qquad (30)$$

where N is the number of points and X_i is the i^{th} data point. The variance is defined as the normalized second moment about the mean and is given as

$$\sigma^2 = \frac{1}{N} \sum_{i=1}^{N} (\bar{X} - X_i)^2 \qquad (31)$$

The standard deviation (σ) is simply the positive square root of the variance. For the group in question,

$$\bar{X} = 0.0725 \text{ kg-sec}$$

$$\sigma^2 = 0.000006 \text{ kg}^2\text{-sec}^2$$

$$\sigma = 0.00241 \text{ kg-sec}$$

When a small quantity of data is analyzed, it is often convenient to apply Sturges' Rule to provide a near optimum grouping for a graphical display. This is stated as

$$K = 1 + 3.3 \log_{10} N \qquad (32)$$

where K is the number of sub groups into which the N data points are divided for the display. For N = 20, K is approximately equal to five. The data points are now divided in the five groups as follows:

Group	Range	Data Points
1	$0.0667 \leq X < 0.0689$	1
2	$0.0689 \leq X < 0.0712$	6
3	$0.0712 \leq X < 0.0735$	6
4	$0.0735 \leq X < 0.0758$	5
5	$0.0758 \leq X < 0.0780$	2

This is shown as a bar graph in the sketch below. Superimposed in this sketch is a Gaussian distribution having the same variance as the population of data points under consideration.

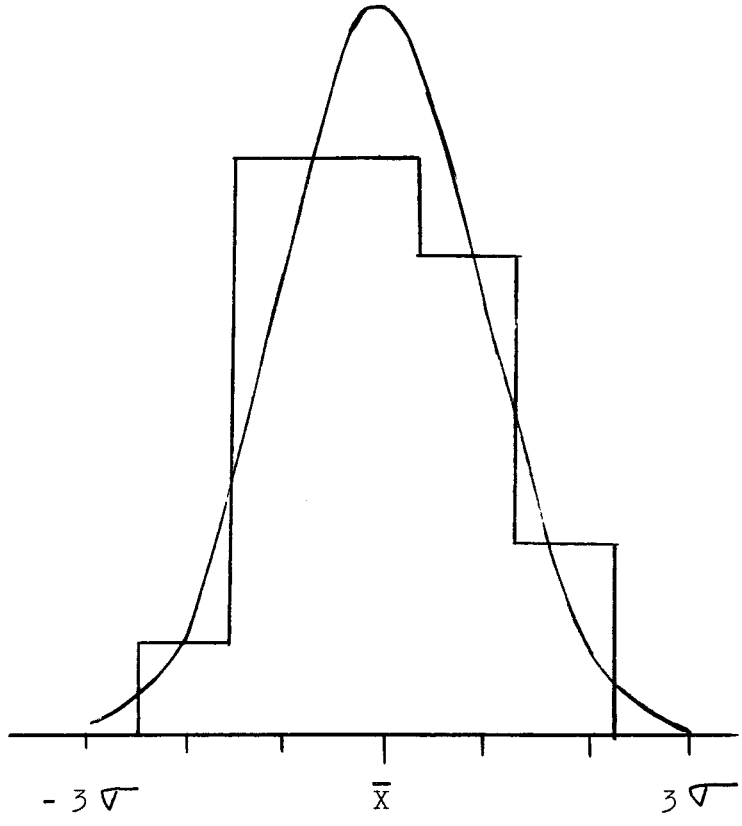

Sketch 5

Similar operations are performed on the group associated with the 12-millisecond pulse width. For this group, the following values were obtained:

$$\bar{X} = 0.08705 \text{ kg sec}$$

$$\sigma^2 = 0.00005341 \text{ kg}^2\text{-sec}^2$$

$$\sigma = 0.00731 \text{ kg-sec}$$

An application of Sturges' Rule yields approximately seven groups as shown below:

Group	Range	Data Points
1	$0.0685 \leq X < 0.0739$	1
2	$0.0739 \leq X < 0.0794$	2
3	$0.0794 \leq X < 0.0848$	8
4	$0.0848 \leq X < 0.0903$	9
5	$0.0903 \leq X < 0.0957$	4
6	$0.0957 \leq X < 0.101$	2
7	$0.101 \leq X < 0.1066$	2

These data are shown below as a bar chart with a superimposed Gaussian distribution having the same variance as the data population.

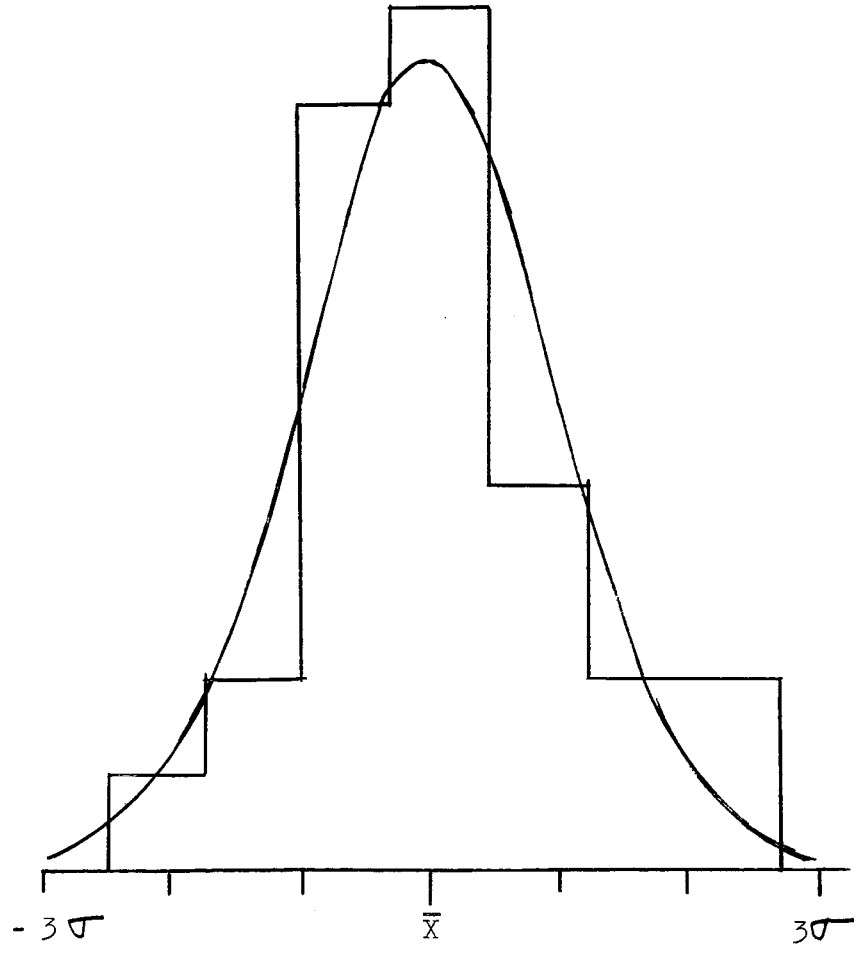

Sketch 6

TMC A673

The number of points upon which the present analysis is based is too small to provide a reasonable level of confidence. It is presented essentially to demonstrate the form of the results expected from a more extensive survey and analysis. The probability density of those errors which are time variant may be assumed to be approximately Gaussian or normal. However, any reasonable distribution may be included in the digital computer program without undue difficulty. The mechanization of the number generation to provide a specified distribution is an established routine and is discussed in Section VI-C.

A survey of immediately available rocket impulse data was also made to determine the magnitude and source (transient or steady state) of impulse errors as a function of pulse width. Approximately 100 pulses from 66.84 and 445.6 Newton nominal thrust level engines were used. Figure 7 presents the mean values of these data points for the most probable impulse error and the 3σ total impulse error. These curves are correct to within 10% for the data used.

A mean value of specific impulse as a function of pulse width was obtained from available pulse firings. This curve (shown in Figure 8) was used in the computer program. Figure 8 is based on approximately a thousand pulses of various thrust levels and it is accurate to within 8% of the data used. There is a heavy dependency on the engine and injector design. The engine could be designed for good steady state performance in which case the shorter pulse performance would be degraded or vice versa.

Another source of error is attributed to the effects of finite or nonidealized thrusting. The thrusting on-time may safely be considered to be short compared with the mean time between pulses so the assumption was made that the thrust duration is effectively zero and all errors exist simultaneously.

Since the impulse bits were delivered as Dirac delta functions or impulses, the results are suspect when finite thrusting is considered. However the effects of finite thrusting are predictable and may be compensated for by system intelligence and do not affect the results of the present computer program as long as Δt firing $\leq \Delta t$ 1/2 total deadband in the worst case. These statements require proof before their validity is accepted.

Finite thrusting will affect the time at which the thrust should be applied and also the trajectory of position versus time. Since these factors affect the residual rate after the final pulse firing of any control cycle, the nonlinearities must be considered. The residual rate is the determining factor in a performance evaluation of the damped limit cycle control technique. The purpose of the following analysis is to obtain a convenient method of analyzing the control techniques with the associated nonlinearities accounted for.

A method ideally suited to this problem is available. This method allows all the nonlinear aspects of the system to be easily evaluated, and the system errors to be lumped into two convenient parameters defined by experimental

data. The method, first investigated by R. W. Adlhoch, simplifies the problem of analyzing, understanding, and using the control techniques. The correct characteristics are obtained before and after the pulse firing, but information is not obtained during the thrusting phase. The motion imparted to the vehicle during a finite pulse firing is shown to be exactly that which would result from an impulse of zero duration and total impulse equal to $\int_{t_1}^{t_1'} F dt$ applied at the centroidal coordinate of the area under the thrust versus time curve.

A general curve of rate versus time would resemble that shown below:

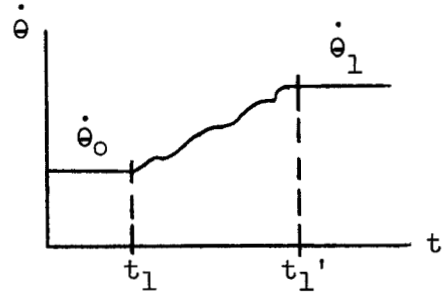

Sketch 7

Equation (15) shows that the angular rate can be expressed as the following function of time:

$$\dot{\theta} - \dot{\theta}_o = \frac{1}{K_1} \int_{t_1}^{t} F dt \tag{33}$$

Where $K_1 = I/L$

$$\frac{d\theta}{dt} = \dot{\theta}_o + \frac{1}{K_1} \int_{t_1}^{t} F dt \tag{34}$$

$$\int_{t_1}^{t} d\theta = \dot{\theta}_o \int_{t_1}^{t} dt + \int_{t_1}^{t} \left\{ \frac{1}{K_1} \int_{t_1}^{t} F dt \right\} dt \tag{35}$$

$$\theta(t) - \theta(t_1) = \dot{\theta}_o (t - t_1) + \frac{1}{K_1} \int_{t_1}^{t} \int_{t_1}^{t} F d\gamma\, dt \tag{36}$$

TMC A673

Prior to thrusting, the vehicle will have a constant rate in the absence of disturbance torques, and the position is defined as

$$\theta = \theta_o + \dot{\theta}_o \, (t - t_1) \qquad t \leq t \tag{37}$$

After the pulse firing, the vehicle will have a rate described by

$$\theta = \theta_o + \dot{\theta}_o \, (t - t_o) + \frac{1}{K_1} \int_{t_1}^{t} \int_{t_1}^{t} F \, d\tau \, dt \qquad t \geq t_1' \tag{38}$$

The double integral can be written as

$$\frac{1}{K_1} \int_{t_1}^{t} \int_{t_1}^{t} F \, d\tau \, dt = \frac{1}{K_1} \int_{t_1}^{t_1'} \int_{t_1}^{t} F \, d\tau \, dt + \frac{1}{K_1} \int_{t_1'}^{t} \int_{t_1}^{t_1'} F \, d\tau \, dt \qquad t \geq t_1' \tag{39}$$

and since

$$\int_{t_1}^{t_1'} F dt = I_T$$

$$\int_{t_1}^{t} \int_{t_1}^{t} F \, d\tau \, dt = \int_{t_1}^{t_1'} \int_{t_1}^{t} F \, d\tau \, dt + \int_{t_1'}^{t} I_T \, dt \tag{40}$$

Since the energy is expended by t_1', I_T becomes a constant in the second integral.

$$\int_{t_1}^{t} \int_{t_1}^{t} F \, d\tau \, dt = \int_{t_1}^{t_1'} \int_{t_1}^{t} F \, d\tau \, dt + I_T \, (t - t_1') \tag{41}$$

TMC 6673

Combination of Equations (38) and (41) yields

$$\theta = \theta_o + \dot{\theta}_o (t - t_o) + \frac{1}{K_1} \int_{t_1}^{t_1'} \int_{t_1}^{t_1'} F \, d\tau \, dt + \frac{1}{K_1} I_T (t - t_1') \quad (42)$$

which describes θ as a function of time for the period $t \geq t_1'$.

The motion of the vehicle is now described for $t \leq t_1$ (Equation (37)) and for $t \geq t_1'$ Equation (42)). The value of t is now sought which makes these two equations equal when the lines are extended into the region $t_1 \leq t \leq t_1'$. This is shown below.

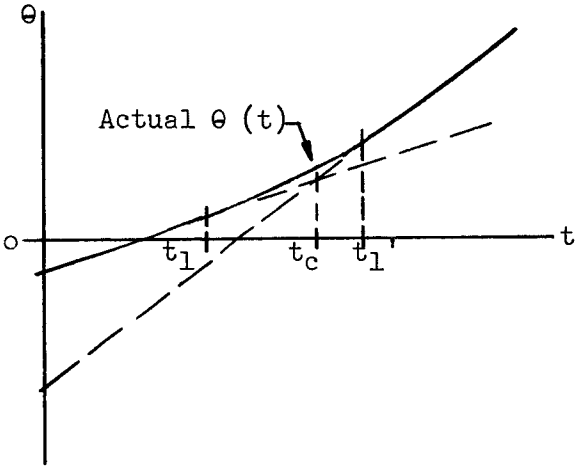

Sketch 8

The point at which these two lines cross is described by

$$\theta_o + \dot{\theta}_o (t - t_o) = \theta_o + \dot{\theta}_o (t - t_o) + \frac{1}{K_1} \int_{t_1}^{t_1'} \int_{t_1}^{t} F d\tau dt + \frac{1}{K_1} I_T (t - t_1) \quad (43)$$

which reduces to

$$\int_{t_1}^{t_1'} \int_{t_1}^{t} F \, d\tau \, dt = - I_T (t - t_1') \quad (44)$$

TMC 6-63

or

$$t = t_c = -\frac{1}{I_T} \int_{t_1}^{t_1'} \int_{t_1}^{t} F \, d\tau \, dt + t_1' \tag{45}$$

Now consider

$$\int_{t_1}^{t_1'} \int_{t_1}^{t} F \, d\tau \, dt$$

set

$$\int_{t_1}^{t} F \, d\tau = I(t) \tag{46}$$

The integral

$$\int_{t_1}^{t_1'} \int_{t_1}^{t} F \, d\tau \, dt = \int_{t_1}^{t_1'} I(t) \, dt$$

may be integrated by parts to yield

$$\int_{t_1}^{t_1'} I(t) \, dt = t \, I(t) \Big|_{t_1}^{t_1'} - \int_{t_1}^{t_1'} t \left\{ \frac{d}{dt} I(t) \right\} dt \tag{47}$$

now

$$t \, I(t) \Big|_{t_1}^{t_1'} = t_1 = \int_{t_1}^{t_1'} F \, d\tau - t_1 \int_{t_1}^{t_1} F \, d\tau = t_1' \, I_T \tag{48}$$

and

$$\frac{d}{dt} I(t) = \frac{d}{dt} \int_{t_1}^{t} F \, d\tau = F(t) \tag{49}$$

TMC A 673

Substituting Equations (48) and (49) into Equation (47) yields

$$\int_{t_1}^{t_1'} \int_{t_1}^{t} F \, d\tau \, dt = t_1' \, I_T - \int_{t_1}^{t_1'} t \, F(t) \, dt \tag{50}$$

and

$$\frac{1}{I_T} \int_{t_1}^{t_1'} \int_{t_1}^{t} F \, d\tau \, dt = t_1' - \frac{1}{I_T} \int_{t_1}^{t_1'} t \, F(t) \, dt \tag{51}$$

However, the last term in this expression can be recognized as the centroidal coordinate of the area under the thrust versus time trace when put in the form

$$\frac{1}{I_T} \int_{t_1}^{t_1'} t \, F(t) \, dt = \frac{\int_{t_1}^{t_1'} t \, F(t) \, dt}{\int_{t_1}^{t_1'} F(t) \, dt} \triangleq \bar{F}(t) \tag{52}$$

Re-examination of Equation (45) in light of the above yields

$$t_c = -t_1' + \bar{F}(t) + t_1' \tag{53}$$

or

$$t_c = \bar{F}(t) \tag{54}$$

Therefore, the point at which these lines cross is exactly the centroidal coordinate (t_c) of the area under the thrust versus time trace for a constant moment of inertia system. This can be interpreted in terms of vehicle motion

TMC A 673

to imply that, if an impulse bit equal to $\int_{t_1}^{t} F dt$ was applied at t_c, it would impart the same motion as that imparted during the finite pulse (F (t)) except for the region $t_1 < t < t_1'$. Since the present program is not interested in this region and only interested in the fact that the total time or time and position of the next pulse firing remain valid, the effects of finite pulse firing need not be considered as long as Δ t firing $\leq \Delta$t 1/2 total deadband (in the worst case).

VI. DESCRIPTION OF COMPUTER PROGRAM

A. General Considerations

The nature of this study lends itself well to general computer methods. Since the time history of any individual cycling sequence may be described by a series of linear algebraic expressions whose coefficients contain random errors, digital computer methods are particularly well suited. The inherent nonlinearities and discontinuities which plague the purely analytical methods are no cause for concern in digital methods. A basic flow chart for the general digital computer program is shown in Figure 9.

The input information required for the computer program consists of the following groups of data:

1. Initial Conditions.- Angular position and rates, time, pulses, propellant, standard deviation of normal distribution, epsilon or error coefficients, position-deadband, and installation angular errors

2. Vehicle parameters.- Moment arms, moments of inertia, minimum impulse bit, and configuration of interest

3. Control system parameters.- Control system of interest, rate sensor errors for System 4, and constants for amplifying the position and rate feedback information for all systems

4. General information.- W_p vs. I_T curve for the thrust levels of interest, delay times of firing additional corrective pulses when the control band has been exceeded, and the nature and amount of printout information desired

Initial conditions were determined which will allow some degree of parameterization.

TMC A673

The current output format is not optimum from a standpoint of data handling; it is primarily designed to facilitate program monitoring. The output may be modified to a more desirable form without difficulty. It is anticipated that as a result of the early runs, the need for particular forms of output data not originally provided for will suggest itself, therefore requiring a format change for this reason alone. The final printout format includes the following parameters:

1. Total mission time elapsed
2. Indication of engine or engines fired
3. Number of engines fired
4. Total propellant for engines fired
5. Propellant consumption rate for engines fired
6. Total number of firings per engine
7. Angular position and rate for each axis
8. Impulse bit commanded for engines fired
9. Impulse bit delivered per axis with polarity

If desired, the program may include a subroutine to generate statistical information. This would include a frequency distribution of mean time between cycling, propellant consumption, or other system variables. In this way, a realistic measure of worst case conditions and the probability of their occurrance may be directly obtained. The following description of the general program will trace through the numbered operations of Figure 9.

1. The function of this operation is to print out the parameters of interest.

2. This operation will determine the time of the next firing for each axis of the control technique employed. The angular errors and drift rates for each of the three vehicle axes following a pulse in any axis are employed in this operation. For each system, there exists a functional relationship involving angular error and drift rate which defines the time of the next pulse firing. In the case of the simple limit cycle, for example, whenever the angular deadband is reached, a pulse is fired. The required time lapse from the previous pulse to the following one is calculated for each axis by employing the functional relationship mentioned above. These three drift times are also stored in this operation.

3. The three drift times from the previous operation are compared to determine the lowest value. This value is passed to the next operation, and the remaining two are passed to a storage location. The axis associated with this particular time is also selected.

4. The angular errors for the next pulse replace those of the last pulse.

5. According to the operational philosophy in effect, the total impulse of the next pulse for the selected axis is calculated. The magnitude of this pulse is a function of the axis which is activated, the numerical order of the pulse is its sequence and, in some cases, the previous pulsing history. All required inputs are supplied from appropriate sources within the program. This operation calculates the pulse width for a given fixed thrust level engine. This pulse width combined with a thrust level represents the nominal or ideal impulse bit.

6. The output of Operation 3 is the total impulse value required for ideal system performance. The present operation introduces errors to the system. Particular errors, for example, will be obtained from a random number generator used in conjunction with a normal distribution curve. The system errors are discussed in another part of this report.

7. Following the pulse, the system dynamics are changed primarily in the axis being controlled. These changes are calculated during this operation.

8. Due to thrust misalignment, the two inactive axes also experience dynamic changes. These changes are calculated during this operation.

9. The outputs of Operations 7 and 8 are used to compute the previous inputs to Operation 1 which have not yet been altered. All variables for the next pulse have now been evaluated.

The computer program to simulate the behavior of the attitude control systems in question is built around a structure of a fundamental "driver program". This driver program provides the basic logic to direct the various activities and establish the proper sequencing of events throughout the simulation. The detail functioning of the simulation takes place in the various subroutines such as the random number generating routine and the routine which handles the evaluation of the system dynamics together with the system and impulse errors.

The program is constructed to provide torque impulses in the proper sense when appropriate conditions are met. These conditions are determined by the particular operating philosophy in force and the order of that impulse in the firing sequence. For example, the firing criteria for the advanced limit cycle with velocity calculations are given below:

Pulse No.	Magnitude	When to Fire	Time
1	I_o	$\lvert\theta\rvert = \Delta\theta$	t_1
2	$I_o + \frac{2J}{r}\left(\frac{\Delta\theta}{t_2 - t_1}\right)$	$\lvert\theta\rvert = \Delta\theta$	t_2
3	I_o	$t_2 + \frac{J\Delta\theta}{r I_o}$	t_3

In addition to the firing criteria shown above, several other constraints are placed upon the systems operation. These concern themselves with unlikely but entirely possible situations such as a compounding of errors in such a way that at some point a single pulse is unable to execute its proper function and the vehicle angular position drifts beyond its limits. In this case, sufficient additional pulses are fired in the proper sense to return the vehicle to its deadband and the cycling sequence is again initiated. Other system safeguards concern themselves with simultaneous pulsing in two or more axes. The program is so constructed to avoid confusion at such times.

When a torque impulse is delivered to any particular axis, the ideal impulse is modified to contain both random and bias errors in all three vehicle axes simultaneously. These delivered impulses are then applied to the system dynamics to produce angular velocity changes about all applicable vehicle axes. This operation is discussed more thoroughly in the following section.

B. System Errors and Dynamics

The subroutine of the digital computer program containing the errors and dynamics is described as follows: For each commanded impulse of each engine configuration there are three linear algebraic equations, one for the active axis and one each for the two passive axes. A block of three equations is reserved for each couple or single engine firing possible under any of the control philosophies.

TMC 673

Due to the large number of combinations of specified system configurations, control philosophies, and individual component bias errors, the operation of the computer program under development can be very prone to human operator error. For this reason, a convenient method of parameter identification has been evolved which minimizes errors of the above-mentioned type.

The vector and numbering convention used is shown in the following diagram where the numbers indicate both positive and negative directions of each of the three axes. Positive rotation is shown in the diagram according to the right-hand rule.

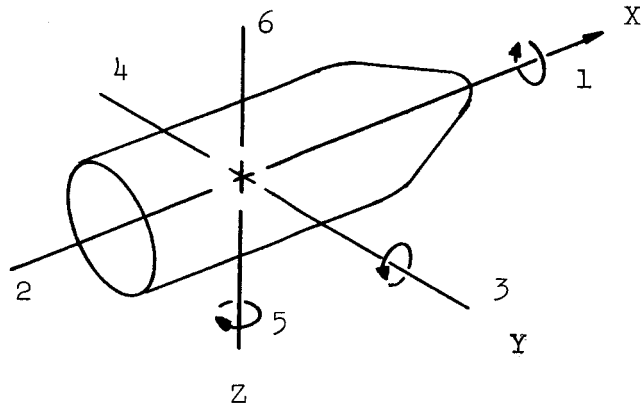

Sketch 9

Designation of system errors is accomplished by means of a triple subscript on the quantities in question. The first digit of the subscript denotes the axis from which the engine stems. The second digit denotes the direction in which the engine is pointing, and the third denotes the direction in which the positive direction of the error vector points. The engine numbering system is illustrated in Figure 1.

As a typical example, the 6-unit configuration given a positive yaw command is shown in the following illustration where I_o represents the commanded impulse, β the biased or fixed error, and ϵ the random error.

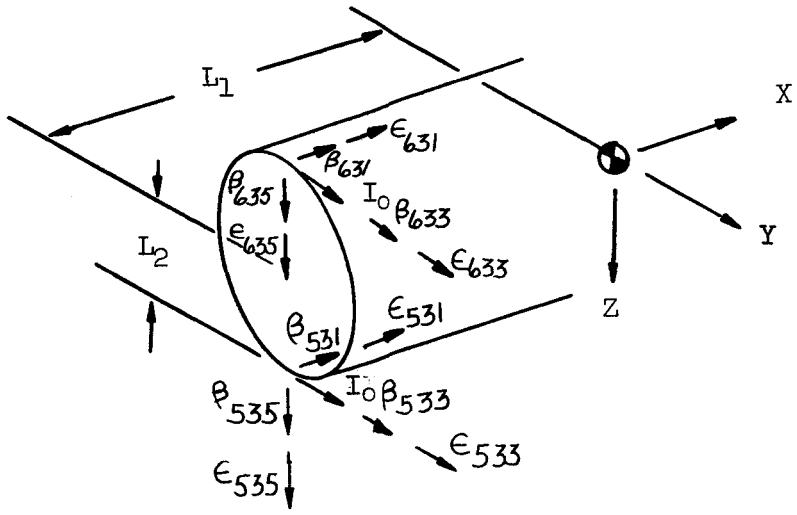

Sketch 10

The vector sum of the ϵ's therefore represents the total random error due to such factors as unsymmetric combustion, command error, etc. Similarly the vector sum of the β's represents the total fixed error due to engine attachment misalignment and machining errors.

In general, a pair of engines designated to provide a torque impulse about one axis also torques the other two axes to the extent of its out of plane errors. This situation necessitates the use of the six "blocks" of three equations mentioned previously. The role of each of these blocks is best shown by example. For the engine configuration shown in the previous illustration and with a positive roll command, the appropriate block is as follows:

$$\dot{\Delta\theta}_R = I_o L_2 \,(2 + \epsilon_{644} + \beta_{644} + \epsilon_{533} + \beta_{533})/J_R$$

$$\Delta\theta_P = I_o L_2 \,(\epsilon_{641} + \beta_{641} - \epsilon_{531} - \beta_{531}) + I_o L_1 \,(-\epsilon_{645} - \beta_{645} - \epsilon_{535} - \beta_{535}) \;/J_P$$

$$\Delta\theta_Y = I_o L_1 \,(\epsilon_{533} + \beta_{533} - \epsilon_{644} - \beta_{644})/J_Y$$

The biased errors (β) in the above expressions are introduced into the program as input data, that is to say, the values are assigned before executing

TMC A673

a program run. The random errors (ϵ), on the other hand, are introduced into the program by the random number subroutine as each error is called for in the program execution. The random errors (ϵ) are determined by the following equations:

$$\epsilon_{ijk} = \frac{(\text{2nd } \epsilon_{coef})(\text{1st } \epsilon_{coef})}{\sigma_1 \ \sigma_2} R_1 R_2 + (1 - \text{2nd } \epsilon_{coef} \frac{I_T}{I_o} \frac{\text{1st } \epsilon_{coef}}{\sigma_1 \ \sigma_2} R_1 R_2$$

$$\epsilon_{ijj} = \text{3rd } \epsilon_{coef} \frac{(\text{2nd } \epsilon_{coef})(\text{1st } \epsilon_{coef})}{\sigma_1 \ \sigma_2} R_1 R_2 + (1 - \text{2nd } \epsilon_{coef}) \frac{I_T}{I_o} \frac{\text{1st } \epsilon_{coef}}{\sigma_1 \ \sigma_2} R_1 R_2$$

where R is a random number normally distributed between $-\sigma$ and $+\sigma$. The random number generator subroutine is modified to reflect normally disturbed random errors (R_1, R_2). All random errors are symmetrically distributed with respect to sign. That is, it is equally likely for an error to be positive as negative and all random errors are independent events. The numerical limits placed on the biased and random errors will be in accordance with the ground rules established in Section III.

The 3σ total impulse error curve (Figure 7) was used in the computer program to establish the impulse magnitude errors. The total impulse magnitude error is composed of both steady state and transient errors. If the steady state error is represented by $\pm$ x and the transient error by $\pm$ y, then the total impulse magnitude error is represented by $\epsilon' = x + y$.

If we let k equal the ratio of steady state error to total error

$$k = \frac{x}{x + y}$$

then

$$\epsilon' = \frac{x}{k}$$

It also follows that $k\ \epsilon' = x$ and $(1 - k)\ \epsilon' = y$

TMC A673

If k = 1 all errors arise from steady state sources

If k = 0 all errors arise from the transient portion of the pulse

An abbreviation of the random error equations used in the computer program is

$$\epsilon = k\,A + (1 - k)\,B\,I_T/I_o$$

This function allows the errors to be weighted according to where they arise, either transient or steady state where k is the weighting factor. The values of k, which in the printout is labeled 2nd ϵ_{coef}, were derived from Figure 7 and are presented in Figure 10.

Two other epsilon coefficients were designated in the random error equations. One is required to define the total impulse magnitude error. Another is required to account for the angular errors. In terms of computer printout, the 1st ϵ_{coef} equals the total angular error in radians. This angle is then selected by a random number normally distributed between -1 and +1. The third ϵ_{coef} equals the total percent steady state impulse error divided by the 1st ϵ_{coef}. Therefore, the quantity (1st ϵ_{coef})(3rd ϵ_{coef}) equals the total percent steady state impulse error.

The mean value of specific impulse (I_{sp}) versus pulse width (Figure 8) was used in the computer program to obtain W_p versus I_T curves. A nonlinear operation (thrust times pulse width divided by specific impulse) was performed to obtain the propellant consumption for a given impulse command. The computer program is set up in such a manner that once the impulse is computed, the corresponding W_p for that pulse firing is obtained from the above information.

C. Random Number Generation

The foundation of the entire investigation rests on the nature of the systems thrust impulse errors. Of particular interest are the individual unpredictable portions of these errors and their collective effect upon system behavior. It is the generation of these random errors which is discussed here.

A standard subroutine in use for the IBM 7040 Electronic Digital Computer for the generation of random numbers supplies an output of numbers which show no repetition of pattern within a range of approximately 8.5×10^9 outputs. These numbers are approximately rectangularly distributed within an interval of zero to unity. The numbers introduced into the computer program to simulate the attitude control system errors are different in both range and distribution from those available from the above-mentioned subroutine. For this reason, the output

of the random number generator is properly modified to produce a Gaussian, or normal, distribution having the desired variance and truncated at the desired value of standard deviations from the null value. The distribution is centered about a value of zero; any shift in the distribution is incorporated into the bias error which is introduced as a separate parameter. The truncation of the ideal Gaussian distribution is a necessary measure due to its unbounded nature. Real system errors are approximately normally distributed in the vicinity of zero, but larger values are bounded between definite limits.

The modification of the random number generator output may be accomplished in either of two ways: First by a direct conversion, or second by a linear combination of variables.

1. Direct Conversion

Designate X as a random variable having a frequency distribution f (X). Define a new variable, y = h (X). The classical expression for the frequency distribution, F (y), of y is given as

$$F(y) = f\left(h^{-1}(y)\right) \frac{dh^{-1}(y)}{dy}$$

where $h^{-1}(y)$ is the inverse function of h (X). The above expression is the basis of a differential equation in the variables y and $h^{-1}(y)$ when F (y) is specified. For most cases, the resulting equation is very nonlinear and does not lend itself to a ready solution. When f (X) is constant, however, the problem simplifies greatly. In this case

$$F(y) = C \frac{dh^{-1}(y)}{}$$

where C is the value of f (X) in a finite interval of appropriate length.

Now

$$F(y)\, dy = C\, dh^{-1}(y)$$

or

$$\int_{\infty}^{y} F(y)\, dy = C \int_{a}^{h^{-1}(y)} dh^{-1}(y)$$

TMC A673

where a is the lower bound of the interval (X). This expression simplifies to the following

$$\frac{1}{C}\int_{-\infty}^{y} F(y)\,dy = h^{-1}(y) - a$$

When y is normally distributed, the above integral is written as

$$\int_{-\infty}^{y} F(y)\,dy = \frac{1}{\sqrt{2\pi\sigma}}\int_{-\infty}^{y} e^{-\frac{y^2}{2\sigma^2}}\,dy$$

for which extensive tables exist. Therefore, the inverse function $h^{-1}(y)$, is readily available in graphical form. A proper reflection of the inverse function about the origin yields a plot of the desired function, h (X). Since this function is not available in analytic form, it is to be closely approximated in polynomial form,

$$h(X) \approx \Sigma_i\, a_i\, X^i$$

This function will be applied to the output (X) of the random number generator to produce the new random variable (y) having the desired frequency distribution.

2. Linear Combination

Let X_i denote the i^{th} output of the random number generator. A new random variable is now given as

$$y = \Sigma_i\, b_i\, X_i$$

As i becomes large and the b's remain bounded, it may be shown that the distribution of y approaches that of a Gaussian distribution. When i is limited to a relatively low value (four or five), the closeness of approach of the variable (y) to a Gaussian distribution depends largely upon the choice of the coefficients (b_i).

Both of the methods described above produce output variables which are approximately Gaussian in distribution. The former method, however, is more versatile and it was chosen to produce the desired variables. A table of (X, h (X)) points is input, and interpolation is performed by fitting parabolas on triples of these points. The latter method is initially simpler to mechanize but is limited to producing only a Gaussian distribution.

VII. COMPUTER RESULTS

A. Parametric Results

A series of eighteen computer runs were made with 100 pulses in order to check out the computer logic. The initial conditions used for these runs were as follows:

3 σ error distribution--5% total steady state impulse magnitude error

2 degree constant thrust vector angular error

$k = 0.4$	$\Delta\theta = 1$ deg	$\theta_o = 0$ deg
$\dot{\theta}_{o_p} = 0.0010$ deg/sec	$X = 17.28$ m	$J_R = 17{,}000$ kg-m-sec^2
$\dot{\theta}_{o_y} = 0.0100$ deg/sec	$Y = Z - 3.55$ m	$J_y = J_p = 500{,}000$ kg-m-sec^2
$\dot{\theta}_{o_R} = 0.0001$ deg/sec	$\gamma = 0$	
$f = 668.4$ Newtons	$I_T = 2.04$ kg sec and 4.76 kg sec	Installation angular errors (β_{ijk}) = 0

Configurations 1 and 2 for Systems 1 through 4, described in Section III, were investigated. These initial conditions were used for all data presented in this section except where noted.

1. Mission Time

In order to determine whether or not these runs would produce a mean propellant consumption rate, the propellant consumption rate versus time was plotted. Typical curves for Configuration 2 ($I_T = 2.04$ kg sec) are shown in Figures 11 and 12. Although the mission times were not long enough to produce a mean propellant consumption rate in some cases, the values of propellant consumption rate after 100 pulses were used to obtain preliminary system comparative trends. The results in normalized form are shown in Figure 13. The three System 1 plots present the propellant consumption for the maximum theoretical, average theoretical, and the computer results.

In order to determine the mission time required before a mean propellant consumption value becomes valid, a system was run for 82.5 days. Figure 14 presents the propellant consumption rate as a function of time. Random points in time were used. The total propellant at that total time was used to compute the mean propellant consumption rate. Figure 14 shows that, for this system, the mean

TMC A673

propellant consumption rate was valid after approximately 3×10^6 sec. A flight time was used as a boundary limit for the computer run time, but if this time is insufficient the final conditions can be used as initial conditions for another run and data will be obtained for a longer effective total mission time. Figure 14 shows that the random values which were picked deviated no more than $\pm$ 1.2% after 3×10^6 sec.

2. Minimum Pulse Width

The effect of varying the minimum pulse width on system performance was investigated for Configuration 1 with an advanced limit cycle method (System 2) and a simple limit cycle method (System 1). The theoretical (no error) simple limit cycle propellant consumption rate as previously derived can be expressed as

$$\dot{\omega}_p = K \frac{I_T^2}{I_{sp}}$$

This function is plotted along with the other two curves in Figure 15. The deviation from the theoretical value, although exaggerated in the curve due to the method of plotting, is seen to be substantial. This illustrates the importance of the system errors. The importance of using the smallest impulse bit obtainable is also stressed. The reduction in propellant consumption by using the advanced control techniques is realized for all pulse widths. The propellant consumption has been normalized since only the ratios are of importance at this time. The initial conditions for this case are the same as those noted at the beginning of this section except that a 4% total steady state impulse magnitude error was used and the initial rates were $\theta_{o_R} = 0.0001$ deg sec, $\theta_{o_p} = 0.01$ deg sec, and $\theta_{o_y} = 0.001$ deg/sec.

3. Accuracy Deadband and Thrust Vector Angular Error

System 2 was run with the same initial conditions used for evaluating the effects of minimum pulse width to determine the effects of varying the accuracy deadband and thrust vector angular error. The results for System 2 with a minimum impulse bit of 2.04 kg sec are shown in Figure 16.

The theoretical (no error) propellant consumption is an inverse function of the deadband angle ($\dot{\omega}_p = K/\Delta\theta$). For comparative purposes, this function was checked and the advanced limit cycle error case was found to support the theoretical prediction. The deadband angle is therefore not believed to be a significant parameter in future studies since the basic effect of this parameter follows theoretical predictions.

TMC A 673

Changing the thrust vector angular error within the region shown is seen to have little effect on the total system performance. Up to this point, all thrust vector angular errors had been constant, that is, each pulse firing had the same rather than random angular errors. The constant angular error of 2 degrees total was assumed to be at a 45 degree angle to the axes. Also, the roll was controlled by pitch engines in Configuration 2. These were changed for the final control system comparison runs. The roll was controlled by the yaw engines and the angular error was picked at random from a normal distribution whose 3σ value was 2 degrees.

4. System 4 Errors

There are two significant errors associated with Control System 4. Specifically, these are the impulse error after the electrical signal is commanded off and the angular rate sensor error. The impulse error is treated in the computer program by taking only one-half the impulse error for a given pulse. This results in good first order answers since the pulse of interest (the last pulse of the control cycle) is the minimum pulse width and the error of one-half the pulse for this case is very close to the error after the electrical signal is commanded off. The angular rate sensor errors were reflected by the β_{ijj} coefficients through the impulse bit error associated with the angular rate error. All signs were taken as positive. For the final system runs, however, (used for comparison of control techniques) signs were arbitrarily assigned as $+\beta_{roll}$ and $+\beta_{yaw}$ and $-\beta_{pitch}$. The β's are associated with specific engines whereas the sensor errors are associated with vehicle axes. This led to a problem when one engine was used for control of more than one axis. This problem was resolved by giving the β a value proportional to the firing frequency for each axis controlled. The sensor errors used to parameterize the effect of this variable were as follows:

$\dot{\theta}$ Sensor Errors	
deg/sec	rad/sec
0	0
0.00006	1.046×10^{-6} most sophisticated rate sensors
0.0001	1.745×10^{-6}
0.001	1.745×10^{-5}
0.002	0.349×10^{-4}
0.006	1.046×10^{-4} state of the art rate gyros
0.01	1.745×10^{-4}

TMC A673

Figure 17 shows the effect of angular rate sensor errors. The results were that for angular rate sensor errors equal to or greater than 0.006 deg/sec, the angular rates and therefore the propellant consumption became divergent. Rate sensors better than state of the art gyros are therefore required for this method. The effects are shown in normalized form since the propellant consumption rate for this case is presented in the comparison of control systems section. The initial conditions for this case are the same as those noted for the accuracy deadband investigation.

5. Initial Angular Rates (With and Without Errors)

The simple box limit cycle was the only technique under investigation for which an analytical expression of mean propellant consumption had been derived. It was thus possible to predict these flow rates and compare them with the actual computer results. Configuration 1 was used for this study with the following error conditions:

Runs No. 35, 36, 37: Error conditions as discussed for evaluating minimum pulse width effects. Each run had different initial rate conditions.

Runs No. 43, 43-1: Error conditions as discussed in Section VII-B for the comparison of control systems. Each run had different initial rate conditions.

Run No. 43*: This run was made with no system errors in order to check the theoretical calculations.

The equations previously established for straight limit cycle propellant consumption per axis are as follows:

$$\left.\begin{aligned} \overline{\dot{\omega}}_p &= \frac{(I_T)^2 \; L}{3 \Delta\theta \; J \; I_{sp}} \\ \overline{\dot{\omega}}_{p_{max}} &= \frac{(I_T)^2 \; L}{2 \Delta\theta \; J \; I_{sp}} \end{aligned}\right\} \quad \text{2 pairs of coupled engines}$$

TMC A673

$$\left.\begin{aligned} \overline{\dot{\omega}}_{p_{max}} &= \frac{(I_T)^2 \, L}{12 \Delta\theta \, J \, I_{sp}} \\ \overline{\dot{\omega}}_{p_{avg}} &= \frac{(I_T)^2 \, L}{8 \Delta\theta \, J \, I_{sp}} \end{aligned}\right\} \quad \text{2 uncoupled engines}$$

The first two equations result from having four engines about each axis for a total of 12 engines as in Configuration 3. The last two equations result from two engines about each axis or a total of six engines. The Configuration 1 study uses coupled engines for roll and yaw and an uncoupled engine for pitch.

Due to the nature of the advanced limit techniques (presence of active damping), the system performance is completely independent of the initial angular rates. However, this is not the case in the simple limit cycle techniques. The difference in coefficients arises from the fact that theoretically the propellant consumption depends upon the initial angular rates. The maximum flow rate is predicted for the case in which the initial angular rate is one-half the angular rate increment delivered per pulse. This is the reason for presenting the results as shown in Figure 18. The average and maximum theoretical propellant consumption rates are presented in Table I as well as the predicted flow rates for Runs 43, 43-1 and 43*. The important vehicle and initial rate information is also repeated in Table I. It should be noted that in two Runs (43 and 43*) the initial angular rates in the pitch axis were higher than the angular rate increment. The effective initial rate was thus taken after two firings.

The results of these investigations are presented in Figure 18. Due to the cross coupling of engines for roll and yaw control, the propellant consumption rates for these two axes were combined in Runs 43, 43-1, and 43*. Similarly, only the total propellant consumption rate for all three axes was computed in Runs 35, 36, and 37. It was thus necessary to establish an effective initial rate ratio for Runs 43, 43-1 and 43*. The ratio of initial rate to rate increment was selected to be the same in all three axes, however, for Runs 35-37.

The results of the no error case (Run 43*) substantiated the theoretical calculations showing the validity of this derivation. The data from the cases in which firing errors were incorporated show two different trends.

1. The propellant consumption rate is still dependent on initial rate conditions even when these errors are present.

2. All propellant consumption rates will converge to a value of 0.67 maximum theoretical flow rate after sufficient operating times.

Although these two statements are apparently contradictory, they may be compatible when the operating time is taken into consideration. Of the nine data points, five are within 5 percent of the most probable flow rate ratio and only one has a deviation greater than 19 percent. The longest run time, however, was only one million seconds with some runs as short as a quarter million seconds.

From the random nature of the errors, it appears that the propellant consumption rate will converge to the predicted most probable value after a sufficient period (which appears to be about three million seconds). Initially, the propellant consumption should follow the theoretical values, based on initial conditions, due to the small magnitudes of the errors. As these errors accumulate, the cycling frequency will diverge from initial conditions. The cycling frequency or average flow rate based on any small sample period may vary from zero to the maximum theoretical rate. However, it is the averaging over extended periods of time which results in the most probable value.

B. Control System Comparisons

The control systems were compared using the following initial conditions:

2 degree random thrust vector angular errors, Δt = 30 milliseconds -- k = 0.62

3σ error distribution -- 4% total steady state impulse magnitude error

-- 2% total steady state impulse error (System 4)

$\dot{\theta}_{(\text{sensor error})}$ = 0.002 deg/sec (System 4)

$\Delta\theta$ = 1 deg θ_o = 0 deg -- τ = 0, τ = 0.01 sec (System 5)

$\dot{\theta}_{o_R}$ = 0.0001 deg/sec, $\dot{\theta}_{o_P}$ = 0.01 deg/sec and $\dot{\theta}_{o_Y}$ = 0.001 deg/sec

For System 5, $(a)_{P, R, Y}$ = 1.0 and $(\epsilon_{max})_{P, R, Y,}$ = 1.0 deg

TMC A 673

The roll axis was controlled by yaw engines for Configurations 1 and 2. The particular values for $\beta_{ijk's}$ were selected at random with random signs. These values were then used as constants in the computer program. The $\beta_{ijk's}$ assume one-half of the engines have a 1/2-degree angular error, one-quarter of the engines have a 1-degree angular error, and the remaining engines have zero angular errors. The computer program printed approximately 400 out of every 1000 pulses. The approximate end limits for the computer runs were: Time = 6×10^6 sec, total propellant mass = 2300 kg, or 9000 totalpulses. The vehicle parameters listed in Table II were used for this investigation.

Phase planes for the five control systems were constructed for the purpose of comparing (1). The control systems and (2). The individual axes of each control system. In all cases, it was attempted to obtain data for the phase planes during steady state limit cycle operation. This was essentially accomplished for all systems except System 5 (diamond error matrix). The phase planes are shown in Figures 19 through 27 and a brief description of each control system is given below. All systems were run for Configuration 1, Vehicle Parameter Set 1.

1. Simple Box Limit Cycle

Figures 19, 20, and 21 are representative of the phase plane trajectories for the simple box limit cycle operation without using rate information. As seen in Figure 19, the roll axis limit cycle is completely settled out but Figures 20 and 21 indicate that the yaw and pitch axes limit cycles are drifting. This is explained as disturbances resulting from cross coupling thrust errors and if the trajectories had been drawn at a different starting time, they would appear slightly different. However, since the average error over a long period of time averages to zero, the basic trajectory should be very similar at any time following the initial transient settling time.

2. Advanced Limit Cycle with Velocity Information

The roll axis phase plane for Control System 2 is shown in Figure 22. Only one axis is presented, since the other two axes are nearly identical in form with only the relative drift rates (due to random errors) being slightly different and therefore, commanding various rate corrections.

3. Advanced Limit Cycle with Velocity Calculations (3-Pulse Method)

As in System 2, the trajectories for the three axes in this system are very similar and only the roll axis phase plane is presented (Figure 23). The effect of cross coupling thrust errors is readily seen in this plot wherein the drift rate is initially positive and then switches to negative (as indicated by the dashed line).

4. Advanced Limit Cycle with Rate Cutoff

The trajectories for the three axes in this system, as in the other damped control techniques, are nearly identical with only the drift characteristics differing between pitch, yaw, and roll. Actually, in all of the damped systems, the limit cycle phase planes have lesser meaning than the undamped control techniques due to the fact that once an error band has been reached, the trajectories from that point on will be essentially the same. The roll axis trajectory is shown in Figure 24.

5. Simple Diamond Error Limit Cycle

The phase plane trajectories for the three axes are shown in Figures 25, 26, and 27. It should be noted that interpretation of the roll and yaw axes phase planes for this system is quite difficult. Since the two axes are combined in the switching logic, there is no single angle at which the engines will be pulsed. Therefore, if no steady state limit cycles exist, (and none were found with the system parameters investigated) there are an infinite number of possible phase plane trajectories. These plots are shown here primarily to illustrate the general trend of the limit cycle precession.

Three samples of this System 5 data were analyzed to determine the limit cycle characteristics. Figure 28 indicates the behavior in the combined roll-yaw plane for the conditions of zero fixed and random errors and with zero rate dependent error contribution. These characteristics were extracted from data taken after 78,158 sec. As seen in this plot, there is no apparent steady state limit cycle but rather a pulsating limit cycle which tends to dwell longer along the roll axis than along the yaw axis. Although a greater run time is necessary to absolutely establish this trend, it seems reasonable to conclude that these conditions do exist. Another factor that lends credence to this conclusion is that for a fixed impulse, the roll rates are larger than the yaw rates which results in larger roll angular excursions.

Figures 29 and 30 are for the same system and conditions but with the addition of fixed and random errors. Figure 29 was drawn from data taken from the beginning of the computer run (initial time--t_1 = 3143 sec) and it is obvious from this plot that a steady state condition has not been reached. There are double pulses being fired when the pitch and / or yaw rates are too high which is an undesirable situation from the standpoint of fuel consumption. Figure 30 is at the end of the run and a more consistent pattern has been established. However, the trajectory is still not fixed or predictable in the same manner as the zero error case shown in Figure 28.

From the standpoint of fuel consumption, this system compares unfavorably with the damped techniques, but is about one-half that determined for the simple box limit cycle with errors. These results are reasonable, since a variable pulse width allows for a much finer control than a fixed pulse width

control system. Also, when the diamond error matrix is compared to the simple box error, it should be expected that the diamond error system would consume less fuel on the basis that only one engine, rather than a couple, is being fired per attitude correction.

The influence of the rate switching factor (b) on pulse frequency or propellant consumption is shown in Figure 31. This plot indicates that the rate contribution is valueless. It is concluded that the rate factor would be of value only if a variable pulse width is employed. It can be shown theoretically that the rate factors only tend to reduce the effective error band which in a fixed pulse width case can only cause the error band to be crossed sooner. The equation given below is the time to traverse from an initial value to the first quadrant error limit (+Y +R).

$$\Delta t_{+Y,\ +R} = \left[1 - \frac{\theta_{y_i} - \theta_{R_i} - b_Y \dot{\theta}_Y - b_R \dot{\theta}_R}{\dot{\theta}_y + \dot{\theta}_R} \right]$$

It can be seen in this equation that if both yaw and roll rates are positive the time to intersect the error band is lowered, resulting in more pulses. Figure 31 also indicates that the propellant consumption or pulsing frequency is much more a function of the rate switching factor magnitude than it is of the ratio of the rate switching factors. It should be noted that these conclusions are based on a few select points for the purpose of projecting a general trend.

The only difference between Configurations 1 and 2 is that one engine is used to control pitch (one direction) in Configuration 1 whereas two engines are used in Configuration 2. The time trace of the propellant consumption rate for the pitch axis is shown in Figure 32 for System 2 with Vehicle Parameter Set Number 1. Configuration 2 consumes approximately twice as much propellant as Configuration 1 on the pitch axis. This, however, does not present the total case due to the effects of other axes. The tabulation shown below presents the mean propellant consumption rate and pulsing frequency per engine for each configuration.

Although individual engines or axes have significant differences, the total system performance for the two configurations is seen to be quite similar.

TMC A673

Axis	Engine No.	$\dot{w}_p$ kg/sec x 10^{-6}		fp pulses/hr	
		Conf. 1	Conf. 2	Conf. 1	Conf. 2
+R + Y	53	1.494	1.149	0.5414	0.4156
-R -Y	54	1.490	1.156	0.5422	0.4167
-R +Y	63	1.491	1.149	0.5413	0.4206
+R -Y	64	1.493	1.156	0.5423	0.4117
-P	45	--	0.577	--	0.2095
+P	46	--	0.582	--	0.2095
-P	35	--	0.577	--	0.2095
+P	36	--	0.582	--	0.2095
-P	55	0.571	--	0.2070	--
+P	66	0.580	--	0.2067	--
Totals:		7.119	6.929	2.581	2.5026

Figures 33 and 34 present the total vehicle propellant consumption rate and total vehicle pulsing frequency as a function of vehicle angular acceleration. This is presented for Configuration 3 ($\alpha_P = \alpha_R = \alpha_Y$) which has coupled engines for each axis and no dual usage of engines. Each of the control systems possible with this configuration is presented. As expected, the pulsing frequency is directly proportional to the mean propellant consumption rate for any given vehicle configuration.

Both the propellant consumption rate and the pulsing frequency are proportional to vehicle angular acceleration as expected and the effectiveness of the advanced limit cycle control techniques increases as angular acceleration increases.

In order to investigate the effects of vehicle configuration, the positive yaw engines were investigated for a common yaw axis acceleration of $\alpha = 0.00452$ rad/sec^2 for Control System 2. The results are tabulated below.

TMC A673

Vehicle Configuration	$\dot{w}_{p+Y}$ kg/sec x 10^{-6}	f_{T+Y} pulses/hr
1	2.985	1.0827
2	2.298	0.8362
3	0.001	0.164

Figure 35 presents a mean propellant consumption rate comparison between control systems for Vehicle Parameter Set Number 1 and Configuration 1. The pitch axis contribution is also shown. The dominant factor is seen to be the effect of the yaw and roll engines. As the total system performance improves, the less important this becomes. This effect is minimized in the advanced limit cycle control techniques. Table III summarizes the various control system comparisons. The simple box limit cycle was used as the base point. Although previous results have shown that these comparisons are functions of various system parameters (vehicle angular acceleration, angular rate sensor errors, etc.) a general trend can be formulated. Approximately only 50% of the propellant would be used by employing the diamond error simple limit cycle. The advanced limit cycle techniques (active damping employed) reduce this value to 30%, 16%, and 14% for Control Systems 3, 2, and 4, respectively. These numbers could vary significantly for any given condition and should therefore be used only as gross average values.

When comparing the control systems there are factors to be considered other than system weight and engine duty cycle. The quality of sensors required, the amount of computing equipment required, and the reliability of the system or system complexity are a few of these. Table IV presents a rating system with appropriate weighting factors and general comparison of the control techniques on a total system basis.

VIII. CONCLUSIONS

Although various significant results have been presented and general trends have been established, the main conclusion to be drawn from this study is that quantitative support for previous qualitative thinking has been presented in regard to the advantages of employing advanced limit cycle techniques. The advanced limit cycle techniques are capable of using only 15% of the propellant previously used on a gross average basis (in some cases investigated, only 2% was used). A proportional reduction of engine duty cycle is also realized. These savings are realized with present equipment and without unduly complicating the control system. Further study and development of these control systems is essential and should be of paramount importance.

The damped limit cycle control techniques presented herein were selected because of their ability to reduce the vehicle angular velocity to zero under ideal conditions. The analytical model used to describe the "advanced limit cycle techniques" allowed functional relationships between the mean propellant consumption rate, system parameters, and system errors to be established. The method of treatment also allowed a comparison with the simple box limit cycle technique. System performance degradation for the damped control methods were found to be only a function of the system errors. Since system performance degradation was only a function of the system errors, a more complete understanding of the nature of these errors was obtained by performing a statistical survey of available test data.

Evaluation of the "advanced limit cycle techniques" using actual rocket test data has shown that they are better than the simple limit cycle techniques on a propellant and engine duty cycle basis. Using present hardware and minimum impulse bits, these control methods conserved propellant for all cases. As system hardware is improved, the damped limit cycle techniques will show greater performance advantages. The damped control techniques provide the additional capability of using only one control mode for some entire missions. This provides control circuit simplicity, reduces system weight, and increases the reliability of the control system. Some of the control methods also do not require direct velocity information.

The results of this evaluation were of a preliminary nature due to the neglect of higher order terms, incomplete error and error distribution data, limited computer runs and run time, and the assumption of no external disturbance torques. The number of variables involved allowed only a preliminary parametric evaluation.

IX. RECOMMENDATIONS

The present program developed the tools for obtaining attitude control system performance. The study established major areas of interest and investigated such areas as desired parameter variations, importance of various parameters, and input-output formats. Shortcuts were taken in the computer program in order to allow a number of gross effects to be evaluated under the present program.

What is now required is another degree of sophistication added to the present program in order to allow evaluation of detail (2nd order effects) system performance. This program can then be used as a tool for efficiently optimizing and designing various control techniques.

In order to substantiate the conclusions, additional conditions should be investigated with individual as well as compounded axis or engine information. Since mission operating time was an important factor in each system and configuration, the individual systems should be further studied to see how various mission times influence the conclusions. This would also include a greater error dispersion so that the time required to reach the average values can be determined. It would also be necessary to extend the study to cover the additional vehicle configurations and sizes necessary for a complete evaluation.

Specifically, the following information should be obtained or integrated into this program:

1. Statistical quantities should be obtained from the computer program, especially for propellant consumption and engine duty cycle. Although the mean values are important in a gross comparative study, the vehicle designers will want to know the worst case, the most probable case, etc. as a function of omission time in order to allow freedom in the selection of the design values. In some cases, mission times are too short to reach mean values.

2. Longer mission times will have to be run in order to further substantiate the results, especially in the case of the simple limit cycle methods.

3. A moment arm callout per engine rather than on a per axis basis is required. This would allow offset engine configurations to be investigated.

4. The exact errors after the electrical signal is commanded off should be used in System 4 along with more exact rate sensor error treatment. Also, the jet cutoff threshold for System 4 should be further evaluated.

5. Rate switching should be further investigated for all control systems.

6. A more refined treatment of all sensor and timing errors should be sought.

7. System 5 should be investigated for the case of yaw roll plus pitch roll engine coupling plus variable pulse widths.

8. The critical parameters affecting engine operating efficiencies should be isolated and their effects on system performance should be determined.

9. More accurate thrust vector and hardware installation angular errors should be used.

10. The control philosophies should be investigated for areas of possible modification which might improve the overall system performance and efficiency in the presence of component errors or disturbance torques (i.e., using past history of previous pulses to update control logic, etc.)

11. Such areas as two- or three-axis simultaneous engine firings and the effect of more than one pulse firing should be investigated and the statistical frequency of these plus other special events (corner conditions) should be sought.

12. The effects of vehicle mass changes (main propulsion, etc.) on system performance should be evaluated. One area to investigate would be the automatic compensation for variable mass.

13. The system performance should be evaluated for the case when the present systems are used with fine control modes (passive techniques, momentum wheels, etc.)

Failure to consider even extremely low outside disturbing torques produces severe limitations upon the interpretation of the results. It is suspected that propellant consumption rates are strongly influenced by the presence of this condition. Therefore, one major area of study should be devoted to the determination of the quantitative effects of disturbing torque on system performance and efficiency. The disturbance torques vary in magnitude and are of a steady, cyclic, or random nature. In a general limit cycle control system analysis, the disturbance torques are not treated rigorously since the limit cycle rate is usually orders of magnitude greater than the disturbances. Most of the disturbances tend to be automatically compensating without regard to origin. However, when the control system is closed loop or contains damping, the disturbance torques acting at each point in the orbit become important in determining the effectiveness of the control method and cannot be disregarded. The relationship between the mean angular rate for each control system and the mean

disturbance torque rate should be evaluated. It is recommended that random as well as predictable bias torques be taken under consideration.

Since the degradation of system operating efficiency is a consequence only of system errors, a better knowledge of the error distribution should be secured. It is also recommended that the complete attitude equations of motion be used to obtain a more refined performance analysis.

Simulations which combine the computer with hardware elements are recommended. A number of simulations are possible under this general item. The simulation of vehicle motion can be directly handled on either analog or digital computers. However, the nonlinear nature of the sensors, controller, and moment producers are the least accurate and most critical part of this problem to simulate. The actual hardware elements should become an integral part of computer simulations. Optimum three-axis controller design could then be obtained.

The present investigations brought out some interesting facts and show a very definite need for a more refined study which would provide more support for the trends which were established. In order to rigorously establish the performance tradeoffs, the computer program should be employed with minor modifications. This study would result in definite answers to the question of what the optimum design parameters are of more sophisticated mass expulsion attitude control techniques. This program could be handled on a parametric basis with the goal of presenting results which would allow the selection of an optimal control technique for whatever specific conditions (vehicle and mission) desired.

An actual space flight demonstration of these control techniques would also be desirable. If this flight experiment supports previous results, a definite advancement of the state of the art will be realized.

This study has provided tools which will allow the various control techniques for operational and planned vehicles to be evaluated and compared on a realistic basis. This program could save considerable time and cost in the design and postflight modification phases of spacecraft development programs. This program is also adaptable to other maneuver phases such as rendezvous and docking, re-entry, and midcourse correction.

X. REFERENCES

1. The Marquardt Corporation P.D. Study No. 586, "Advanced Limit Cycle Analysis", R. W. Adlhoch, 15 February 1963. UNCLASSIFIED

2. Englehart, W. C., "Synthesis of a Damped Limit Cycle Reaction Jet Attitude Control System", Master of Science Thesis -- UCLA, June 1963.

3. NASA Marshall Space Flight Center Report MTP-ASTR-N-62-14, "A New Concept to Minimize On-Off Jet Fuel Consumption Used for Space Vehicle Attitude Control", Hans F. Kennel and David N. Schultz, 19 December 1962, UNCLASSIFIED.

4. Reeves, D. F., W. P. Boardman, and H. A. Baumann, "Pulsed Rocket Control Techniques", The Marquardt Corporation, ARS Paper 2704-62, presented at the 17th Annual Meeting and Space Flight Exposition, Los Angeles, California, 13-18 November 1962. UNCLASSIFIED.

TABLE 1

SIMPLE BOX LIMIT CYCLE COMPARISONS

	Run Number					
	35	36	37	43	43-1	43*
Roll Axis:						
1. Moments of inertia, kg M sec^2	1.7×10^4	1.7×10^4	1.7×10^4	1.7×10^4	1.7×10^4	1.7×10^4
2. Moment arm (ℓ), M	7.11	7.11	7.11	7.11	7.11	7.11
3. Impulse bit/eng., kg sec	2.04	2.04	2.04	2.04	2.04	2.04
4. Initial angular rate, deg/sec	0.0466	0.0386	0.0245	0.0001	0.01	0.0001
5. Max. prop. consumption rate (theo.), kg/sec	242.4×10^{-6}	242.4×10^{-6}	242.4×10^{-6}	242.4×10^{-6}	242.4×10^{-6}	242.4×10^{-6}
6. Avg. prop. consumption rate (theo.), kg/sec	161.6×10^{-6}	161.6×10^{-6}	161.6×10^{-6}	161.6×10^{-6}	161.6×10^{-6}	161.6×10^{-6}
7. Predicted prop. consumption rate (theo.) kg/sec	--	--	--	--	--	--
8. Total run time, sec	0.822×10^6(a)	0.263×10^6(a)	0.317×10^6(a)	0.415×10^6	1.066×10^6	0.130×10^6
9. Avg. pulse freq., pulse/hr	13.4 (a)	41.7 (a)	34.6 (a)	82.2 (b)	68.9 (b)	7.01 (b)
10. Prop. rate (act.), kg/sec	63.1×10^{-6}(a)	200.7×10^{-6}(a)	167.1×10^{-6}(a)	225.9×10^{-6}(b)	184.5×10^{-6}(b)	19.6×10^{-6}(b)
Pitch Axis:						
1. Moment of inertia, kg M sec^2	0.5×10^6	0.5×10^6	0.5×10^6	0.5×10^6	0.5×10^6	0.5×10^6
2. Moment arm (ℓ), M	34.56	34.56	34.56	34.56	34.56	34.56
3. Impulse bit/eng., kg/sec	2.04	2.04	2.04	2.04	2.04	2.04
4. Initial angular rate, deg/sec	0.00376	0.00312	0.00198	0.01 (c)	0.0001	0.01 (c)

TABLE I (Continued)

	Run Number					
	35	36	37	43	43-1	43*
5. Max. prop. consumption rate, (theo.), kg/sec	10.0×10^{-6}	10.0×10^{-6}	10.0×10^{-6}	10.0×10^{-6}	10.0×10^{-6}	10.0×10^{-6}
6. Avg. prop. consumption rate, (theo.), kg/sec	6.7×10^{-6}	6.7×10^{-6}	6.7×10^{-6}	6.7×10^{-6}	6.7×10^{-6}	6.7×10^{-6}
7. Predicted prop. consumption rate (theo.), kg/sec	--	--	--	10.0×10^{-6}	--	10.0×10^{-6}
8. Total run time, sec	--	--	--	0.413×10^{6}	1.066×10^{6}	0.132×10^{6}
9. Avg pulse freq., pulse, hr	--	--	--	2.56	2.60	3.72
10. Prop. rate (act.), kg/sec	--	--	--	7.0×10^{-6}	7.0×10^{-6}	10.0×10^{-6}
Yaw Axis:						
1. Moment of inertia, kg M sec^2	0.5×10^{6}	0.5×10^{6}	0.5×10^{6}	0.5×10^{6}	0.5×10^{6}	0.5×10^{6}
2. Moment arm (ℓ), M	34.56	34.56	34.56	34.56	34.56	34.56
3. Impulse bit/eng, kg/sec	2.04	2.04	2.04	2.04	2.04	2.04
4. Initial angular rate, deg/sec	0.0079	0.0066	0.0042	0.001	0.001	0.001
5. Max. prop. consumption rate (theo.), kg/sec	40.0×10^{-6}	40.0×10^{-6}	40.0×10^{-6}	40.0×10^{-6}	40.0×10^{-6}	40.0×10^{-6}
6. Avg. prop. consumption rate (theo.), kg/sec	26.7×10^{-6}	26.7×10^{-6}	26.7×10^{-6}	26.7×10^{-6}	26.7×10^{-6}	26.7×10^{-6}
7. Predicted prop. consumption rate (theo.), kg/sec	--	--	--	17.3×10^{-6}	17.3×10^{-6}	17.3×10^{-6}

TABLE I (Continued)

	Run Number					
	35	36	37	43	43-1	43*
8. Total run time, sec	--	--	--	0.415×10^6	1.066×10^6	0.133×10^6
9. Avg. pulse freq., pulse/hr	--	--	--	--	--	--
10. Prop. rate (act.), kg/sec	--	--	--	--	--	--

(a). Pitch plus roll plus yaw engines

(b). Roll plus yaw engines

(c). Two pulses needed for acquisition

TABLE II

VEHICLE PARAMETERS

Vehicle Parameter Set - Configuration	α_P (rad/sec^2)	α_R (rad/sec^2)	α_Y (rad/sec^2)	J_R (kg m sec^2)	$J_Y = J_P$ (kg m sec^2)	F (Newtons)	I_T (kg sec)	X (m)	Y = Z (m)
1 - 1	0.00226	0.02848	0.00452	--	--	--	--	--	--
1 - 2	0.00452	0.02848	0.00452	17,000	500,000	668.4	2.04	17.28	3.55
2 - 1	0.021	0.05	0.042	--	--	--	--	--	--
2 - 2	0.042	0.05	0.042	1,383	4,149	222.8	0.68	3.81	1.52
3 - 1	0.00041	0.04	0.00062	--	--	--	--	--	--
3 - 2	0.00082	0.04	0.00082	346	34,575	22.8	0.068	6.25	3.05
4 - 3	0.02	0.02	0.02	4.15	4.15	0.89	0.0027	0.457	0.457
5 - 3	0.002	0.002	0.002	692	692	2.23	0.0068	3.05	3.05
6 - 3	0.0004	0.0004	0.0004	1,383	1,383	0.89	0.0027	3.05	3.05

TABLE III

COMPARISON OF CONTROL SYSTEMS

System	Preliminary Trend Results		$\dot{\omega}_p / \omega_p$	System 1 Final System Runs Conf. 3 (α = rad/sec^2)		
	Conf. 1	Conf. 2	Conf. 1	α = 0.004	α = 0.01	α = 0.02
l_{max}	6.25	4.95	--	--	--	--
l_{avg}	3.625	3.25	--	--	--	--
1	1.0	1.0	1.0	1.0	1.0	1.0
5	--	--	0.495	--	--	--
3	0.435	0.362	0.104	0.78	0.092	0.104
2	0.215	0.225	0.033	0.39	0.038	0.036
4 (θ_{SE} = 0.002 deg/sec)	0.164	0.115	0.039	0.22	0.021	0.026
4 no sensor errors	0.10	0.10	--	--	--	--

TMC A673

TABLE IV

TOTAL CONTROL SYSTEM COMPARISON

Control Technique	Sensor Difficulty	Computer Difficulty	Actuator Duty Cycle No. of Pulses x 2	Total Propellant Consumption x 3	Total
1. Simple Box Limit Cycle	10	10	2.8	4.2	3.9
2. ALC-Velocity Information	6	5	17.5	26.3	7.8
3. ALC-Velocity Calculations	9	5	9.3	14.0	5.3
4. ALC-Rate Cutoff	2	5	20.0	30.0	8.1
5. Simple Diamond Error Limit Cycle	9	8	5.6	8.4	4.4

Rating:

ALC = Advanced Limit Cycle

10 = Best
1 = Worst

TMC 0673

VEHICLE AND ENGINE CONFIGURATIONS

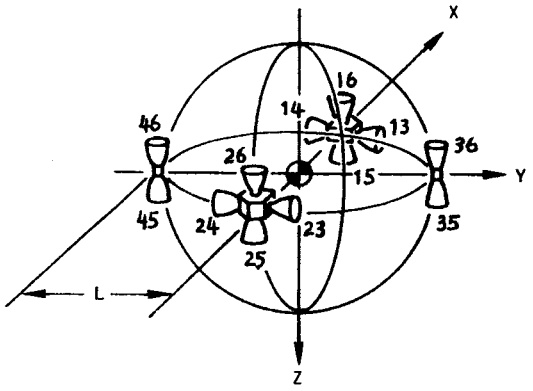

12-UNIT CONFIGURATION NO. 3

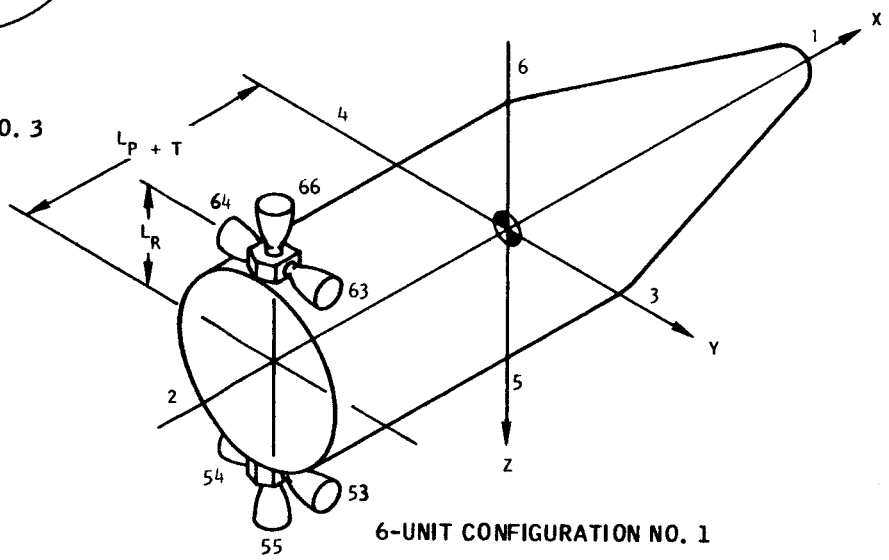

6-UNIT CONFIGURATION NO. 1

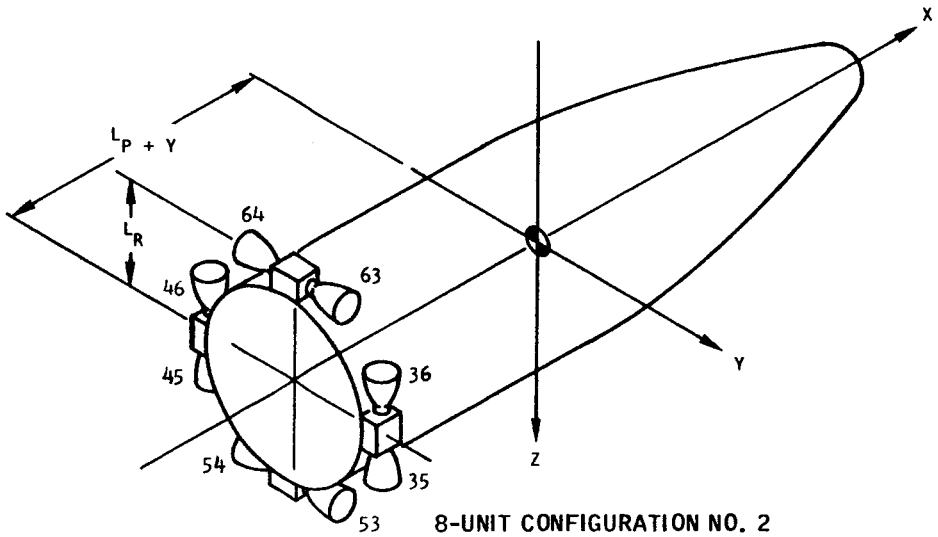

8-UNIT CONFIGURATION NO. 2

NOTES:

1. THE FIRST NUMERAL ON ENGINE CALLOUT REPRESENTS THE AXIS WHICH THE ENGINE STEMS FROM WHILE THE SECOND NUMERAL REPRESENTS THE DIRECTION THE ENGINE IS POINTING.
2. RIGHT-HAND RULE APPLIES FOR ROTATION.

TMC A673

SIMPLE BOX LIMIT CYCLE OPERATION

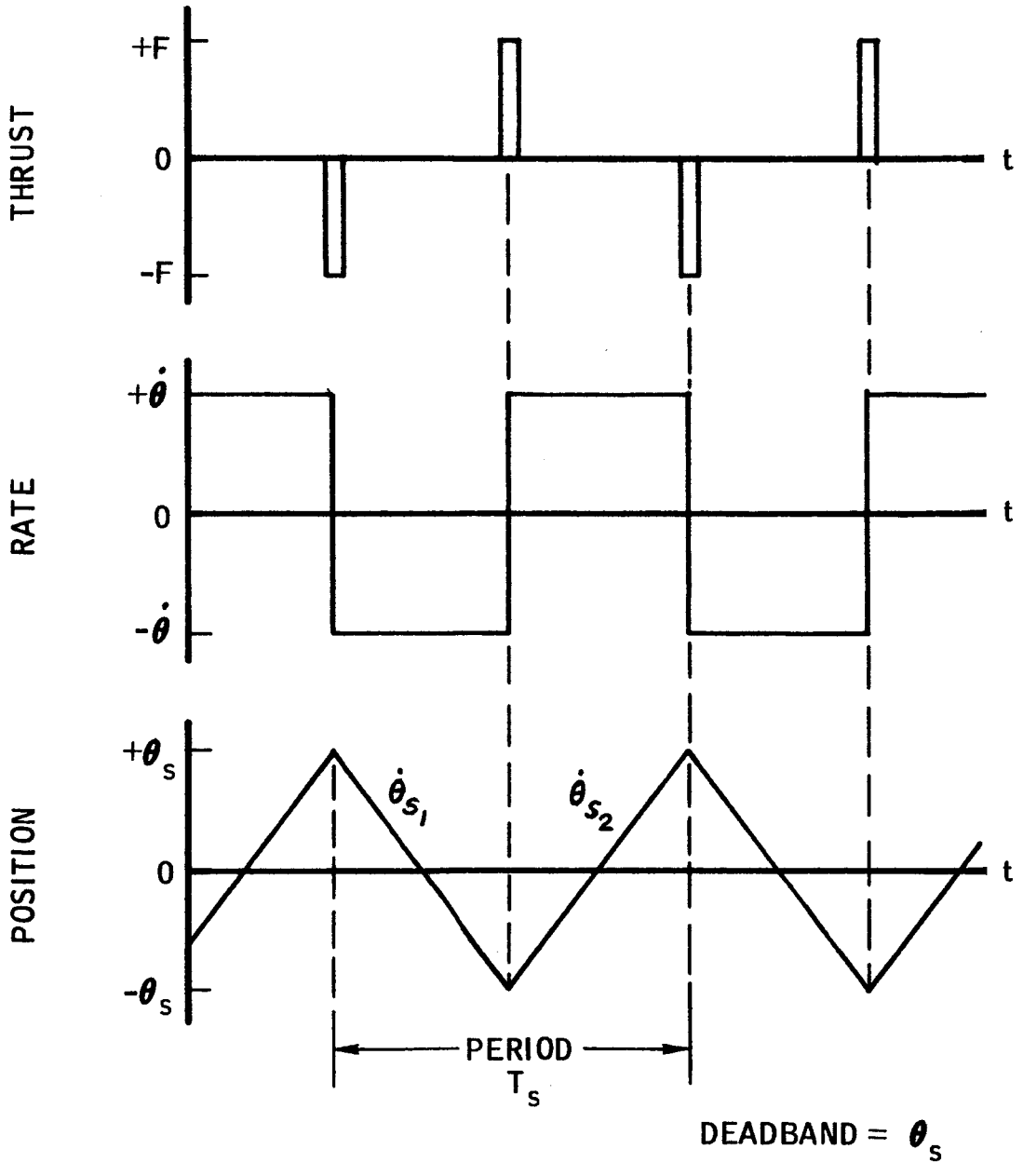

TMC A673

SIMPLE BOX LIMIT CYCLE PHASE PLANE

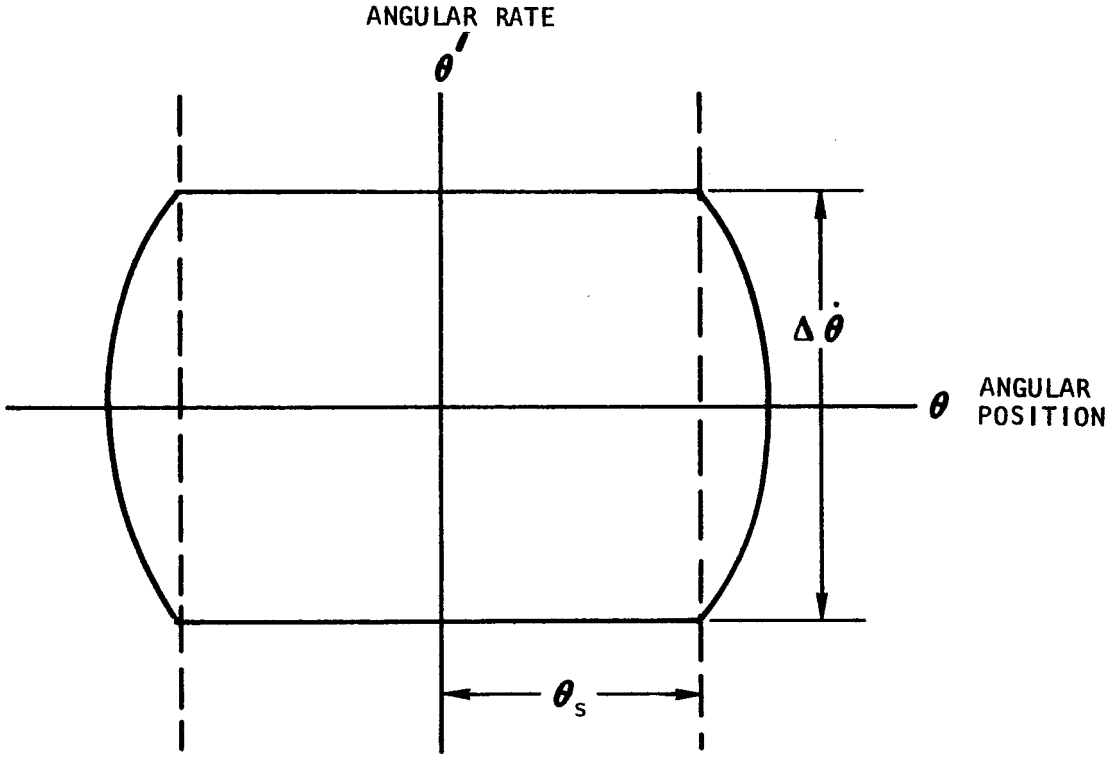

VARIATION OF OSCILLATION FREQUENCY WITH INITIAL ANGULAR RATE

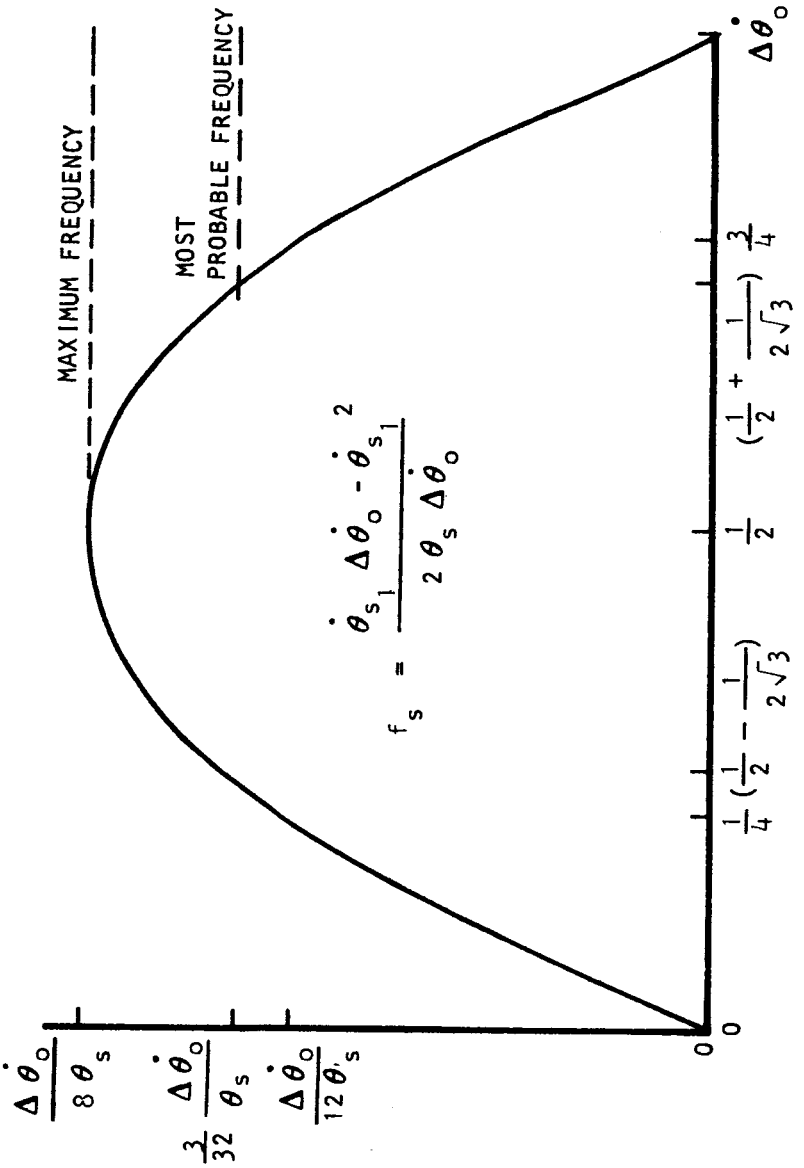

TMC A673

FIGURE 4

ERROR BANDS FOR 6-UNIT CONFIGURATION

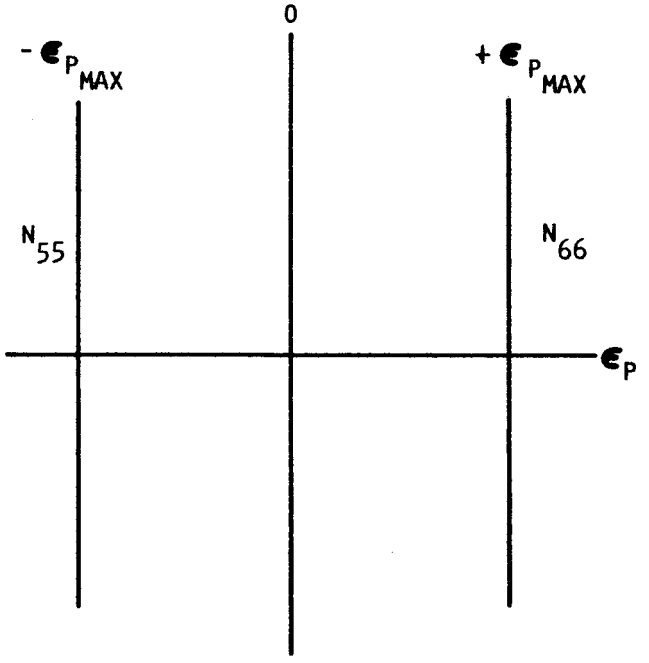

PITCH AXIS ERROR BAND

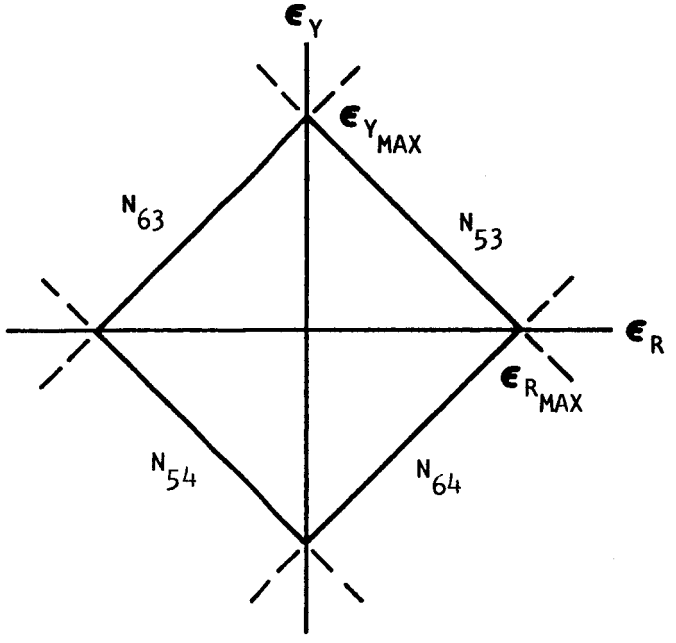

YAW - ROLL AXES ERROR BAND

TMC A673

ERROR BANDS FOR 8-UNIT CONFIGURATION

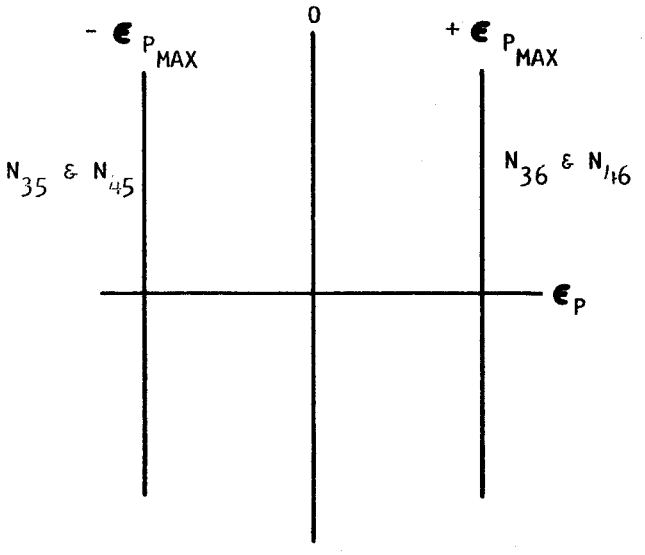

PITCH AXIS
ERROR BAND

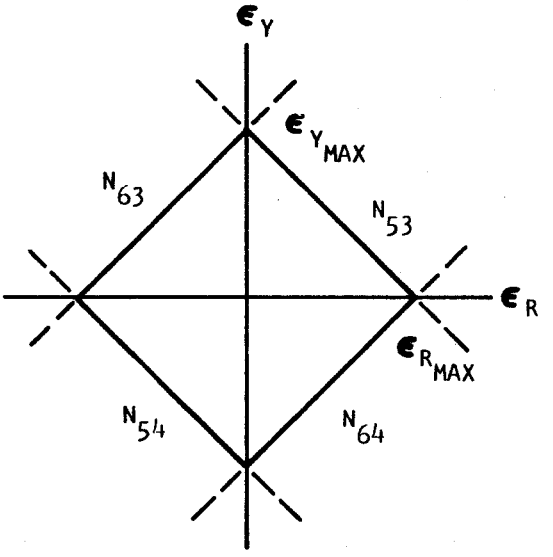

YAW - ROLL AXES
ERROR BAND

(PURE "COUPLE" FOR PITCH)

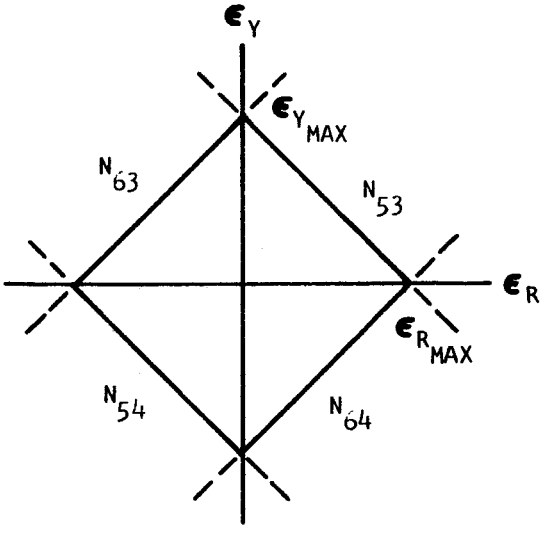

YAW - ROLL AXES
ERROR BAND

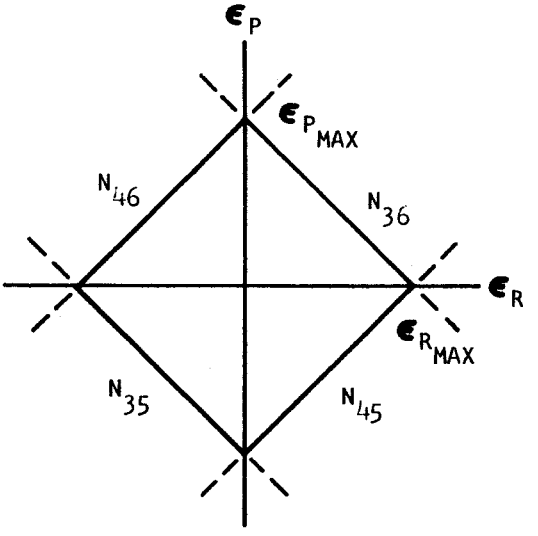

PITCH - ROLL AXES
ERROR BAND

(BOTH YAW AND PITCH AXES
COUPLED TO ROLL AXIS)

TMC A673

TOTAL IMPULSE ERRORS AS A FUNCTION OF PULSE WIDTH

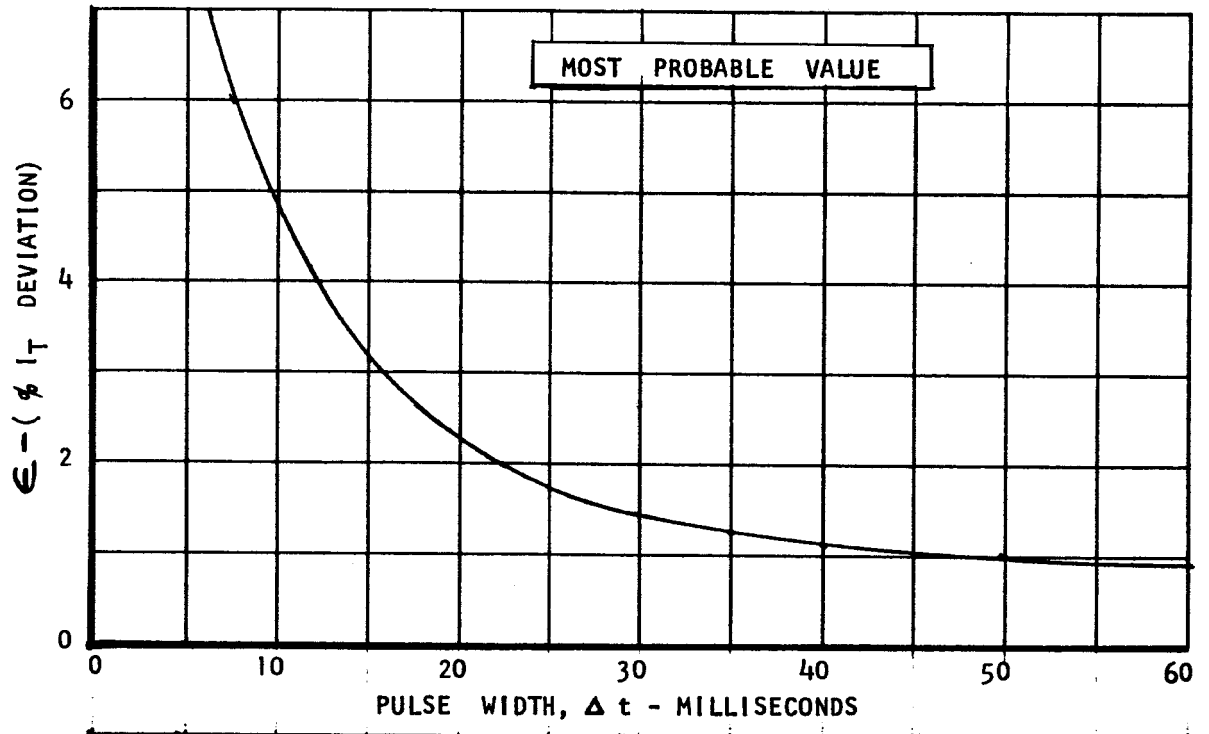

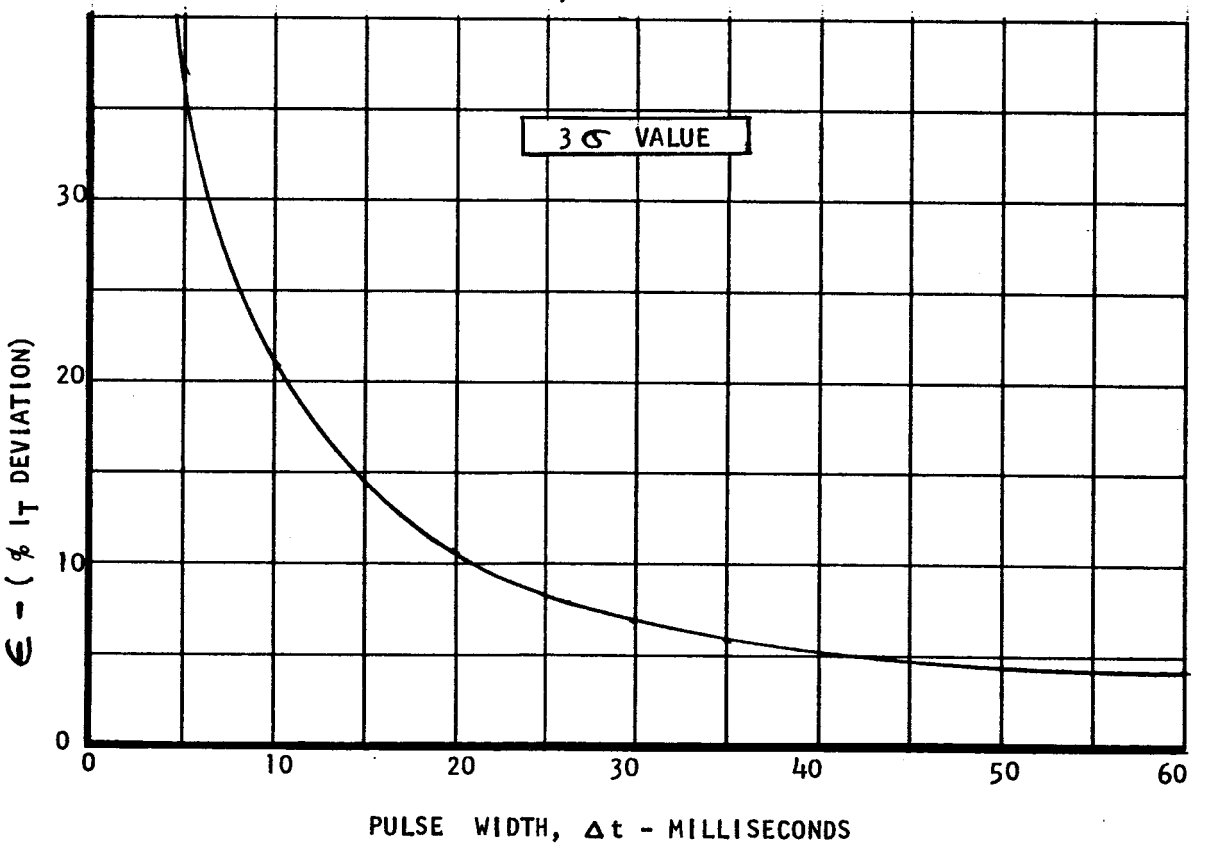

TMC A673

FIGURE 7

MEAN VALUE OF SPECIFIC IMPULSE AS A FUNCTION OF PULSE WIDTH

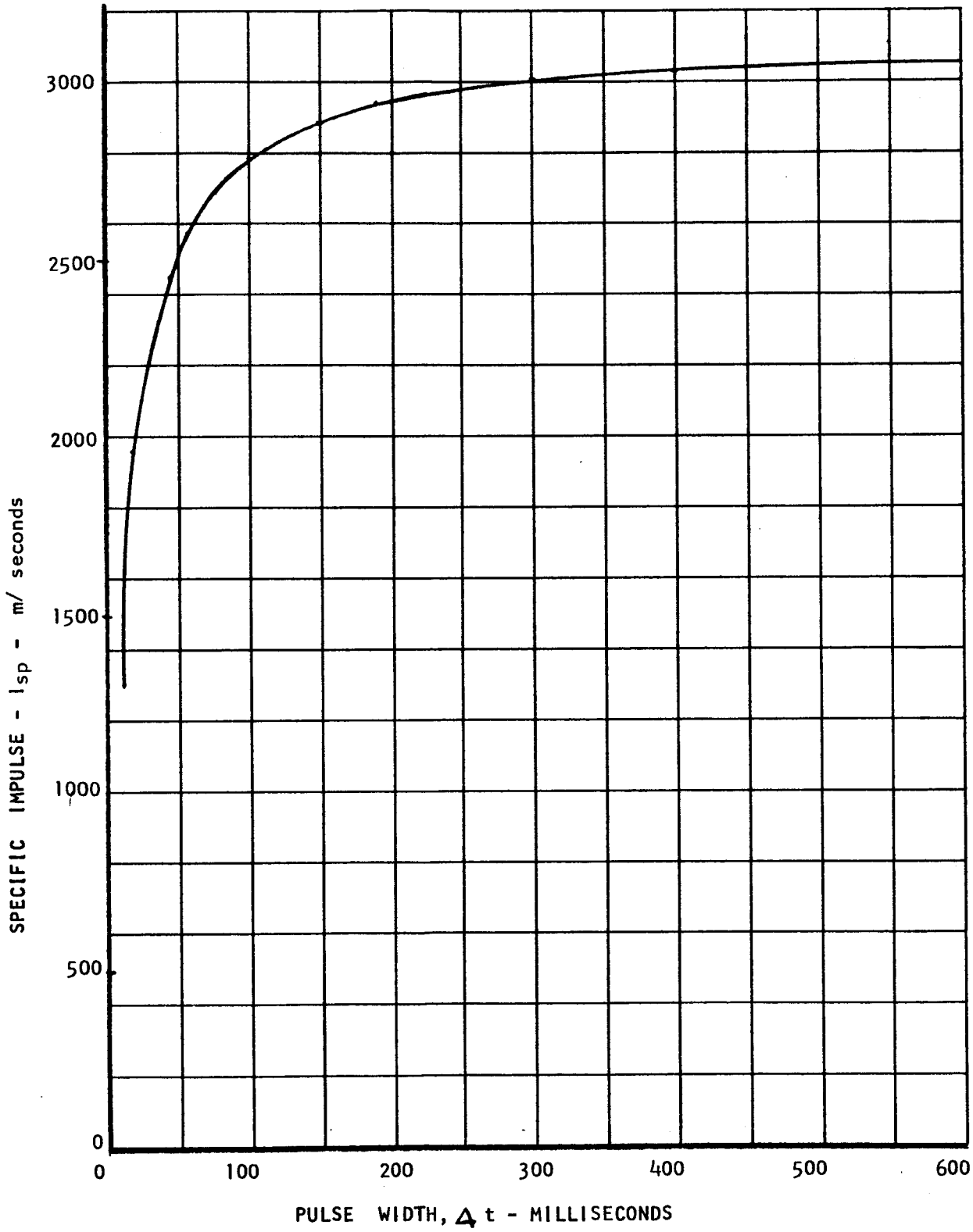

TMC A673

FIGURE 8

GENERAL PROGRAM FLOW CHART FOR ADVANCED ATTITUDE CONTROL TECHNIQUES

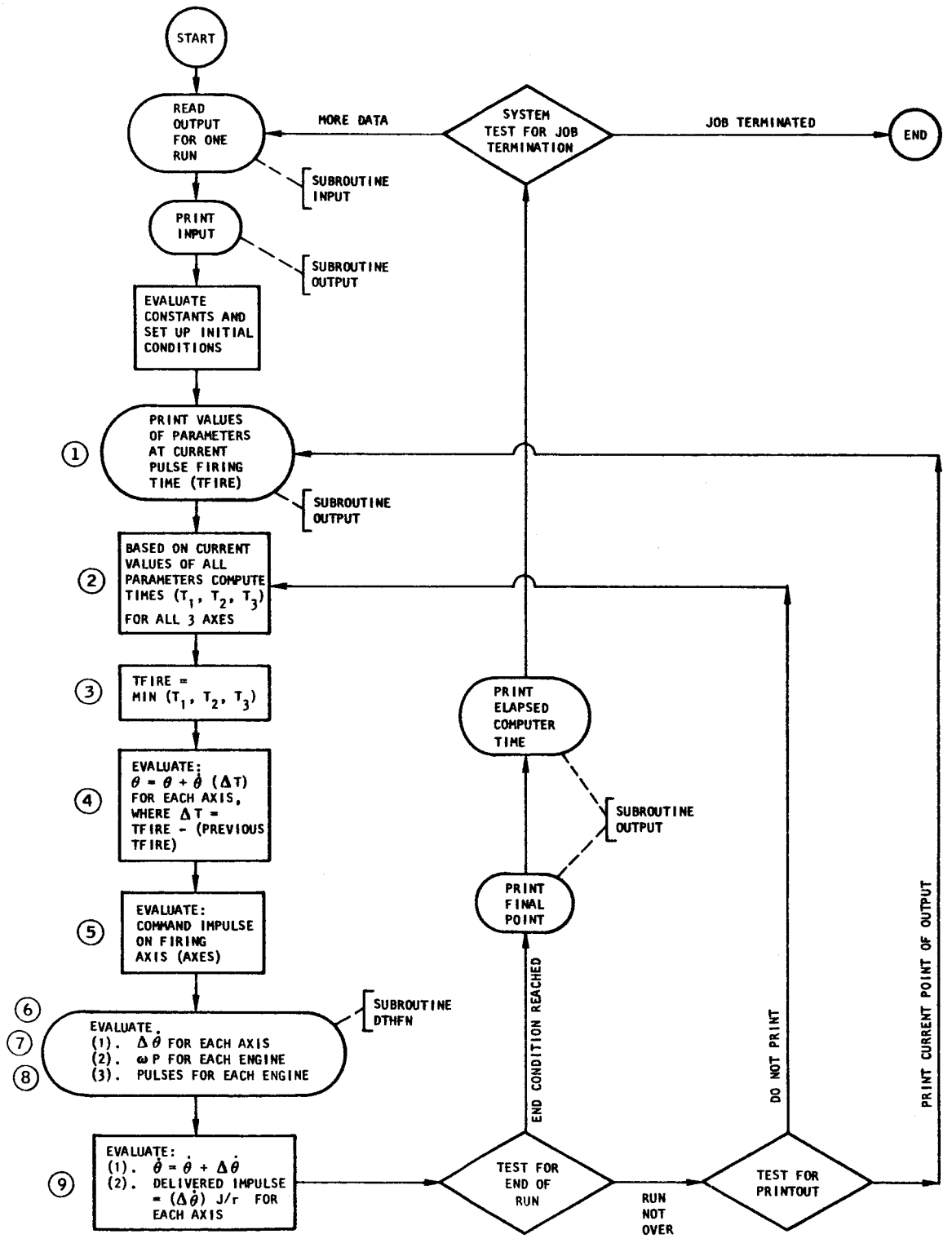

TMC A673

FIGURE 9

WEIGHTING FUNCTION FOR IMPULSE ERROR SOURCE

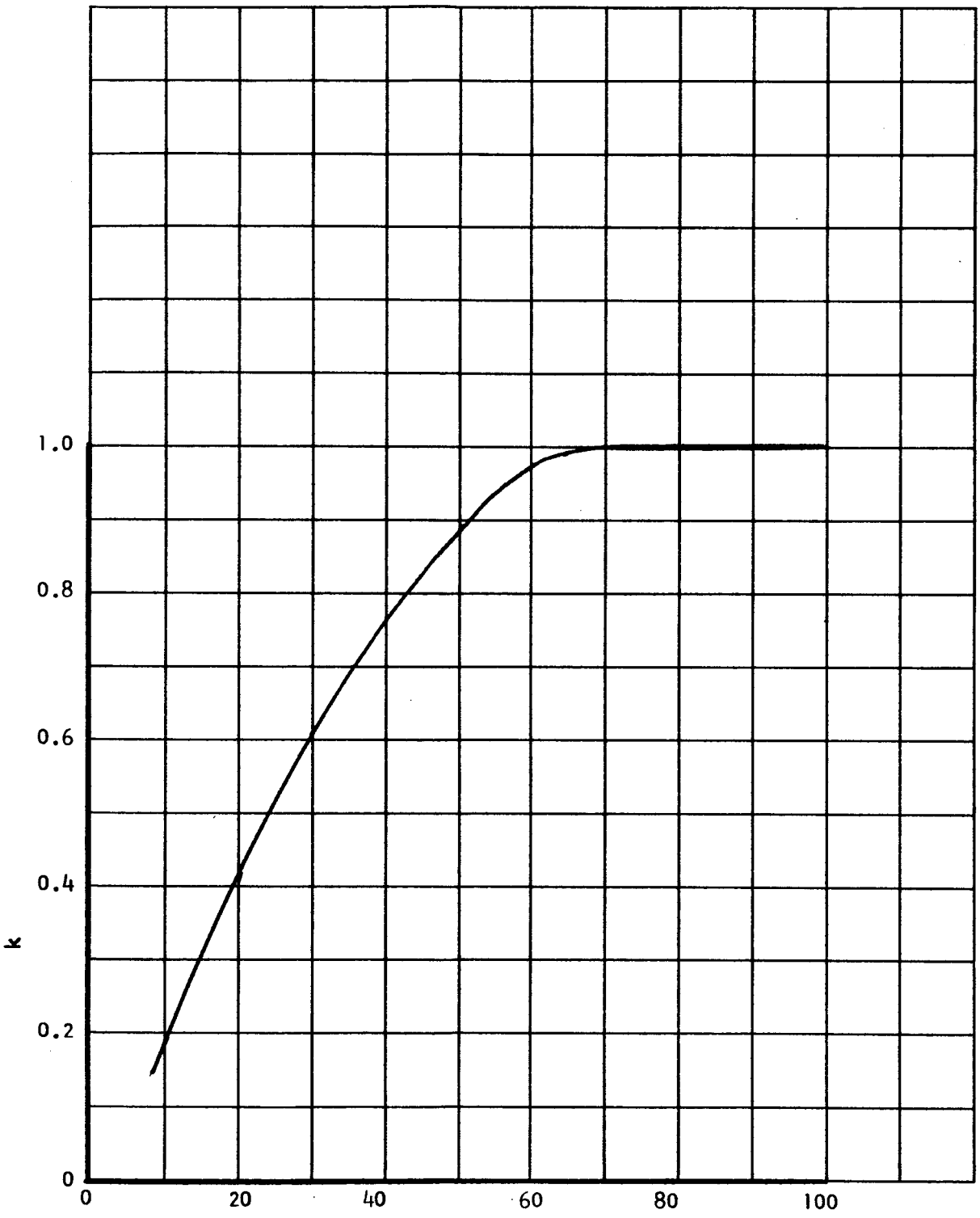

TMC A673

FIGURE 10

PROPELLANT CONSUMPTION RATE VS MISSION TIME --- SYSTEMS 1, 2, AND 3

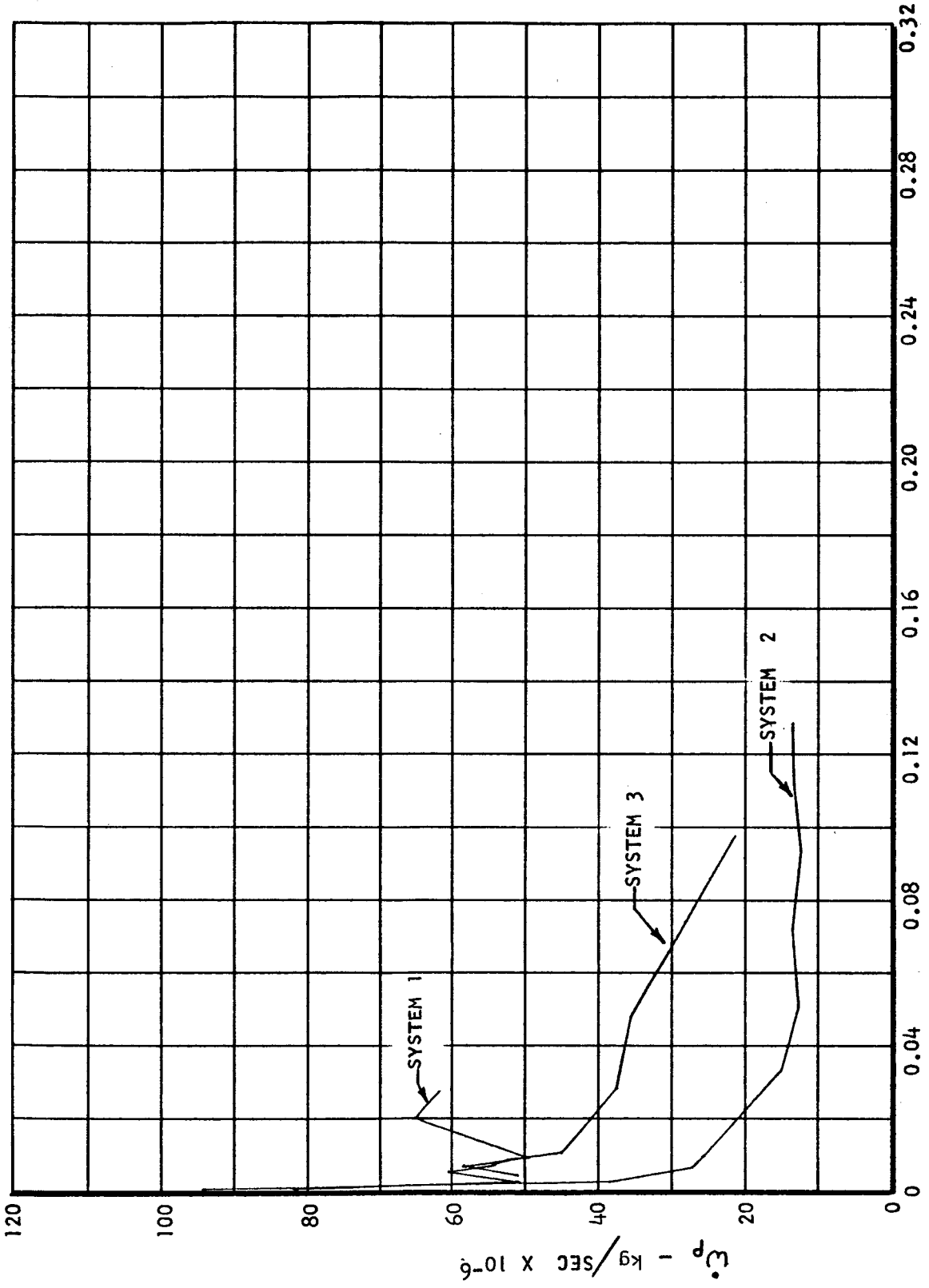

TMC A673

FIGURE 11

PROPELLANT CONSUMPTION RATE VS MISSION TIME --- SYSTEM 4

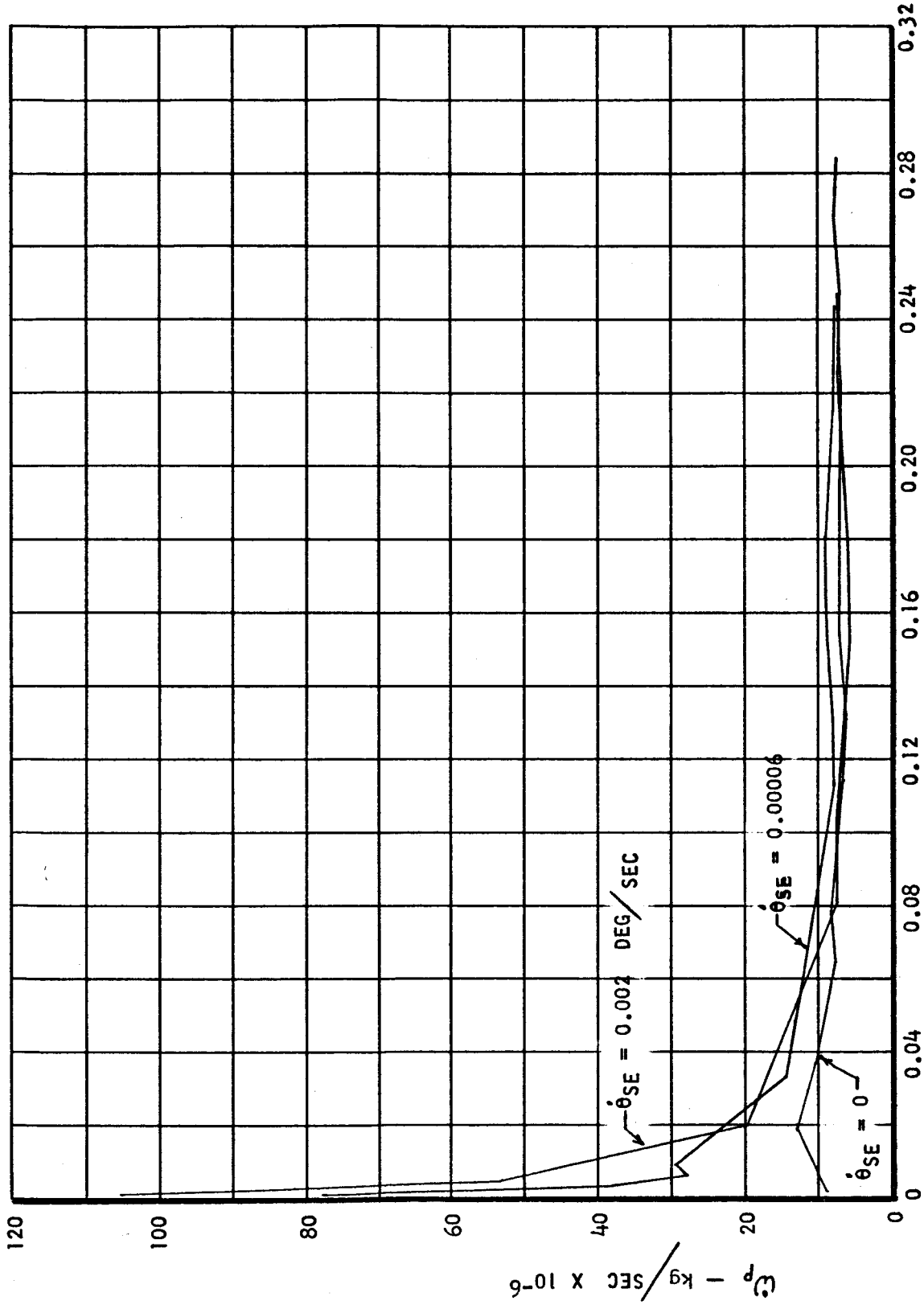

TMC A673

FIGURE 12

CONTROL SYSTEM COMPARATIVE TREND

FINAL PULSE VALUES - (100 PULSES)

$I_{T(MINIMUM)}$ = 2.04 kg/SEC

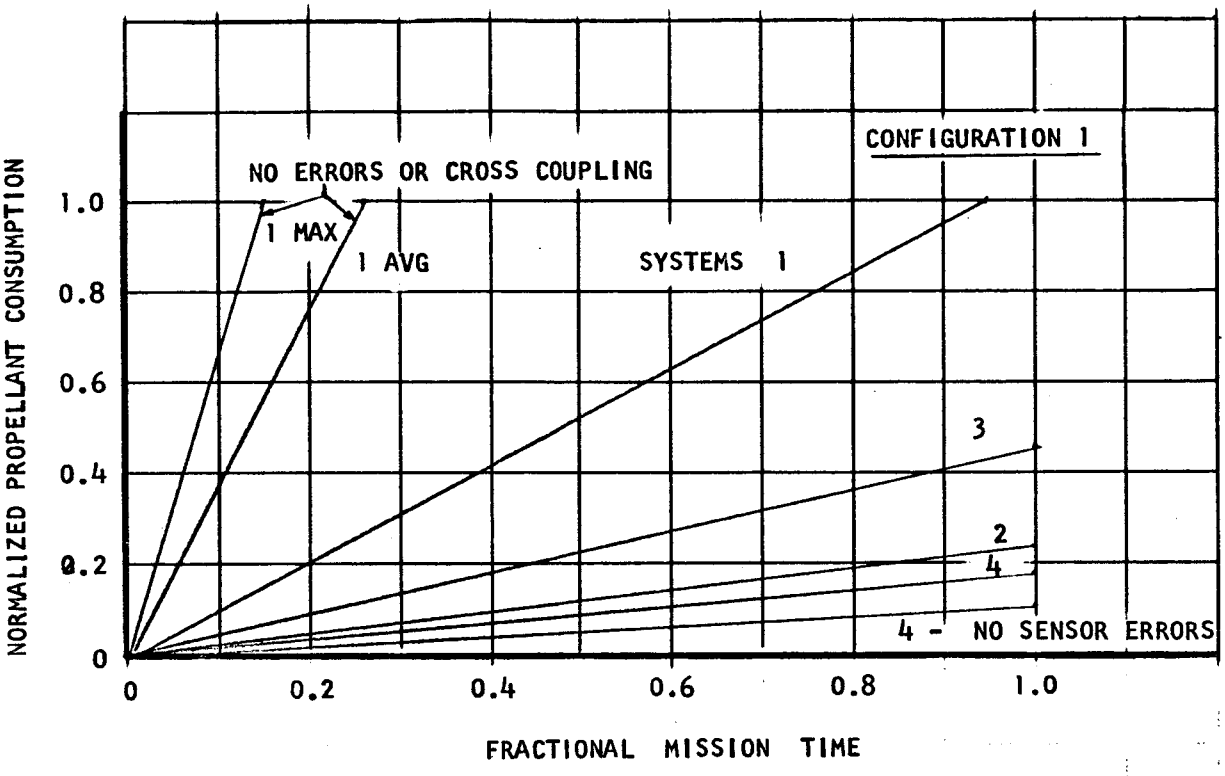

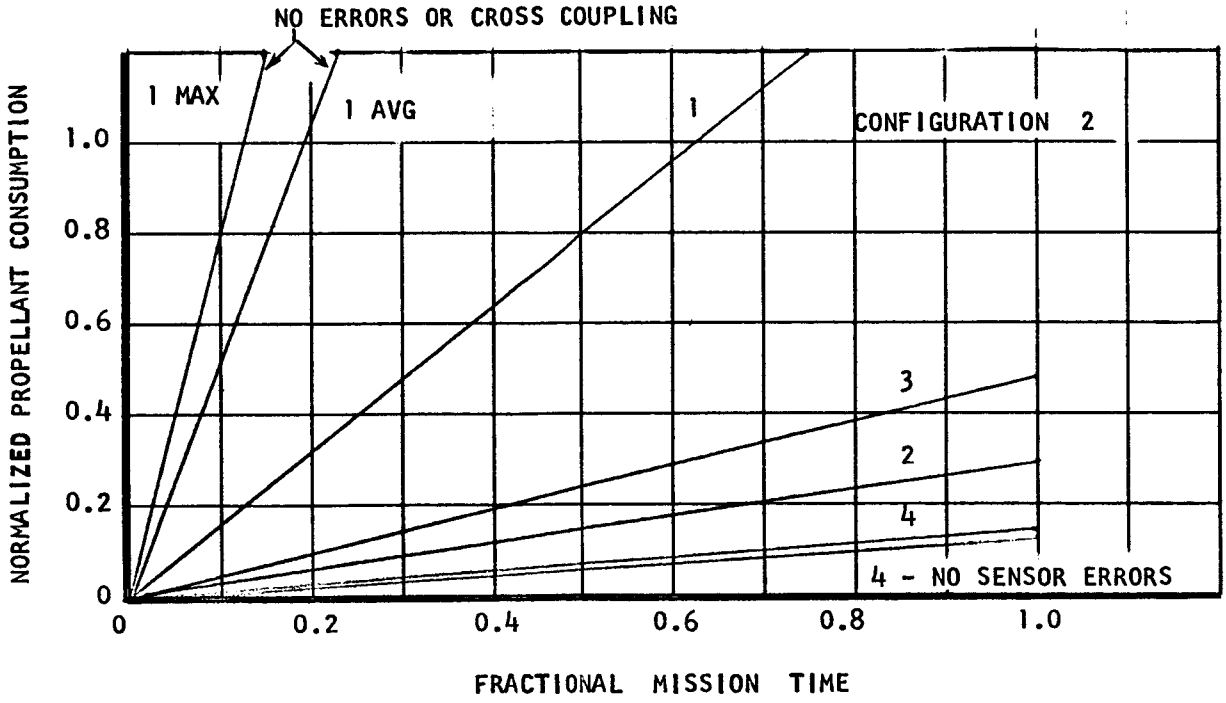

TMC A673

PROPELLANT CONSUMPTION RATE VS MISSION TIME

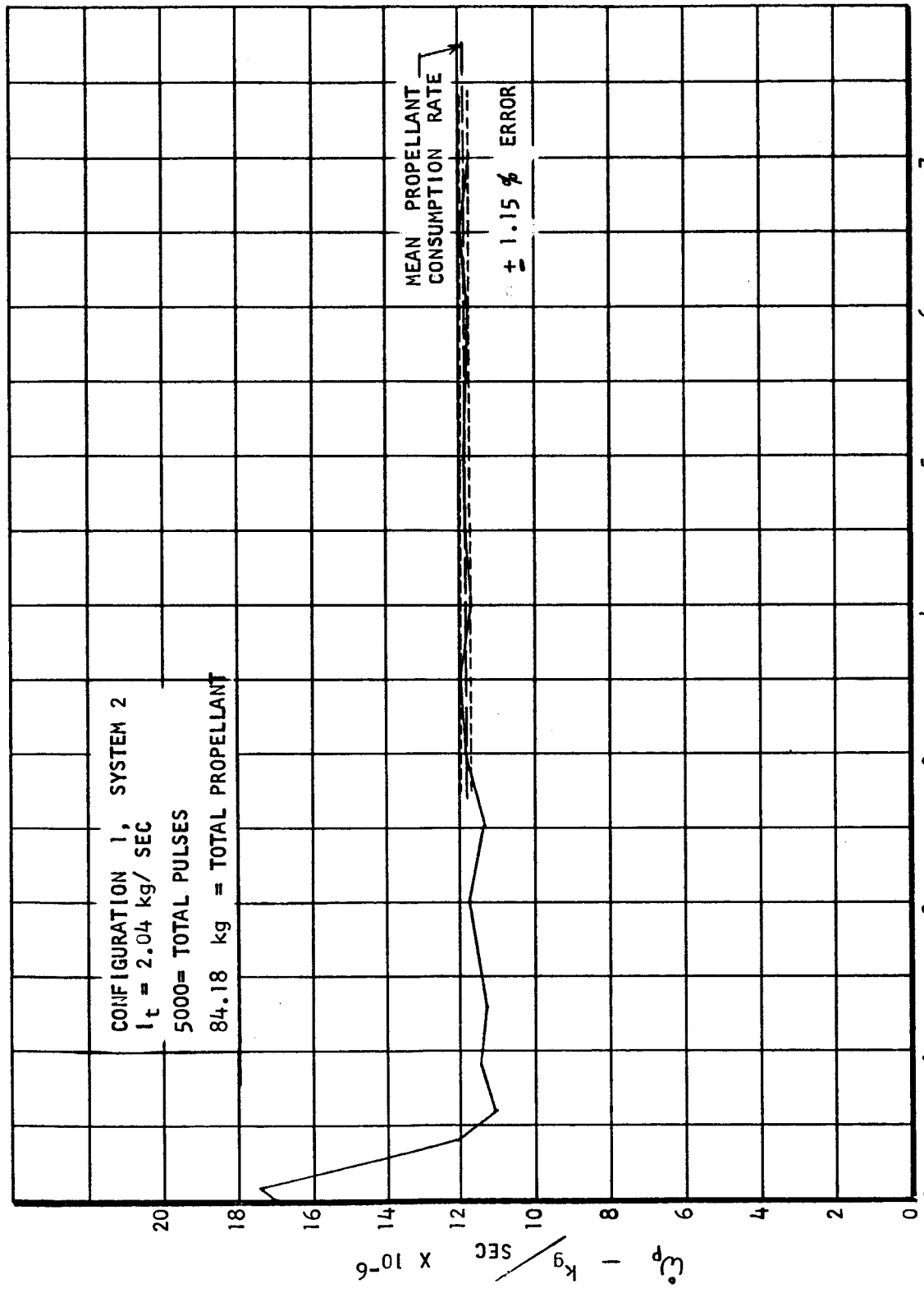

TMC A 673

FIGURE 14

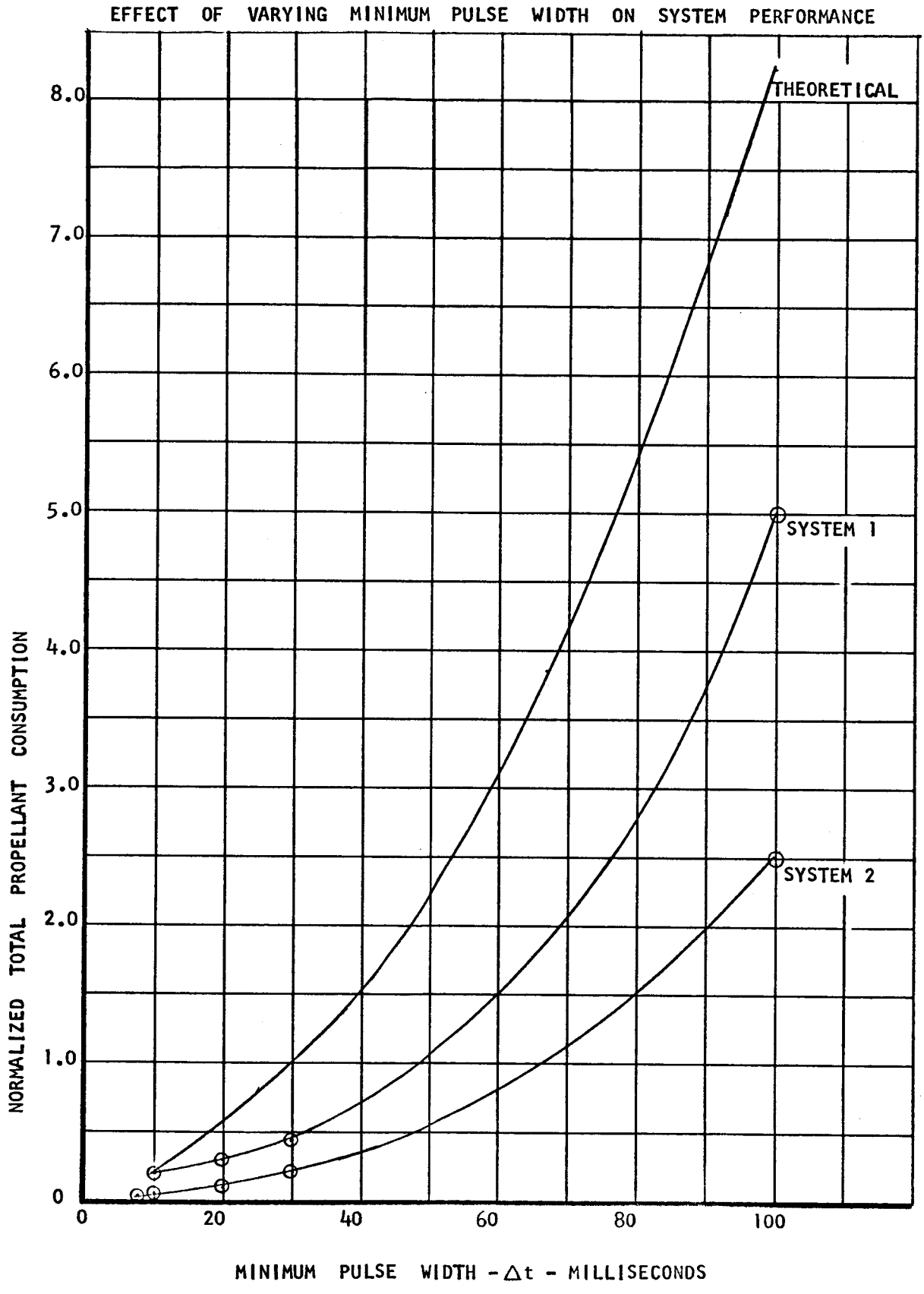

TMC A673

FIGURE 15

EFFECT OF VARYING ACCURACY DEAD BAND AND THRUST VECTOR ANGULAR ERROR

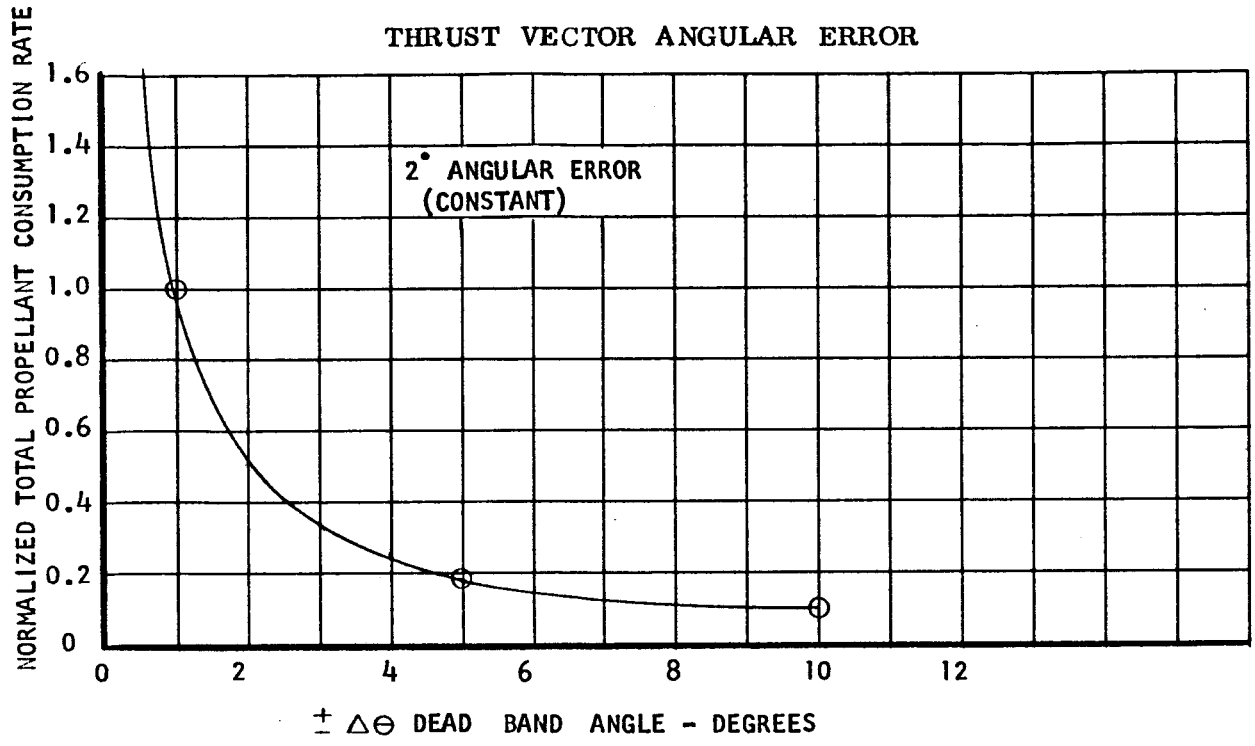

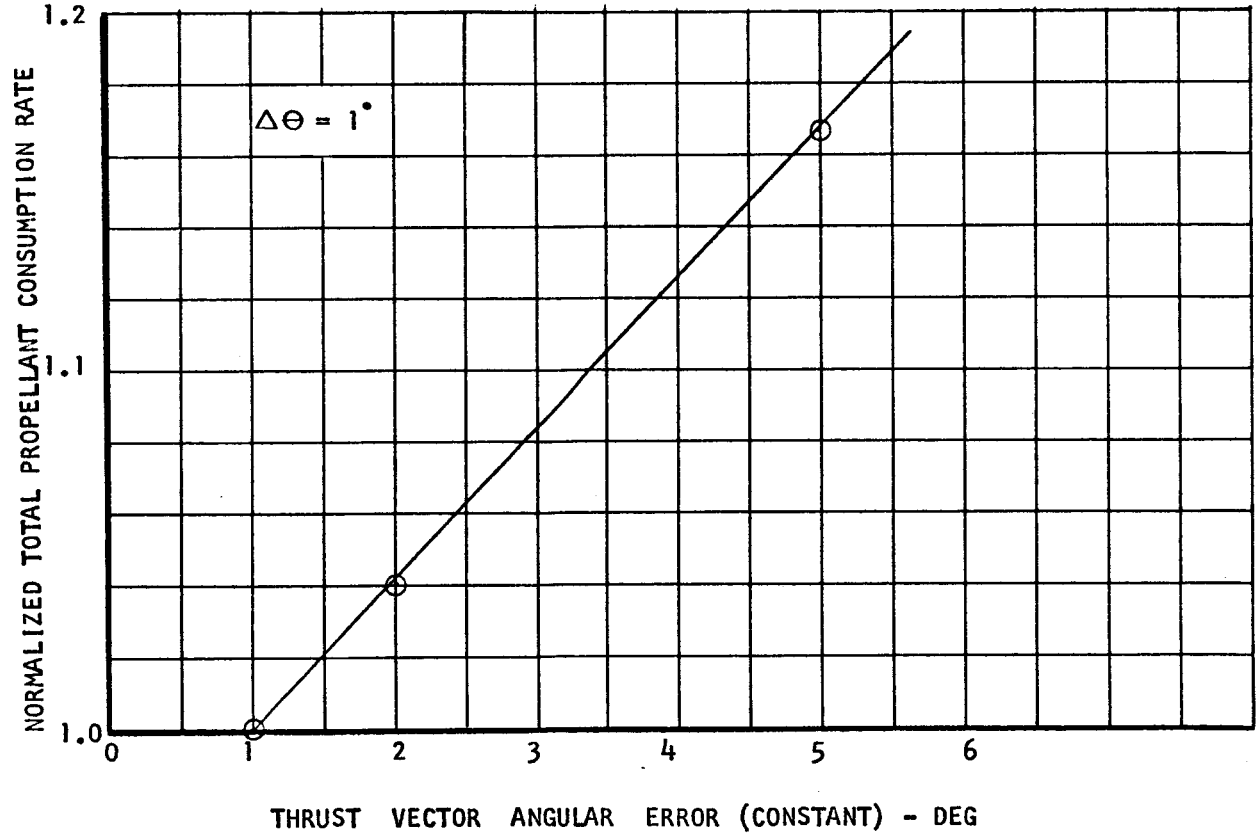

TMC A673

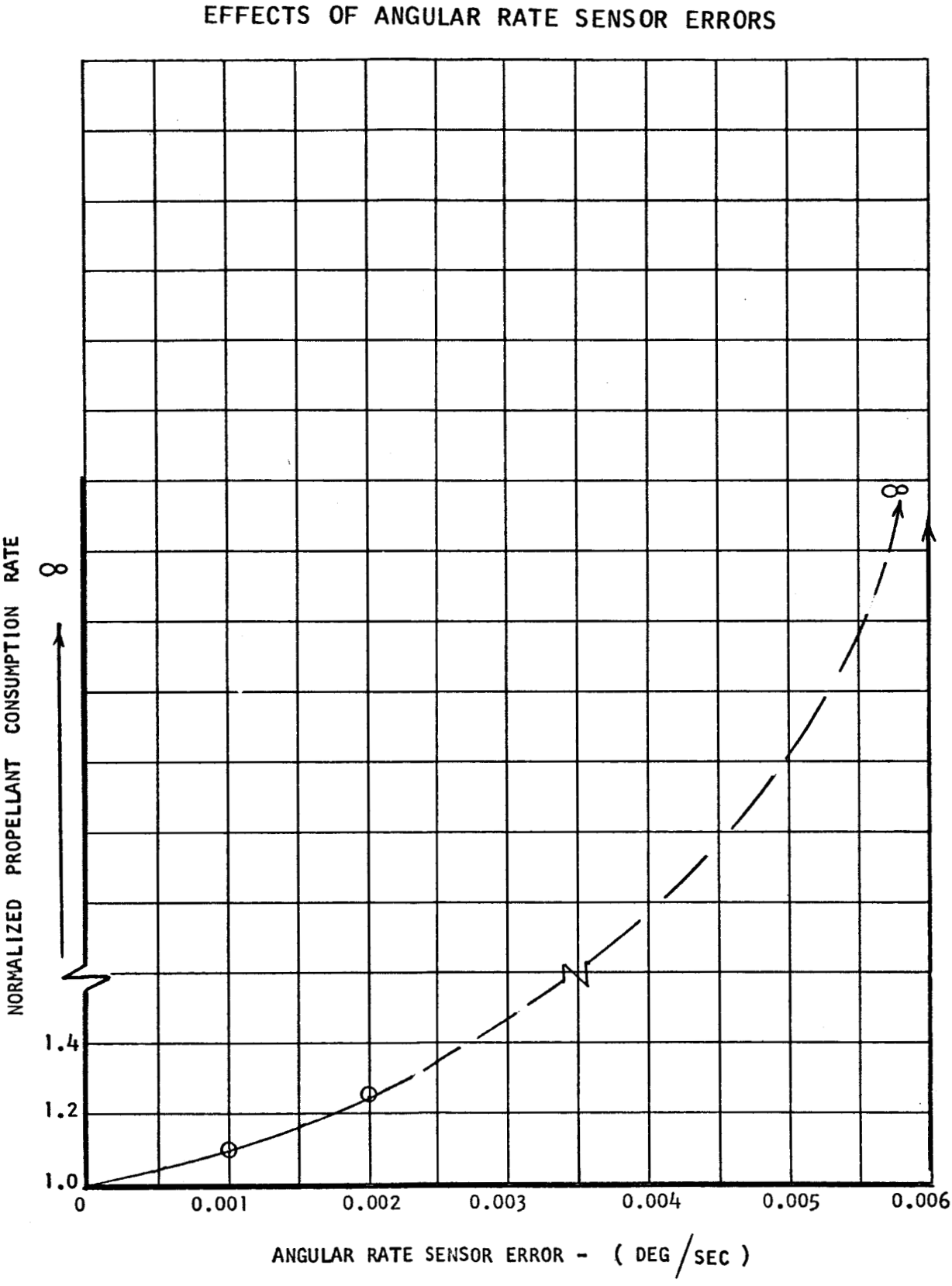

TMC A 673

FIGURE 17

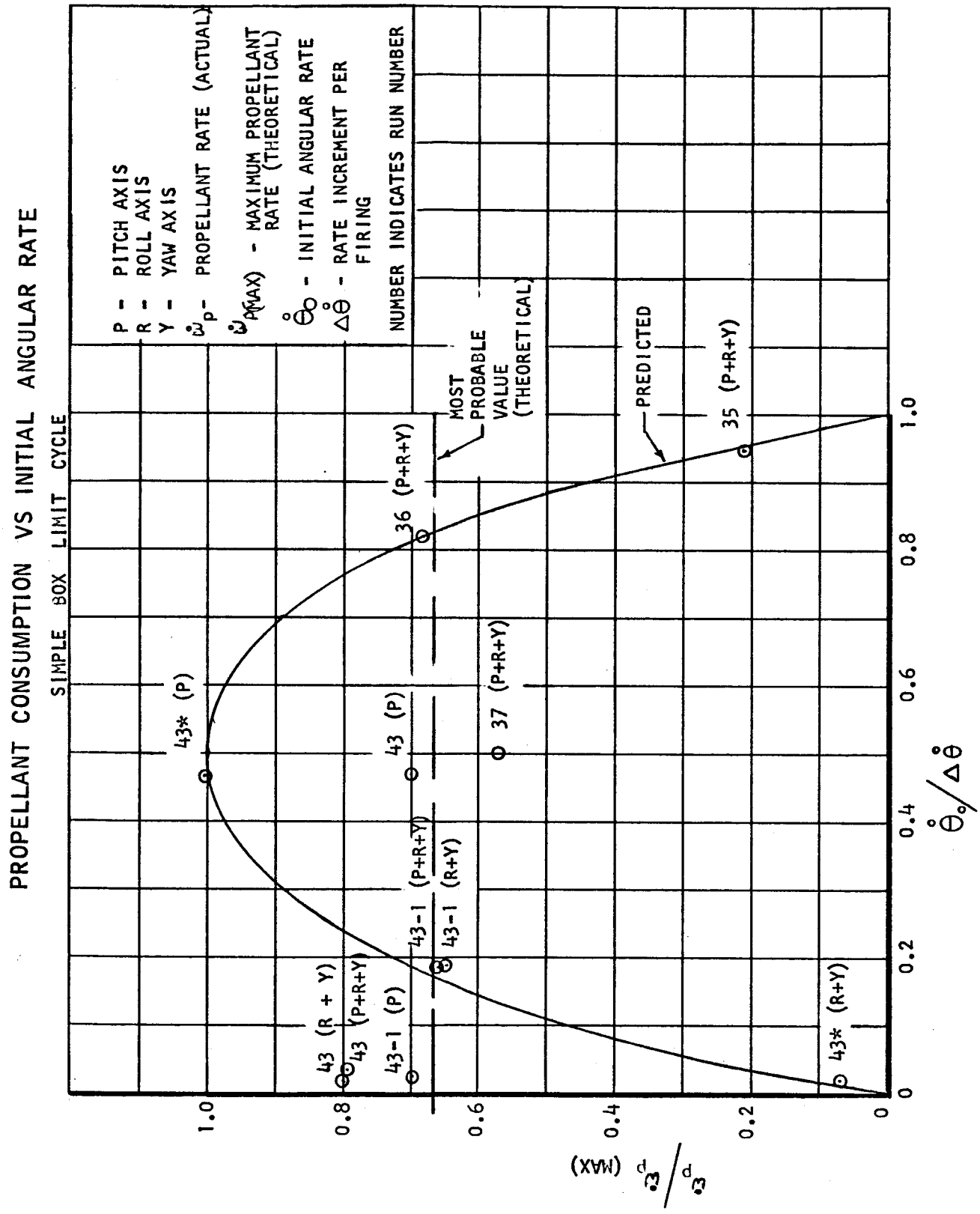

TMC A673

FIGURE 18

PHASE PLANE — SYSTEM I --- ROLL

t_1 = 407,049 SECONDS

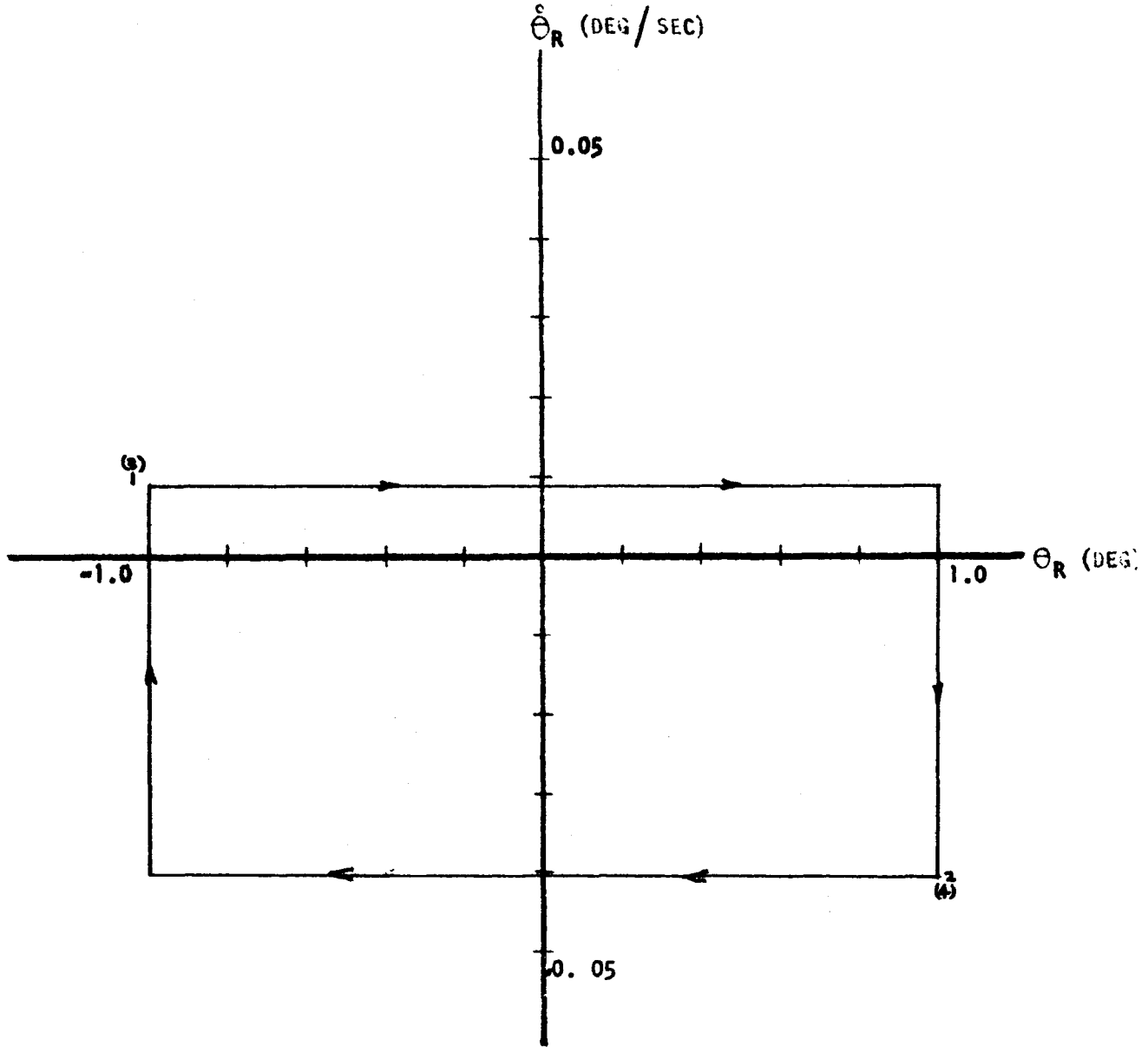

TMC A673

FIGURE 19

PHASE PLANE — SYSTEM I ---YAW

t_1 = 403,456 SECONDS

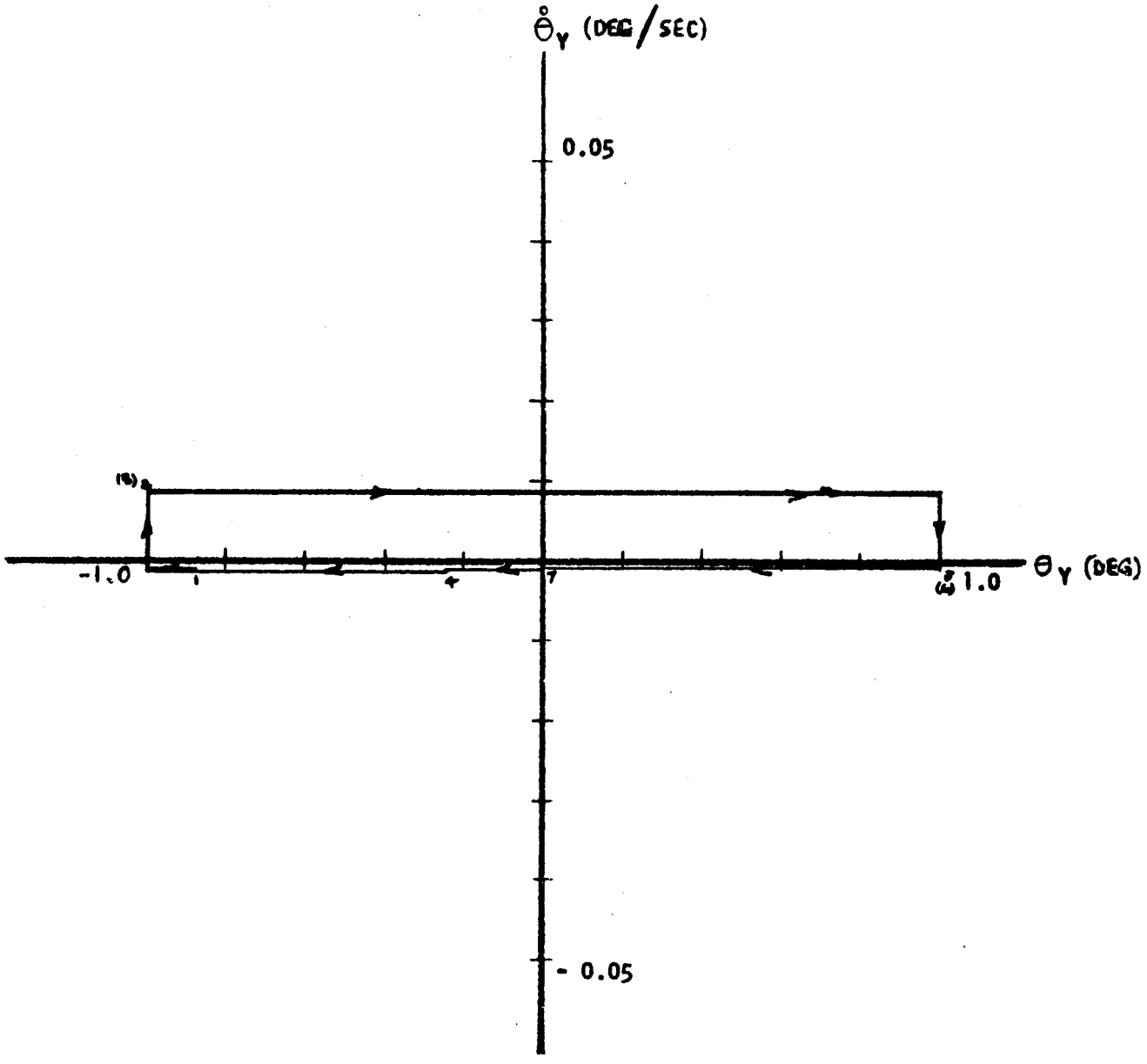

TMC A673

FIGURE 20

PHASE PLANE — SYSTEM I ---- PITCH

t_1 = 398,532 SECONDS

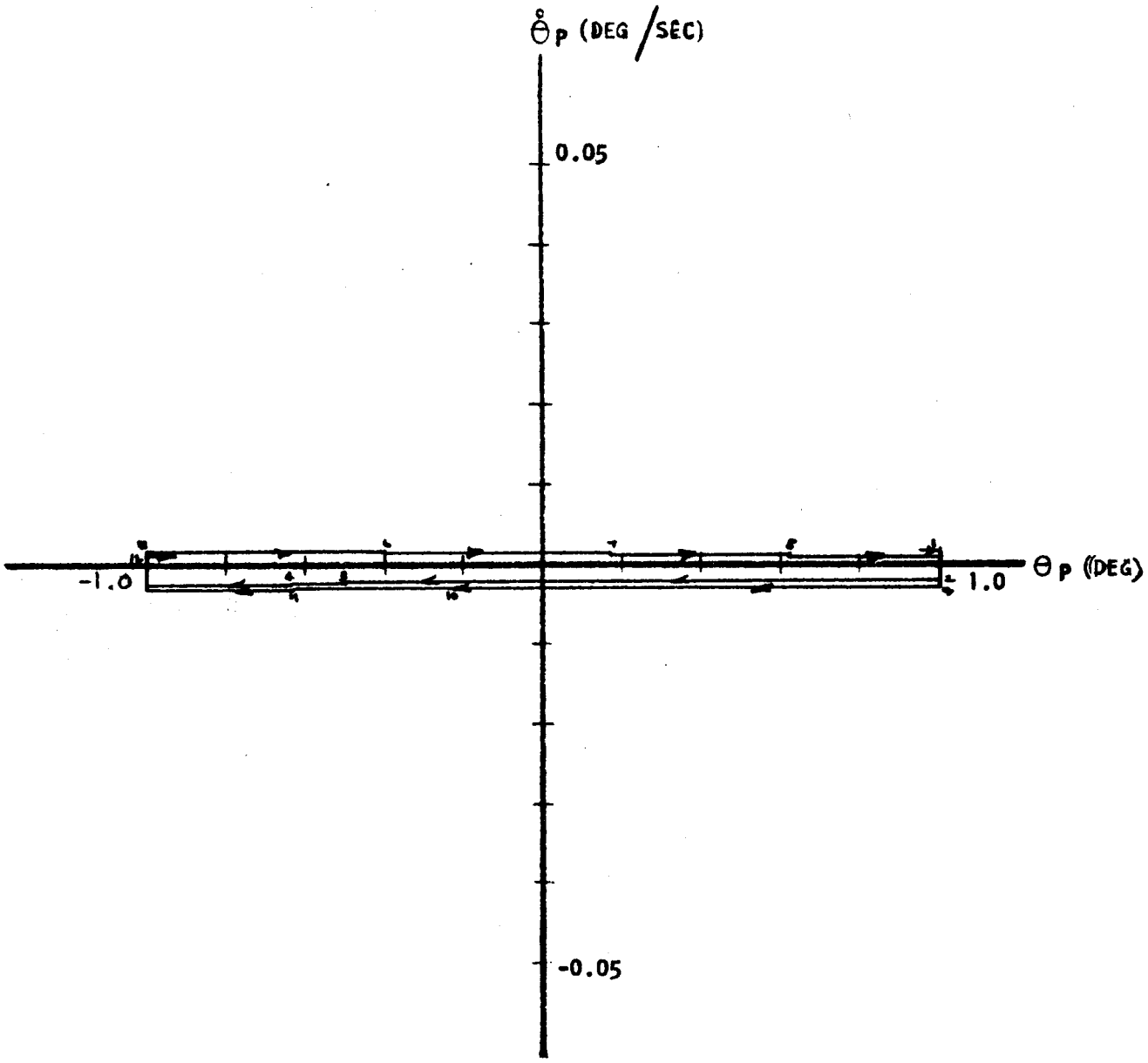

TMC A673

FIGURE 21

PHASE PLANE — SYSTEM 2 ---- ROLL

t_1 = 6,905,625 SECONDS

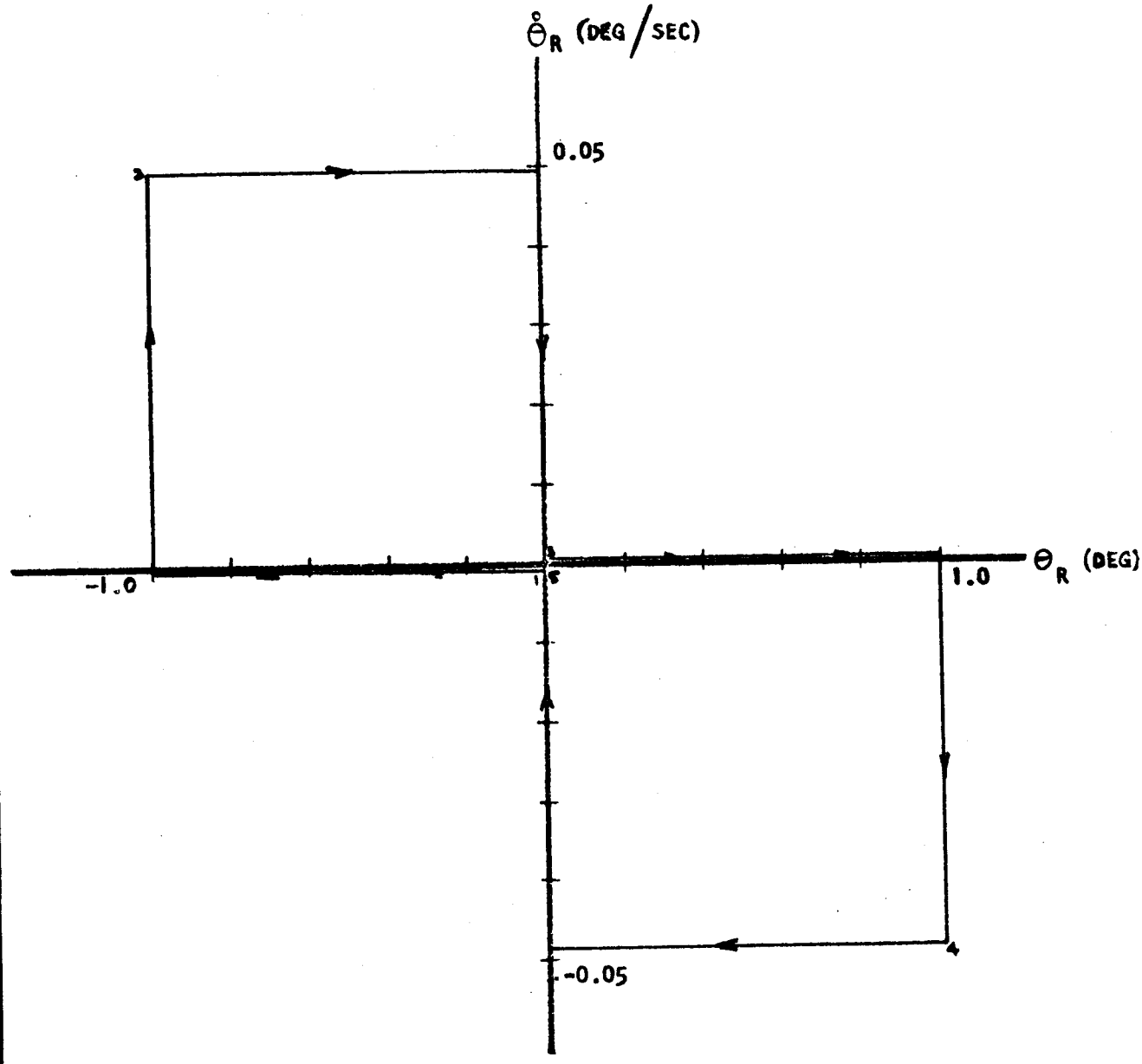

TMC A673

FIGURE 22

PHASE PLANE — SYSTEM 3 ---- ROLL

t_1 = 5,132,164 SECONDS

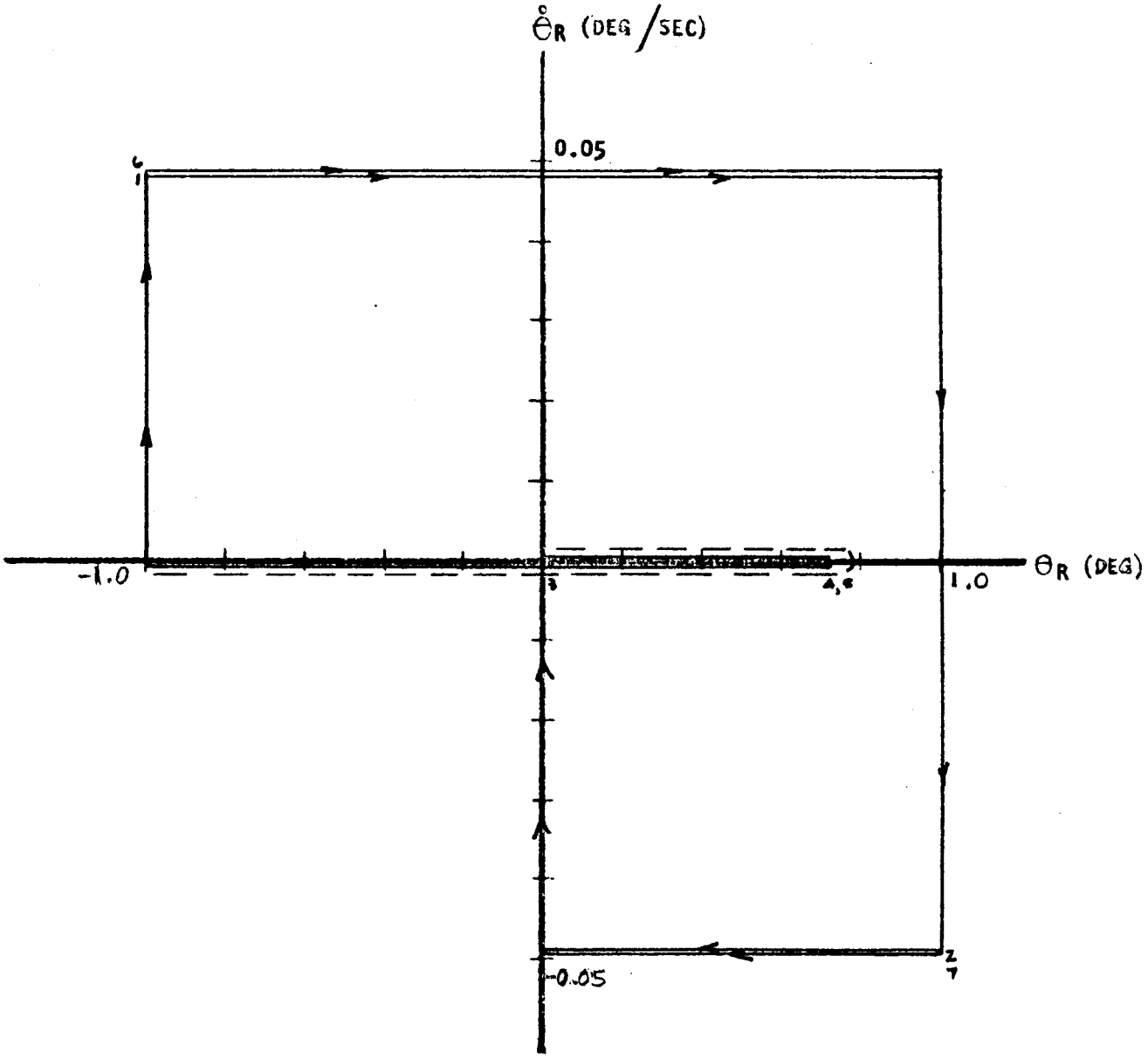

FIGURE 23

PHASE PLANE — SYSTEM 4 ---- ROLL

t_1 = 6,588,433 SECONDS

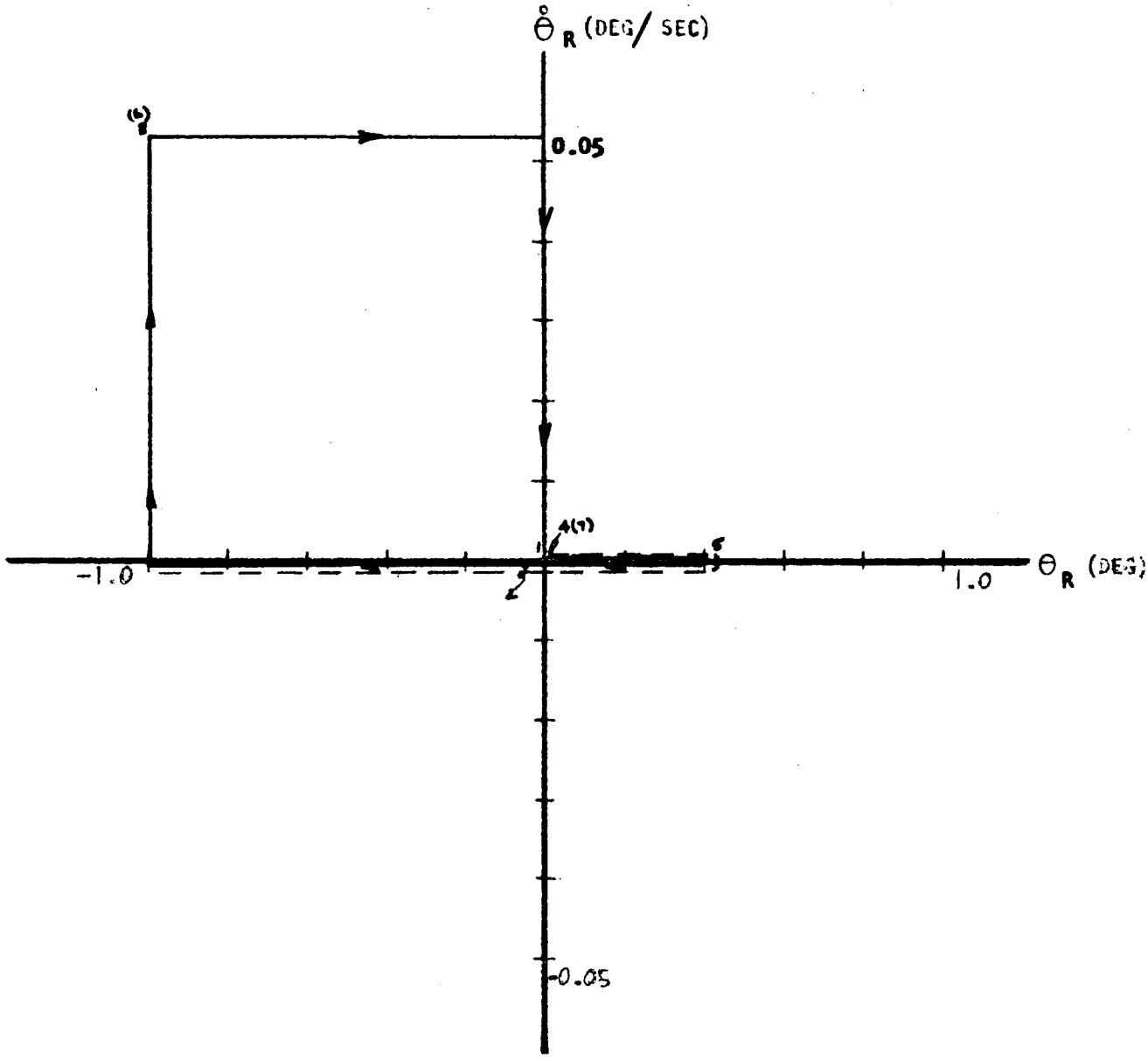

TMC A673

FIGURE 24

PHASE PLANE — SYSTEM 5 --- ROLL

t_1 = 832,512 SECONDS

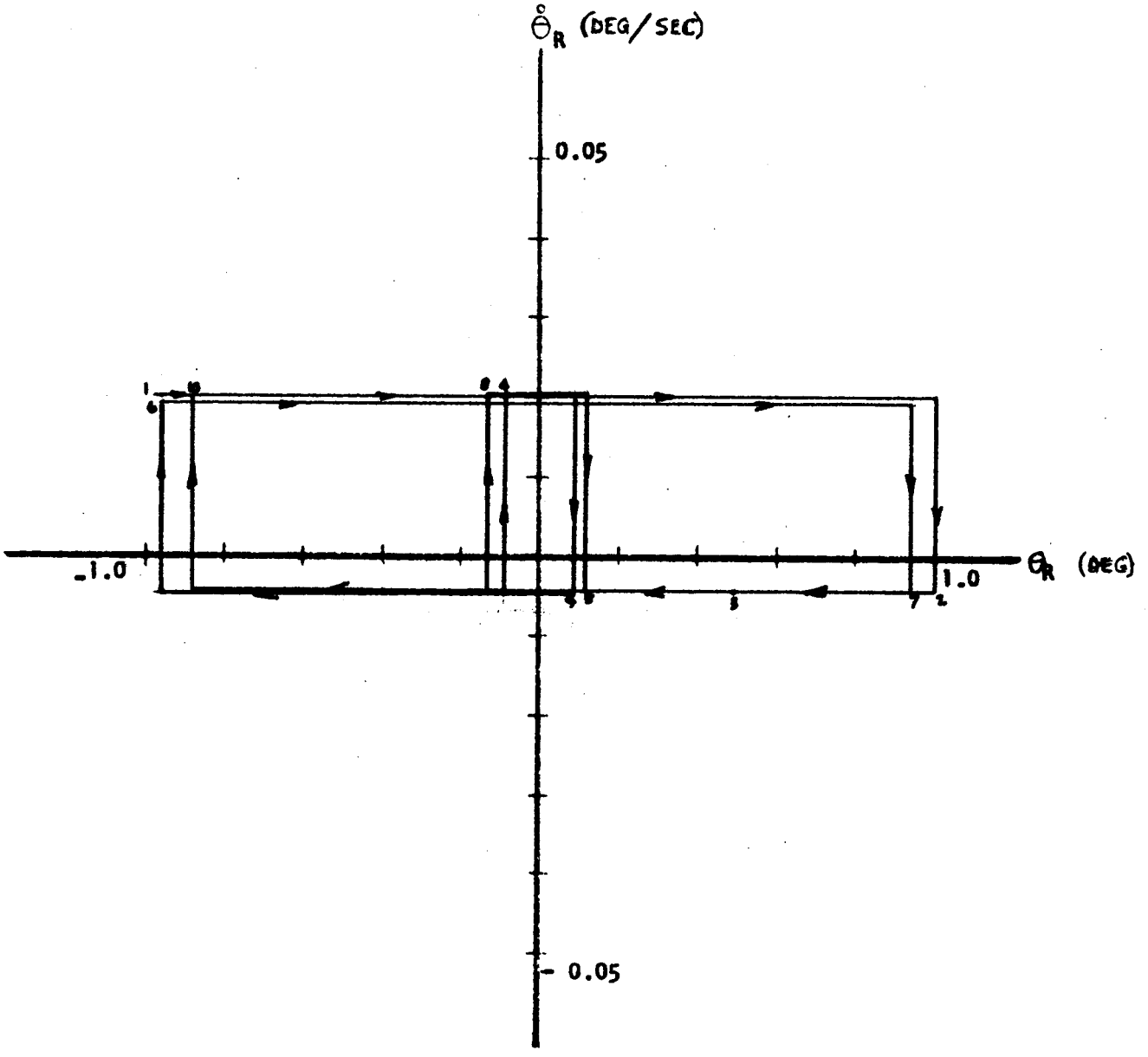

TMC A673

PHASE PLANE — SYSTEM 5 -- YAW AXIS

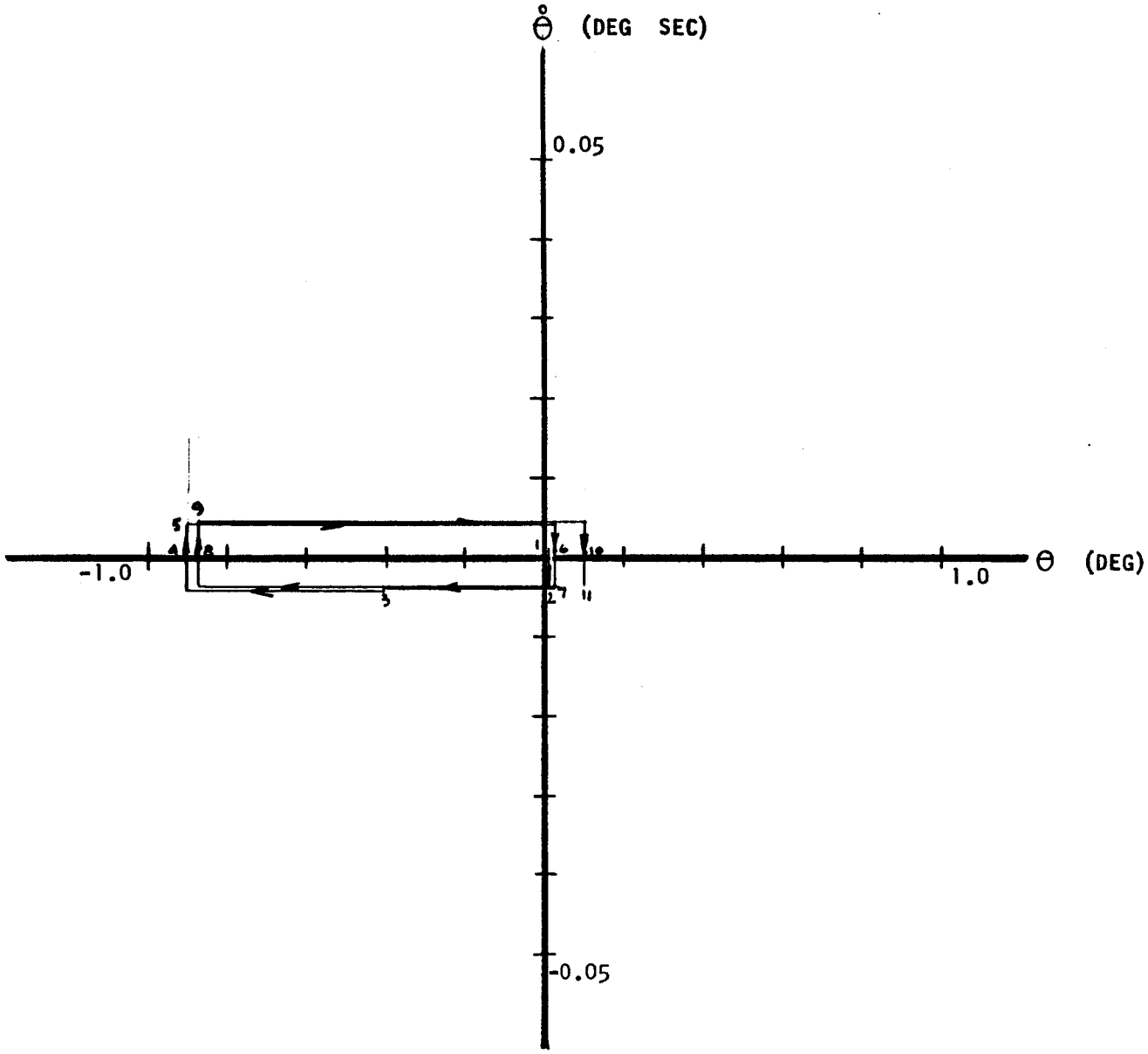

TMC A673

FIGURE 26

PHASE PLANE — SYSTEM 5 ---- PITCH

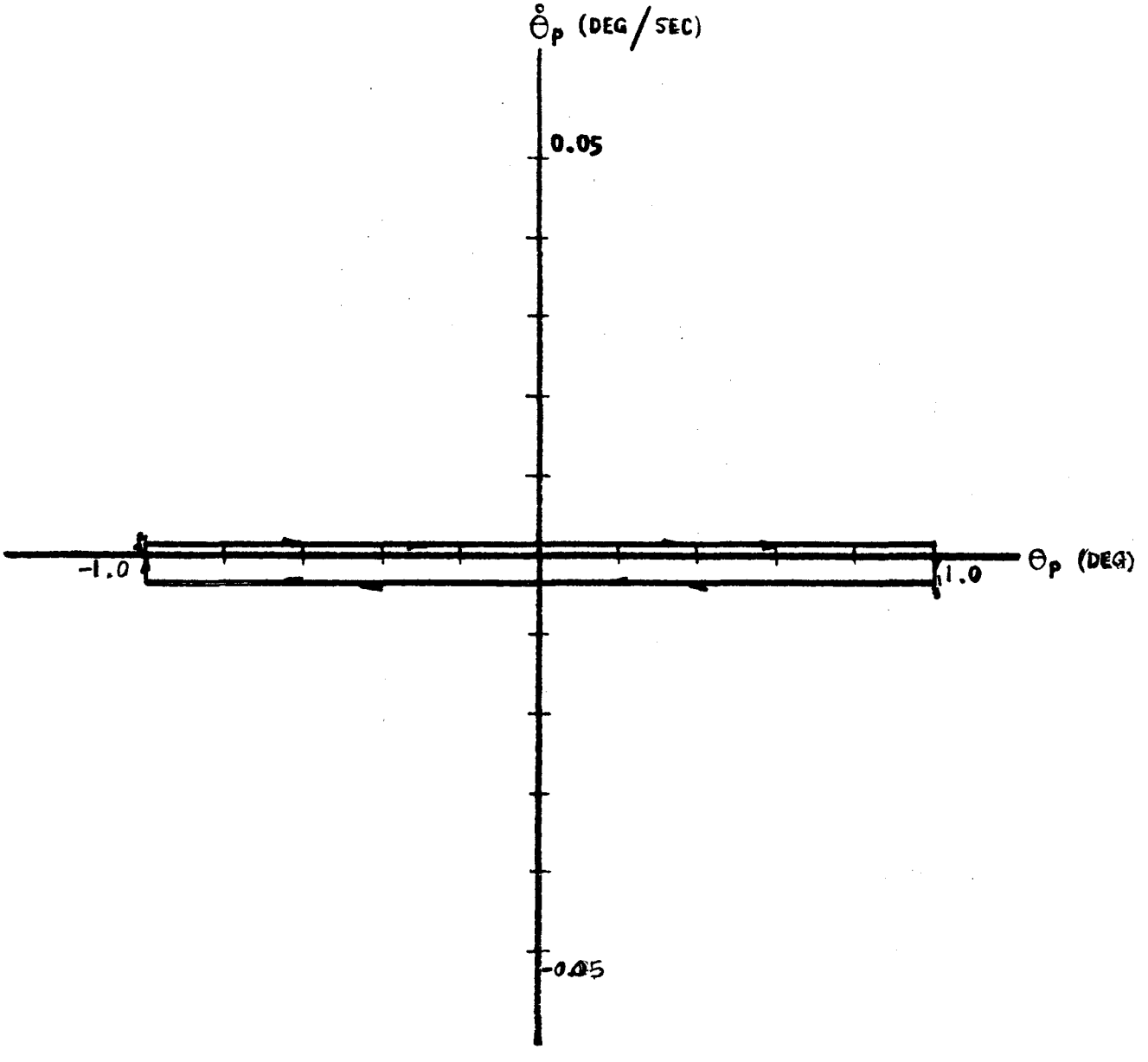

TMC A673

FIGURE 27

COMBINED ROLL-YAW PLANE ----SYSTEM 5

NO ERRORS OR RATE SWITCHING

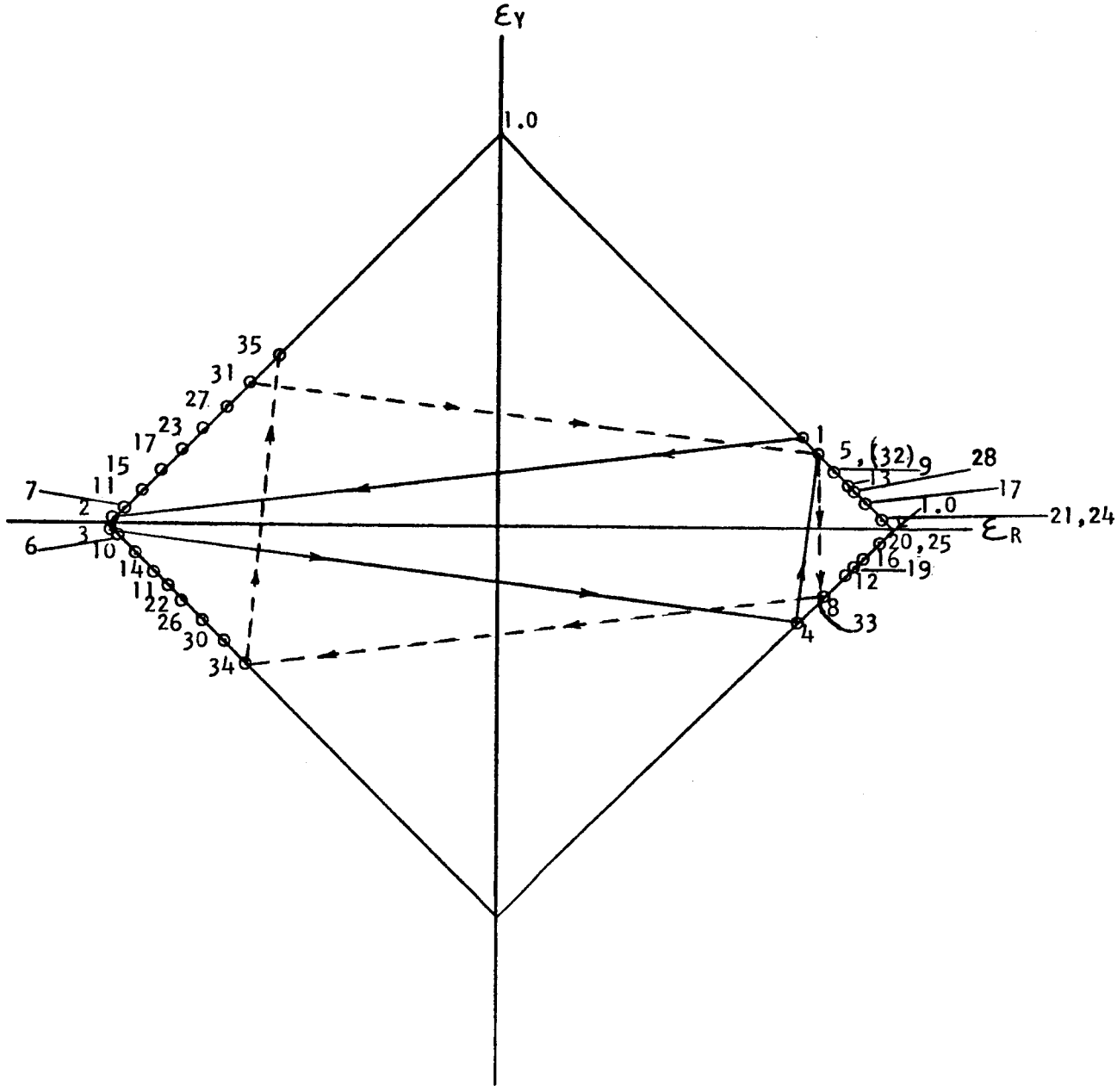

TMC A673

COMBINED ROLL-YAW PLANE ----SYSTEM 5
ERRORS --- NO RATE SWITCHING

t_1 (BEGINNING OF RUN) = 3,143 SEC

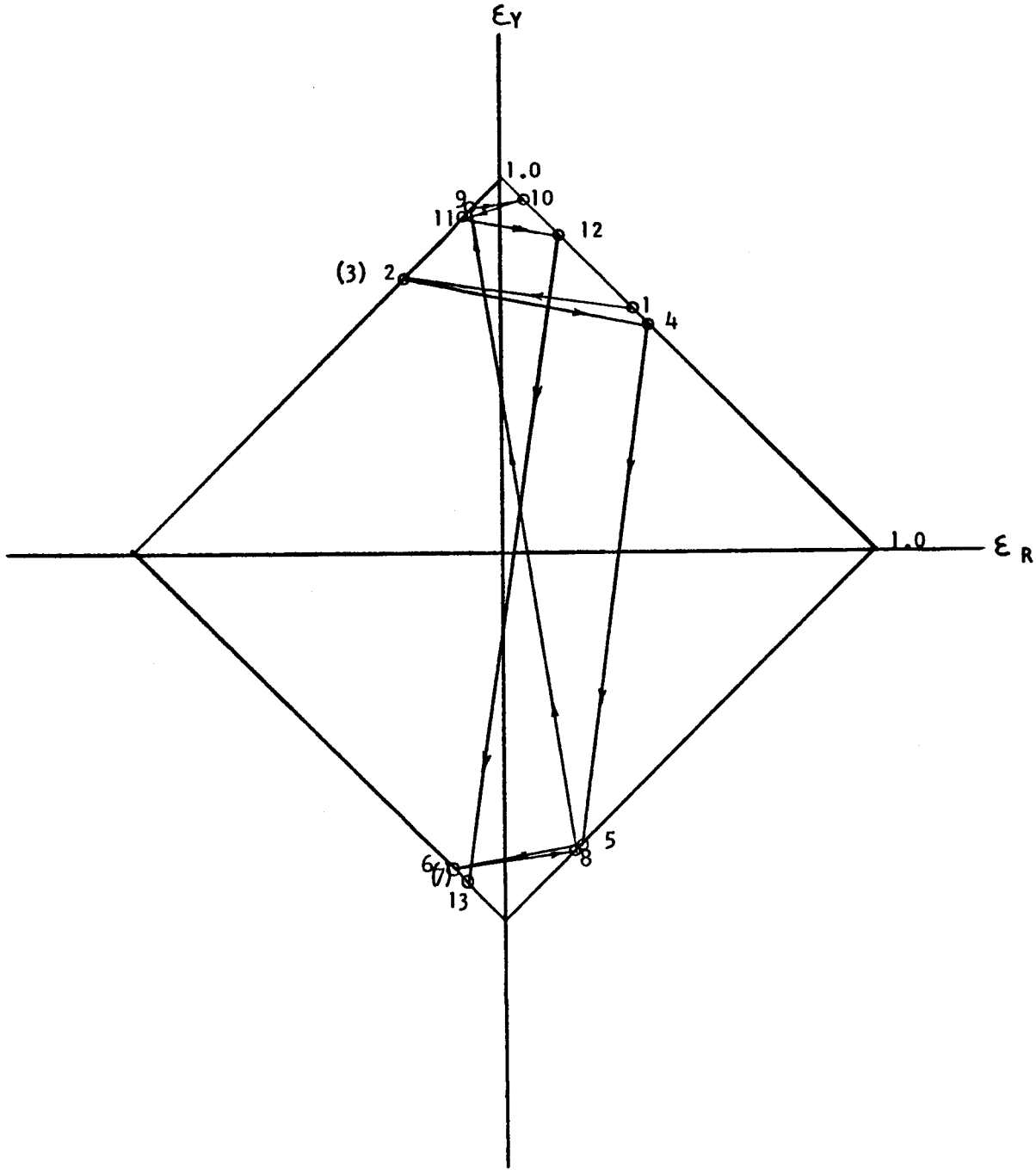

TMC A673

FIGURE 29

COMBINED ROLL-YAW PLANE ----SYSTEM 5
ERRORS --- NO RATE SWITCHING

t_i (END OF RUN) = 832,512 SEC

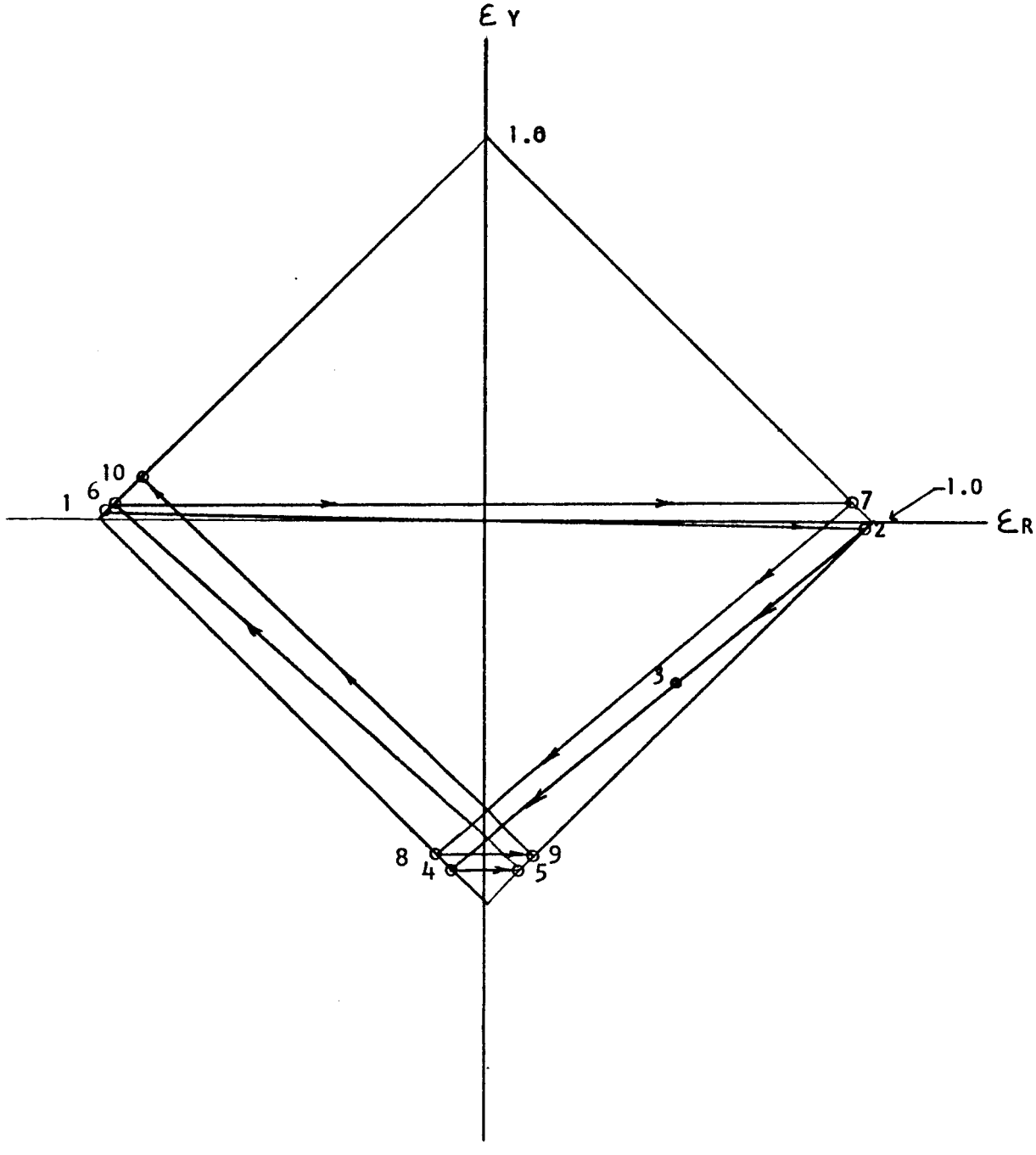

TMC A673

FIGURE 30

INFLUENCE OF RATE SWITCHING FACTORS

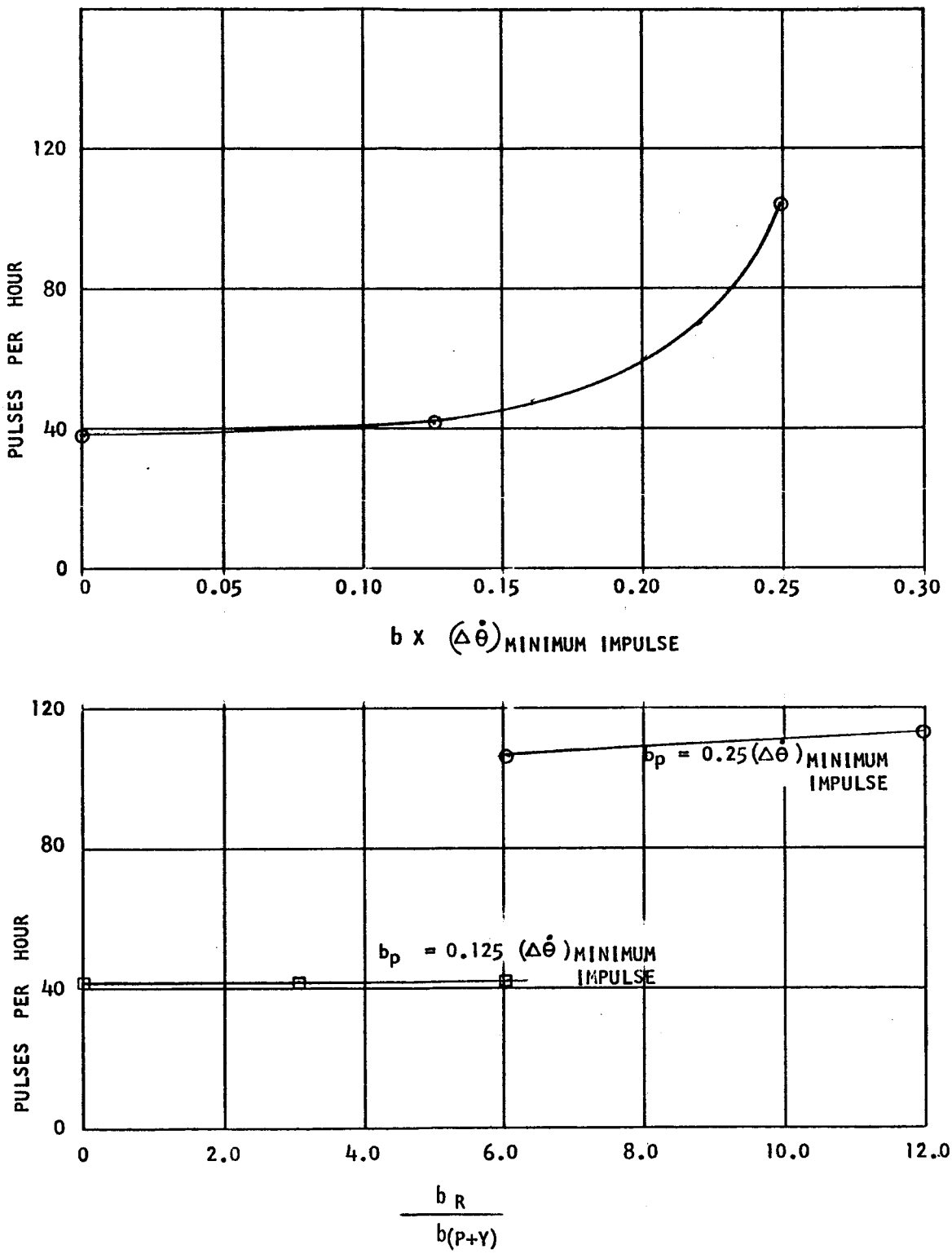

TMC A673

FIGURE 31

PROPELLANT CONSUMPTION COMPARISON - PITCH AXIS

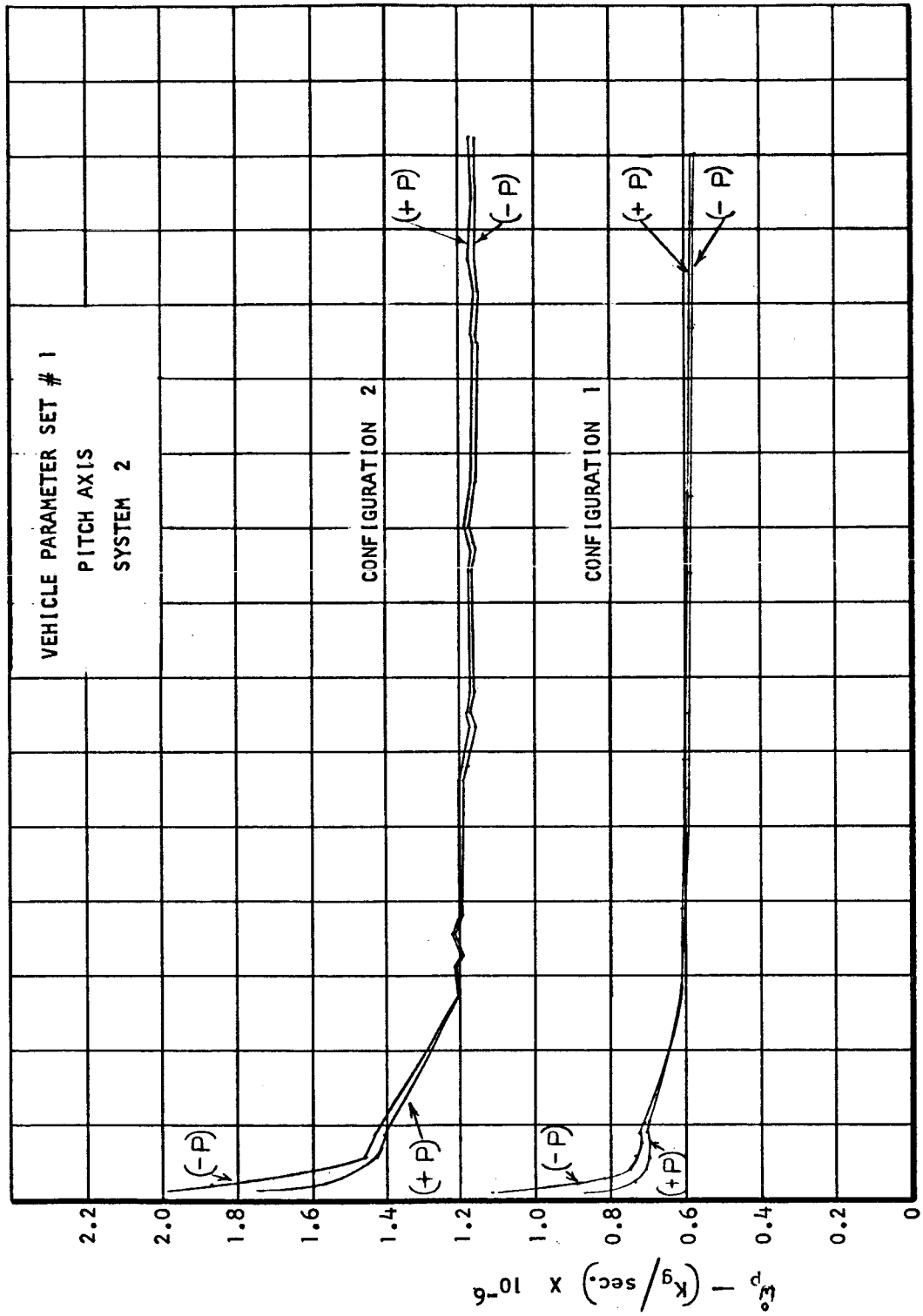

TMC A673

FIGURE 32

MEAN TOTAL PROPELLANT CONSUMPTION RATE VS VEHICLE ANGULAR ACCELERATION --- CONFIGURATION 3

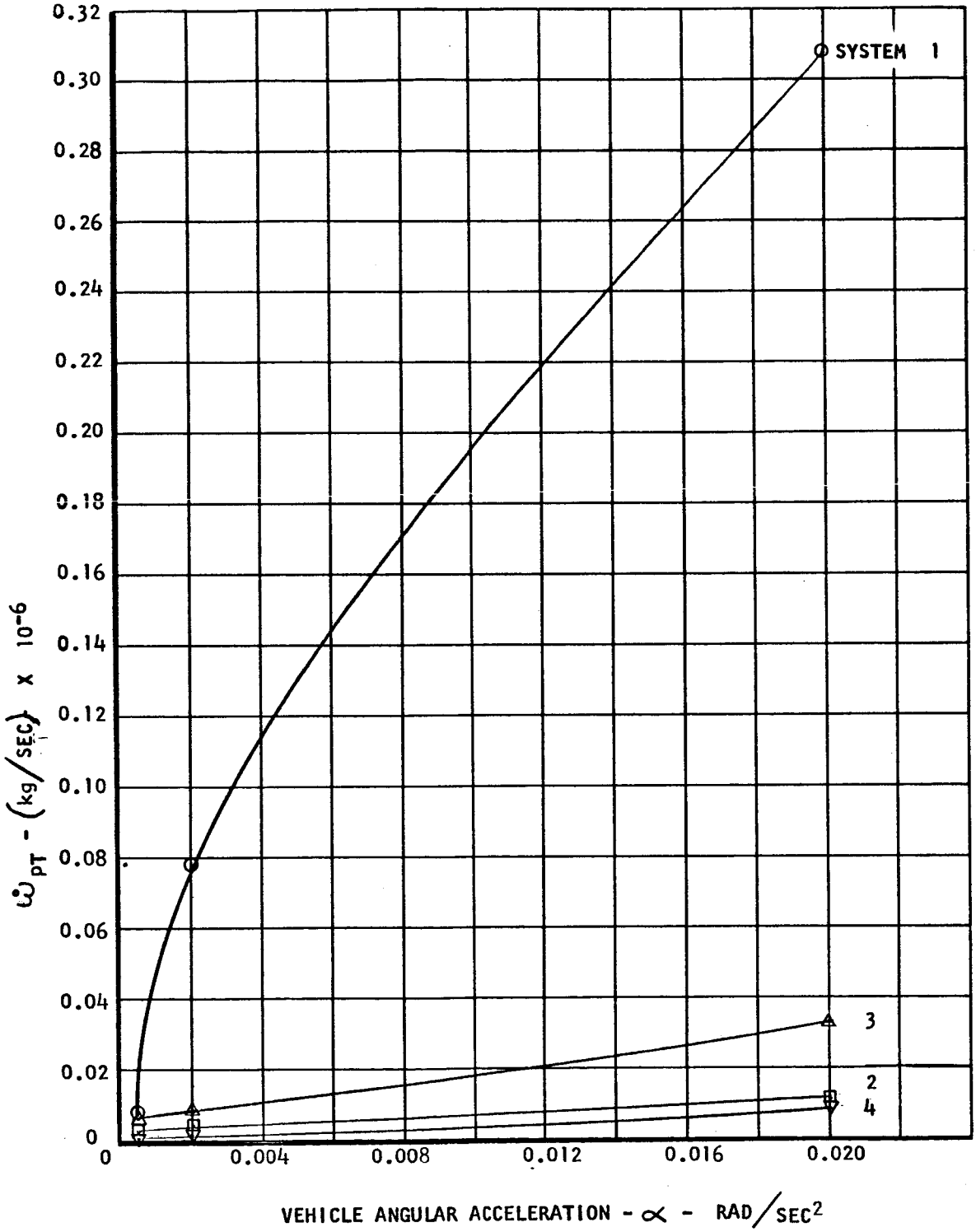

TMC A673

FIGURE 33

TOTAL VEHICLE PULSING FREQUENCY VS VEHICLE ANGULAR ACCELERATION --- CONFIGURATION 3

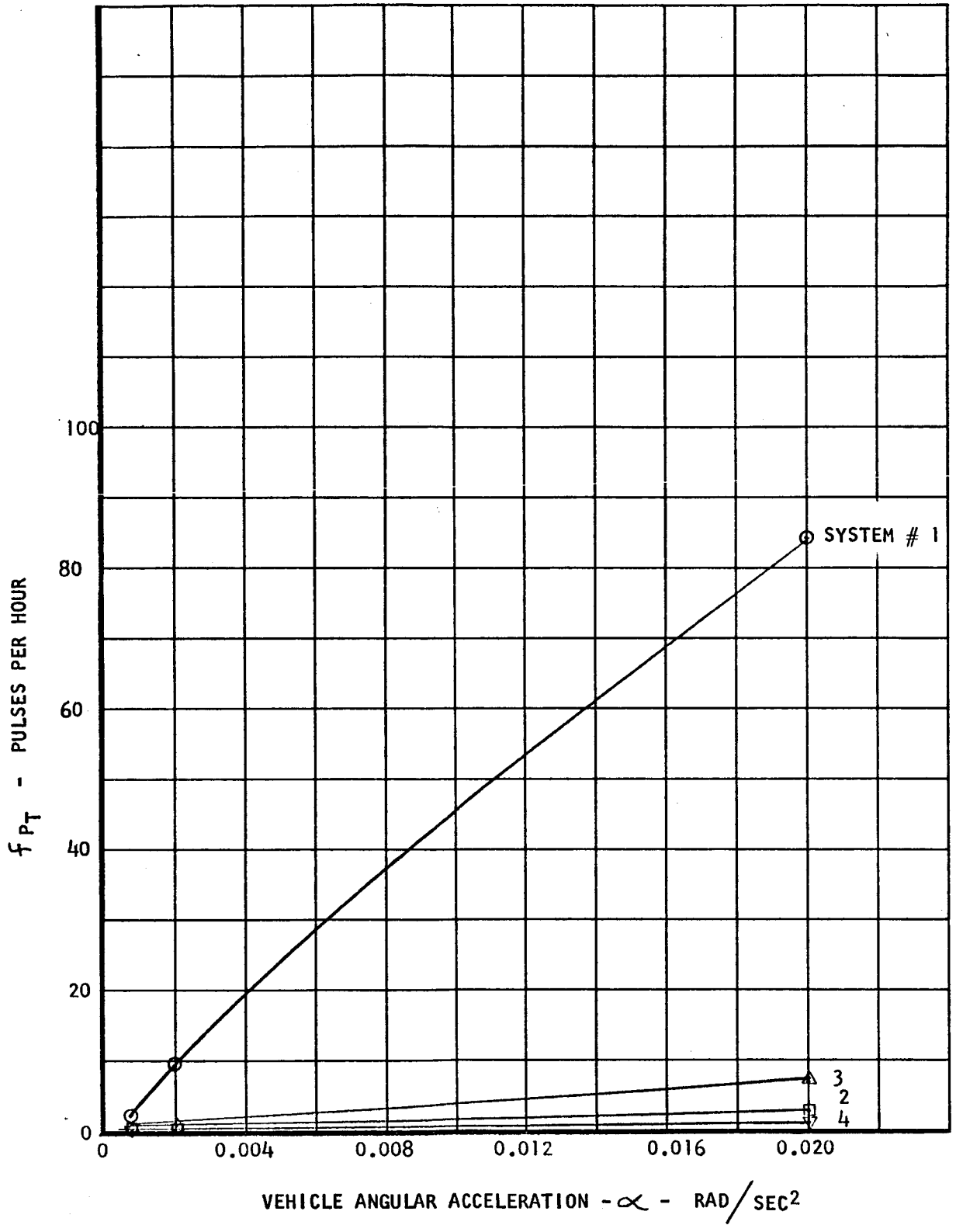

TMC A673

FIGURE 34

MEAN PROPELLANT CONSUMPTION RATE COMPARISON BETWEEN CONTROL SYSTEMS

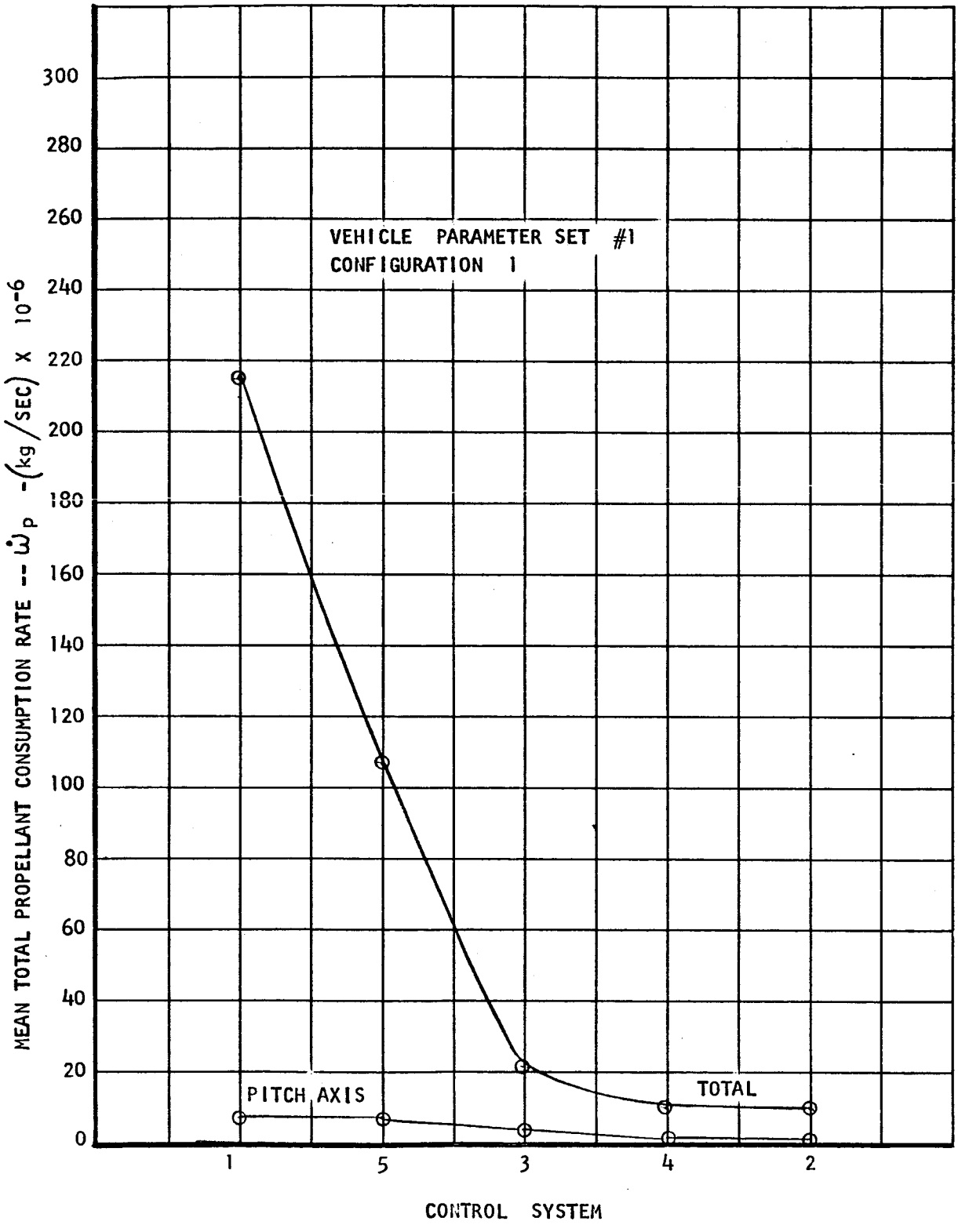

TMC A673

APPENDIX A

SUMMARY OF NOMENCLATURE

Symbol	Description	Units
a	Angular position amplification factor	None
b	Angular rate amplification factor	None
f	Frequency	pulses/hr
F	Thrust	Newtons
F(), f(), h()	Function of	None
I_o	Commanded impulse bit ($\int Fdt$)	kg-sec
I_{sp}	Specific impulse of propellants	n/sec
I_T	Impulse bit	kg-sec
$(J \text{ or } I)_{X,Y,Z}$	Moments of inertia referred to vehicle body axes, X, Y, and Z	kg-m-sec^2
k	Weighting function for impulse error source	None
K	Constant	None
N	Engine number	None
N	Number of sampling points or engine number	None
P()	Probability density function	None
$\dot{\omega}_p$	Propellant consumption rate	kg-sec
r, l, L	Torque or radius arm of rockets	m
R_1, R_2	Random number normally distributed between - and +	None
t	Time	sec
T	Torque	Newton-m
T_s	Period	sec

TMC A673

APPENDIX A (Continued)

Symbol	Description	Units
Δt	Pulse width	milliseconds
W_P	Propellant mass	kg
x, y, z	Moment arms along the body axes	m
$\bar{X}$	Mean value	None
σ	Standard deviation	None
σ_2	Variance	None
Σ	Sum	None
Δ	Increment	None
β	Installation angular error	None
ϵ	Error	None
θ	Angular position	deg
$\Delta\theta$	Angular deadband limit	deg
$\dot{\theta}$	Angular rate	deg/sec
α	Angular acceleration	deg/sec^2
Ψ, O, ϕ	Vehicle attitude angles in yaw, pitch, and roll, respectively	deg
$\ll$	Much less than	None
τ	Time delay	sec

Superscripts

$(\cdot)$	Operator denoting $\frac{d(\ )}{dt}$	
$(\cdot\cdot)$	Operator denoting $\frac{d^2(\ )}{dt}$	

TMC A673

APPENDIX A (Continued)

Coordinate Selection	Positive Direction, Right Hand Coordinate System
θ -- Pitch -- YY Axis	Nose up
ϕ -- Roll -- XX Axis	Clockwise from aft end
Ψ -- Yaw -- ZZ Axis	Nose right

For numbering, let the first numeral equal

1 -- Positive X axis

2 -- Negative X

3 -- Positive Y

4 -- Negative Y

5 -- Positive Z

6 -- Negative Z